MEMBRANE SURFACE MODIFICATION VIA ULTRAVIOLET-PHOTOGRAFTING FOR FORWARD OSMOSIS

AHMAD FIKRI HADI ABDUL RAHMAN

DOCTOR OF PHILOSOPHY

UNIVERSITI MALAYSIA PAHANG

UNIVERSITI MALAYSIA PAHANG

DECLARATION OF THESIS AND COPYRIGHT

Author's Full Name : AHMAD FIKRI HADI BIN ABDUL RAHMAN

Date of Birth : 21 SEPTEMBER 1986

Title : MEMBRANE SURFACE MODIFICATION VIA ULTRAVIOLET PHOTOGRAFTING FOR FORWARD OSMOSIS

Academic Session : SEM 2 2018/2019

I declare that this thesis is classified as:

☐ CONFIDENTIAL	(Contains confidential information under the Official Secret Act 1997)*
☐ RESTRICTED	(Contains restricted information as specified by the organization where research was done)*
☑ OPEN ACCESS	I agree that my thesis to be published as online open access (Full Text)

I acknowledge that Universiti Malaysia Pahang reserves the following rights:

1. The Thesis is the Property of Universiti Malaysia Pahang
2. The Library of Universiti Malaysia Pahang has the right to make copies of the thesis for the purpose of research only.
3. The Library has the right to make copies of the thesis for academic exchange.

Certified by:

_______________________	_______________________
(Student's Signature)	(Supervisor's Signature)
_______________________	_______________________
New IC/Passport Number Date:	Name of Supervisor Date:

NOTE : * If the thesis is CONFIDENTIAL or RESTRICTED, please attach a thesis declaration letter.

SUPERVISOR’S DECLARATION

I hereby declare that I have checked this thesis and, in my opinion, this thesis is adequate in terms of scope and quality for the award of the degree of Doctor of Philosophy.

____

(Supervisor’s Signature)

Full Name : DR. MAZRUL NIZAM BIN ABU SEMAN
Position : ASSOCIATE PROFESSOR
Date :

STUDENT'S DECLARATION

I hereby declare that the work in this thesis is based on my original work except for quotations and citations which have been duly acknowledged. I also declare that it has not been previously or concurrently submitted for any other degree at Universiti Malaysia Pahang or any other institutions.

____

(Student's Signature)

Full Name : AHMAD FIKRI HADI BIN ABDUL RAHMAN

ID Number : PKE 14001

Date :

MEMBRANE SURFACE MODIFICATION VIA ULTRAVIOLET PHOTOGRAFTING FOR FORWARD OSMOSIS

AHMAD FIKRI HADI BIN ABDUL RAHMAN

Thesis submitted in fulfillment of the requirements
for the award of the degree of
Doctor of Philosophy

Faculty of Chemical & Natural Resources Engineering

UNIVERSITI MALAYSIA PAHANG

AUGUST 2019

ACKNOWLEDGEMENTS

This thesis would not have been completed without the help and support of many people who are gratefully acknowledged here.

At the very first, I am honored to express my deepest gratitude to my dedicated supervisor, Assoc. Prof. Dr Mazrul Nizam Abu Seman, with whose notable guidance I could have worked out this thesis. He has offered me valuable ideas and suggestions with his profound knowledge and rich research experiences. His patience and kindness are greatly appreciated. Without him, I could not continue and complete this PhD journey.

I am also grateful to the Faculty of Chemical and Natural Resources Engineering. This work could not have been completed without the help of the lecturers, administration and staff specifically the laboratories used for vigorous experimental works. Thanks for your help and assistance. I also want to thank the Central Lab and Cariff for kindly providing me with an important material for this investigation.

Moreover, I sincerely acknowledge the help I received from my colleagues; without whose support I would not have been able to complete this thesis on time. In particular, the contribution made by Abu Haniffa, Zulsyazwan, Zulhelmi, John, Suhaimi, Mah, Nudra, Amiruls, Amir, Faisal, Nizar, geng sado and PSM students.

I am greatly indebted to my sponsors, Ministry of Higher Education of Malaysia (MyPhD) and Universiti Malaysia Pahang for providing four-year scholarship particularly the Fundamental Research Grant Scheme FRGS/1/2016/TK02/UMP/02/8 and RDU:160127 and Postgraduate Research Grant Scheme PGRS:160336.

There are so many downs than ups throughout the process, and I appreciate the involvement of every person directly and indirectly throughout the process.

ABSTRAK

Kekurangan bekalan air bersih menjadi satu permasalahan global yang semakin kritikal. Bagi mengatasi masalah ini, pelbagai kaedah pemprosesan air bersih makin diterokai. Satu kaedah terbaik untuk menangani masalah ini adalah dengan menggunakan teknologi membran. Pengaplikasian membran osmosis kehadapan (FO) secara khususnya kini meningkatkan kajian untuk menghasilkan membran FO yang baru. Walaubagaimanapun, produk komersil yang dibuat daripada gentian selulosa triacetate mengalami dua isu utama, iaitu kadar serapan garam terundur yang tinggi serta kadar halangan terhadap hidupan biologi serta hidrolisis yang rendah. Di dalam kajian ini, kaedah percambahan sinar ultraviolet (UV) digunakan untuk mengubah membran komersil penapis ultra polietersulfon (UFPES) dan penapis nano polietersulfon (NFPES) untuk kegunaan aplikasi FO. Dua parameter digunakan iaitu kepekatan asid akrilik sebagai monomer (5,15,30 dan 50 g/L) dan masa percambahan (1,3 dan 5 minit). Sifat kendiri membran telah dinilai menggunakan sistem osmosis terbalik untuk menilai fluks air (Jw), ketelapan air (A), ketelapan garam (B) dan penolakan garam (R). Sistem osmosis kehadapan pula di gunakan untuk menilai fluks air (Jv), struktur parameter (S) serta serapan garam terundur (RSD). Pencirian bagi membran telah dilaksanakan untuk menilai struktur kimia permukaan membran, kumpulan berfungsi, kekasaran permukaan, morfologi permukaan dan kadar hidrofilik melalui -analisis transformasi inframerah Fourier (ATR-FTIR), spekstroskopi electron cahaya pembelauan sinar-X (XPS), mikroskop berkuasa atom (AFM), mikroskopi pengimbasan elektron pancaran medan (FESEM) serta sudut sentuhan (CA). Kaedah percambahan sinar UV pada permukaan membran berpotensi untuk digunakan didalam applikasi osmosis kehadapan kerana penambahan kumpulan hidrosil meningkatkan fluks air serta nilai RSD yang setara. Walau bagimanapun, penelitian eksperimen membuktikan bahawa membran UFPES tidak sesuai untuk digunakan di dalam applikasi FO berbanding dengan membran NFPES. Membran UFPES yang belum dimodifikasi telah diuji pada tekanan 3 bar telah menghasilkan penyingkiran garam R sebanyak 0.39 % sahaja apabila larutan sodium klorida berkepekatan 200ppm digunakan. Disamping itu, membran UFPES yang telah menjalani modifikasi juga hanya mampu menghasilkan penyingkiran garam, R dibawah kadar 1%. Ini menyebabkan membran UFPES tidak dipertimbangkan untuk proses model matematik dan seterusnya proses penentuan kondisi optimum. Maka, model matematik hanya dijalankan untuk membran NFPES bagi meramal fluks air pada tekanan osmotik yang berbeza seterusnya untuk meletakkan nilat julat bagi proses pengoptimuman. Kondisi optimum yang telah diperolehi ialah masa percambahan pada 2.81 minit serta kepekatan monomer pada 27.85 g/L. Kondisi ini telah memberikan nilai ketelapan air pada 1.52 ± 0.04 $L.m^{-2}.hr^{-1}$ serta nilai RSD pada 10.09 ± 0.36 $g.m^{-2}.hr^{-1}$. Di dalam kajian ini, didapati bahawa kesan modifikasi permukaan tidak hanya terbatas pada sifat kimia dan fizikal permukaan membran sahaja, tetapi ia telah berlaku jauh ke dalam lapisan berlubang-lubang membran. Sebagai kesimpulan, proses pengubahsuaian ini dinilai sebagai satu kaedah yang berpotensi untuk digunapakai pada membran komersil yang berpacuan tekanan untuk aplikasi FO.

ABSTRACT

The shortage of freshwater has become a severe problem globally. To mitigate this problem, various technologies to cater the demand have been actively explored worldwide. An effective approach to address these water-related issues is via membrane technology. Specifically, the forward osmosis (FO) membrane, it has emerged as promising technology that has attracted much attention especially on the development of new FO membrane. Unfortunately, the commercial asymmetric cellulose triacetate membrane which is built with a low structural parameter and demonstrated decent FO performance suffers from high reverse salt diffusion (RSD) and show poor inhibition to biological attachment and hydrolysis. Thus, this study aims to modify commercial pressure-driven membrane using the surface modification technique for potential FO application. Among different successful membrane surface modification techniques, ultraviolet (UV) photografting is of particular interest, which offers a versatile means for providing the existing polymer with new surface functionalities, without affecting the bulk properties of the substrate. In this study, commercial ultrafiltration polyethersulfone (UFPES) and nanofiltration polyethersulfone (NFPES) membranes were modified via UV-photografting technique for FO application. The membranes were prepared under different acrylic acid monomer concentration (5, 15, 30 and 50 g/L) and grafting time (1,3 and 5 minutes). The membrane intrinsic properties were measured in reverse osmosis mode for water flux (Jw) water permeability (A), salt rejection (R), solute permeability (B) and in FO mode for water flux (Jv), structural parameter (S), and reverse salt diffusion (RSD). Membrane characterization was performed to evaluate the surface chemistry, functional group, surface roughness, surface morphology and hydrophilicity using the attenuated total reflection-Fourier transform infrared spectroscopy, x-ray photoelectron spectroscopy, atomic force microscope, field emission scanning electron microscopy and contact angle, respectively. The surface modification via UV-photografting has the potential in the FO application as incorporation of the carboxyl group enhanced the water flux as well as comparative RSD value. However, the experimental work reveals that UFPES membrane was not suitable for FO application compared to NFPES membrane. Unmodified UFPES was tested at a pressure of 3 bars exhibited salt rejection with R value of 0.39 % only when using the 200 ppm of sodium chloride (NaCl). Moreover, modified UFPES membrane also has R values which ranges below than 1 %. Thus, UFPES membrane has been excluded from the theoretical modelling and optimization processes. Mathematical modelling was performed on NFPES membrane to predict the water flux at different osmotic pressure as well as to suggest the range for the optimization processes. The obtained optimum conditions were 2.81 min grafting time and 27.85 g/L acrylic acid monomer concentration. Under these conditions, a maximum water flux of 1.52 ± 0.04 L.m^{-2}.hr^{-1} was achieved with RSD value of 10.09 ± 0.36 g.m^{-2}.hr^{-1}. It was found that the chemical and physical modification did not only reflect on the surface of the active layer but also the porous support layer of the membrane. As a conclusion, surface modification via UV-photografting offers another route for the usage of the commercial pressure-driven membrane for FO application.

TABLE OF CONTENT

CHAPTER 4 RESULTS AND DISCUSSION 68

LIST OF TABLES

LIST OF FIGURES

LIST OF SYMBOLS

A	Water permeability
atm	Atmospheric pressure
A_m	Membrane active area
B	Solute permeability
c	Velocity of light
C_b	Concentration of bulk
C_p	Concentration of permeate
D	Diffusion coefficient
D_a	Dalton
D_{ϖ}	Bulk diffusivity
E	Energy
G	Gas constant
h	Planck’s constant
J_v	Water flux in FO mode
J_w	Water flux in RO mode
K	Solute resistivity
k	Mass transfer coefficient
ln	Natural logarithm
M	Molar
nm	Nanometre
N_p	Number of points
P	Pressure
Pa	Pascal
psi	Pound per square inch
r	Radius of strirrer
R	Salt rejection
S	Structural parameter
Sh	Sherwood number
S_a	Average roughness
v	Frequency
Z_i	Current height

Greek letters		Unit
π	Osmotic pressure	bar
π_D	Osmotic pressure in draw solution	bar
π_F	Osmotic pressure in feed solution	bar
υ	Van’t Hoff dissociation factor	i
ω	Stirring rate	rad.s^{-1}
λ	Wavelength	nm
υ	Kinematic viscosity	ms-1
µm	Micrometre	1x10^{-6}m
Δ	Changes	

LIST OF ABBREVIATIONS

AA	Acrylic acid
AFM	Atomic force microscope
ANOVA	Analysis of variance
AR	Argon gas
ATR-FTIR	Attenuated total reflection-Fourier transform infrared spectroscopy
BPA	Bisphenol A
CA	Contact angle
CC	Cyanuric chloride
CCD	Central composite design
CF_4	Tetrafluoromethane
CMCNa	Sodium carboxymethyl cellulose
CNF	Carbon nanofiber
CTA	Cellulose triacetate
CP	Concentration polarization
D	Solute diffusivity
DS	Draw solution
ECP	External concentration polarization
FESEM	The field emission scanning electron microscopy
FO	Forward osmosis
FS	Feed solution
GA	Glutaraldehyde
He	Helium gas
HF	Hollow fibre
HNT	Halloysite nanotube
ICP	Internal concentration polarization
IOP	Internal osmotic pressure
IP	Interfacial polymerization
LBL	Layer by layer
MF	Microfiltration
MPD	M-phenylenediamine
MWCO	Molecular weight cut-off
NaCl	Sodium chloride
NF	Nanofiltration

NFPES	Nanofiltration polyethersulfone
ODMPs	Osmotically driven processes
PDA	Polydopamine
PA	Polyamide
PAA	Polyacrylic acid
PAH	Polyallylamine hydrochloride
PAN	Polyacrylonitrile
PAS	Polyarylsulfone
PBI	Polybenzimidazole
PBO	Poly p-phenylene benzobisoxazole
PDADMAC	Poly-diallyl-dimethylammonium chloride
PEI	Polyethyleneimine
PES	Polyethersulfone
PMAA	Polymethacrylic acid
PolyOEGMA	Polymerization of oligo ethylene glycol methacrylate
PolySBMA	Polysulfobetaine methacrylate
PRO	Pressure retarded osmosis
PSS	Polysodium 4-styrene-sulfonate
PVDF	Polyvinylidene fluoride
RF	Radio frequency
RO	Reverse osmosis
RSD	Reverse salt diffusion
RSM	Response surface methodology
SPPO	Sulfonated polyphenylene oxide
TDS	Total dissolved solid
TFC	Thin film composite
TFN	Thin film nanocomposite
TMC	Trimesoyl chloride
UF	Ultrafiltration
UFPES	Ultrafiltration polyethersulfone
UN	United Nations
UV	Ultraviolet
WHO	World Health Organization
XPS	X-ray photoelectron spectroscopy

CHAPTER 1

INTRODUCTION

1.1 Background of the study

Sustainable development can be defined as the development that meets the needs of the present, without compromising the possibility for meeting the needs of future generations. The sustainable development can be achieved by galvanizing three core elements namely economic growth, social inclusion and environmental protection. These elements are interconnected and are all crucial for the well–being of individuals and societies. In the 17th Sustainable Development Goals set by the United Nations (UN), water has become one of the key components under the "Ensure Access to Water and Sanitation for All" (United Nations, 2018).

At the initial stage, the amount of fresh water was adequate to accomplish this developmental goal. However, due to various reasons ranging from climate change, war, unbalanced growth, and pollution from industries, several millions of people are currently faced with challenges emanating from inadequate water supply, sanitation and other hygiene issues. According to the World Health Organization (WHO), only 71% of the world's population has access to safe drinking water services (UNICEF, 2017).

Membrane technology offers an effective approach to address these water-related issues. It has emerged as an important water treatment technology due to its inherent advantages such as small equipment footprint, easy maintenance, and high energy efficiency (Richard, W. B., 2004). In fact, membrane water treatment is expected to play a major role in areas such as drinking water treatment, brackish and seawater desalination, as well as wastewater treatment and reuse (Yin, J. & Deng B. L., 2015).

In addition, the membrane process can be easily scaled down for operation at partial capacity or scaled up by adding membrane modules in stages to suit higher capacities as well as the elimination of chemical consumption in the treatment process (Deshmukh, A. et al., 2015). Extension of the membrane technology and application to various fields, has facilitated the technology of forward osmosis (FO). FO technology has gained recognition as a suitable complement to the reverse osmosis (RO) technology in a niche application. This is particularly notable in applications where the use of reverse osmosis alone is unfeasible or impossible (Cai, T. et al., 2016).

Forward osmosis is a process which movement of water from low concentration to high concentration across a selectively permeable membrane which driven by osmotic pressure. A selectively permeable membrane allows passage of water, but rejects solute molecules or ions. Thus, forward osmosis which usually performed with low or even without hydraulic pressure has been considered as an emerging membrane technology for water reuse and desalination (She, Q. H. et al., 2012a).

Currently, the major challenges of FO technologies are the lack of ideal FO membranes, draw solution with high osmotic pressure and the ability to recover the fresh water from the draw solution. The conventional pressure-driven membrane is asymmetric have been observed to be unsuitable for the FO process as it aggravates concentration polarization effects (McCutcheon, J. R. & Elimelech M., 2008). The desirable FO membranes must have a high water flux and salt retention, low concentration polarization, resistance to chlorine and a wide range of pH plus long-term stability in separation performance (Sairam, M. et al., 2011).

As stated, the selection of draw solution with high osmotic pressure is another limiting factor for commercial applications of FO technology. The ideal characteristics of potential draw solution includes high osmotic pressure, zero toxicity, easy recovery and low cost (She, Q. H. et al., 2012b). Another area of concern in the FO technology is the recovery of pure water from the draw solution which affects the performance of the FO process. However, this research will only focus on the first barrier which is the development of the FO membrane.

In the development of new FO membrane, many approaches have been explored but mainly oriented into two main methods namely the bulk modification and surface modification. Both modifications produced an enhanced membrane with increased hydrophobicity, biocompatibility, and functionality compared to the pristine membrane

(Chekli, L. et al., 2016). The bulk modification is either phase inversion for flat sheet membrane or dry-wet spinning technique for hollow fibre membrane. Bulk modification methods are often more straightforward because they can be applied in the polymer solution. However, the entire membrane modification often yields a lower net effect, with enhanced swelling effect (Van Der Bruggen, B., 2009a). Moreover, the bulk modification is not commercially feasible as the equipment involved may be too costly for large-scale membrane production (Ng, L. Y. et al., 2013c). Another method in the development of FO membrane is via surface modification. This technique varies from interfacial polymerization (Wang, Y. Q. et al., 2016), layer-by-layer deposition of polycations and polyanions on porous charged substrates (Nguyen, A. et al., 2013), as well as the incorporation of nanoparticles into the membrane (Ghanbari, M. et al., 2015).

Another successful technique in the surface modification method is the ultraviolet (UV)-photografting. It is normally applied in various form ranging from flat sheet of microfiltration (MF) membrane (Ren, P. F. et al., 2015), ultrafiltration (UF) membrane (Pieracci, J. et al., 2002) and nanofiltration (NF) membrane (Abu Seman, M. N. et al., 2010a). One of the important selections of this surface modification technique is that can change the surface properties of a membrane without adverse influence on its bulk properties (Rahimpour, A., 2011). Moreover, the membrane used for FO should be hydrophilic to enhance the permeation of water flux without losing the ability to retain the draw solution.

In this research, acrylic acid has been used as the sole monomer, hence the effect of monomer size, chemical group, the degree of polymerization and surface coverage are kept constant (Kato, K. et al., 2003). This monomer has a high hydrophilicity and water solubility have been broadly used to facilitate the water molecules across the membranes in early work. (Abu Seman, M. N. et al., 2010a). However, there is no report on the usage of this technique into FO technology. Therefore, innovation in surface modification technique via UV-photografting for improving the FO to have membrane is thought great potentialities. FO which is an osmotically driven membrane processes (ODMPs) are the emerging technologies in solving the water-related issue. Therefore, there is a pressing need to develop additional route for synthesizing high-performance FO membrane.

1.2 Problem statements

Currently, the production of FO membrane is led by Hydration Technology Inc. (HTI) with the fabrication of asymmetric cellulose triacetate (CTA) membrane (Nguyen, T. P. N. et al., 2015). The membrane, which is built with a low structural parameter, has demonstrated decent FO performance and offers a desirable advantage as conventional pressure-driven membranes which are unsuitable for FO application. Unfortunately, this commercial FO membrane suffers from high reverse salt diffusion (RSD) (Liu, C. et al., 2013) and show poor inhibition to biological attachment and hydrolysis (Gu, Y. et al., 2013). Using 14 types of draw solution, Achilli, A. et al. (2010) has identified that the smaller the anion hydrated size, the higher the value of RSD on the negatively charged CTA membrane.

Conventional pressure-driven membrane is well known to characterized by severe internal concentration polarization (ICP). McCutcheon, J. R. et al. (2005) has mentioned that the conventional membrane consists of an active layer and porous layer which serves as thick support layer to withstand the pressurized condition. This condition leads to the significant lost in the effective driving force and resulting water flux. However, as research progressed, it has been revealed that bulk modification and surface modification on the pressure-driven membrane is applicable in ODMPs application. Bulk modification on thin film composite FO membrane was conducted by modifying the support layer by changing the spongy pore structure with straight finger-like pore structure to minimize ICP (Wei, J. et al., 2011b). Systematic investigations were conducted on FO performance using the influence of monomer concentration, interfacial polymerization and polyamide rejection layer.

On the other hand, the surface modification on commercial thin-film composite membrane works by the addition of polydopamine on the support layer. This research group led by Arena, J. T. et al. (2011) have identified the RO membrane support layers as hydrophobic which inhibit wetting. This poor wetting condition limiting the water and solute transport in the support layer which leads to severe ICP. Thus, the addition of bio-inspired polymer with a similar chemistry to the adhesive secretions of mussels increases the hydrophilicity and promote wetting. The modified membrane shows excellent performance in FO (Arena et al., 2014) and pressure retarded osmosis (Arena et al., 2011) in their respective configurations. Thus, we hypothesized that the similar improvement on the commercial pressure-driven membrane using surface modification via UV-photografting can offer enhanced properties as well.

Another major issue in FO technology is the RSD. It is the movement of solute from the draw solution into the feed solution via the semipermeable membrane. RSD plays an important role in any FO system because it can lead to the loss of draw solute, enhancement of concentration polarization, and the change of feedwater chemistry which may significantly influence the membrane fouling behaviour (She, Q. H. et al., 2016). Thus, RSD is considered a key parameter in the development of high-performance FO membrane. In the membrane development, various polymeric materials have been used in the fabrication of new membranes either in flat sheet or hollow fibre.

In another vein, it is worthy of note that optimization studies are much needed to finalise the development of high-performance FO membrane. In fact, it has been previously concluded that fabrication of high-performance FO membrane requires optimization of the structural properties of the support layer and transport features of the active layer (Tiraferri, A. et al., 2011). Thus, optimization process was conducted using Response Surface Methodology (RSM). The influence of grafting parameters namely monomer concentration and grafting time on the modified membrane will be measured on the performance of water flux and RSD. Developed models can then be subjected to validation process via three confirmation runs to confirm the regression equations.

Therefore, this research has been conducted to investigate the possibilities of using surface modification via UV-photografting technique for modifying the conventional pressure-driven membrane for the application of FO technology. Both ultrafiltration polyethersulfone (UFPES) and nanofiltration polyethersulfone (NFPES) membranes were prepared under different grafting parameters to increase the hydrophilicity as well as decrease the RSD. As such, this research tends to suggest an alternative route to modify the membrane for FO application. Moreover, an optimal condition for surface modification of PES membrane via UV-photografting for the FO application was proposed.

1.3 Research objectives

The main objective of this research is to develop high-performance FO membrane using surface modification technique via UV-photografting. The specific objectives are as follows;

i. To modify, characterize and compare UFPES and NFPES membranes substrate for FO application.
ii. To model the FO membrane performance of water flux using mathematical modelling and investigate the performance of grafting parameters.
iii. To optimize the performance of modified membrane using the response surface methodology for forward osmosis.

1.4 Research scopes

i. Evaluation of the membrane using reverse osmosis (RO) mode to determine the water flux (Jw), water permeability (A), salt rejection (R), solute permeability (B) and forward osmosis (FO) mode to determine the water flux (Jv), reverse salt diffusion (RSD) and structural parameter (S).
ii. Pre-treatment and modification of commercial UFPES and NFPES membranes using acrylic acid (AA) monomer at different AA concentration (5,15,30 and 50 g/L) and different grafting time (1,3 and 5 min).
iii. Characterization of the membrane in term of functional group using attenuated total reflectance-Fourier transforms infrared spectroscopy (ATR-FTIR), the elemental analysis using x-ray photoelectron spectroscopy (XPS), surface roughness using atomic force microscopy (AFM), surface morphology using field emission scanning electron microscopy (FESEM) and hydrophilicity using contact angle.
iv. Comparison of the performance of UFPES and NFPES membranes to enable proper selection of the membrane support for the FO application.
v. Prediction of the membrane performance at different draw solution concentration (0-1.5M) using developed theoretical modelling.
vi. Optimization of UV-photografting condition in response surface methodology (RSM) using two factors namely monomer concentration and grafting time and two responses namely water flux and reverse salt diffusion as well as the

evaluation of the regression equations using the validation test to suggest the accuracy of experimental results.

1.5 Thesis outline

This chapter focused on the fundamental understanding of the importance of the research which is necessary to the body of knowledge. We implement the standard methodology for evaluating the membrane performance which has been developed by Cath, T. Y. et al. (2013). The procedures are configured initially in reverse osmosis (RO) mode to determine the membrane intrinsic properties (J_w, A, B and R) before proceeding with the FO mode to determine the membrane performances (J_v, J_s and S). Chapter 1 contains the background of the study, the problem statement, objectives, and scope of the study. The literature review, which is in Chapter 2 presents the fundamentals of membrane technology and FO technology, membrane development on both bulk modification and surface modification specifically relating to FO application, mathematical modelling and ends with the optimization process. Chapter 3 contains the research methodology employed in this study and include important details such as the materials, experimental procedures, evaluation of the membrane performance, the process of mathematical modelling as well as the design of experiment for the optimization process.

The development of high-performance FO membrane in Chapter 4 was divided into four main phases. In the first phase, UFPES membrane was modified using the UV-photografting technique. The second phase is the modification of NFPES membrane. The modification of UFPES and NFPES membranes are using the same grafting parameter under the same protocols for modification and experimental works. The third phase is the comparison between these two membranes followed by mathematical modelling to predict the water flux at different osmotic pressure. Details of graft polymerization mechanism namely the effective grafting and chain scission are provided. Next, NFPES membrane was selected for optimization after evaluation and performance comparison. Response Surface Methodology (RSM) using a central composite design (CCD) was performed using two factors and two responses. Finally, the optimized grafting condition was re-fabricated to confirm the development of high-performance FO membrane using the UV-photografting technique. Chapter 5 contains the conclusion of the study and provide suggestions for future work relating to this study.

CHAPTER 2

LITERATURE REVIEW

2.1 Introduction

The membrane is defined as the material which allows selective mass transport of certain species (Wang, L. K. et al., 2008). The membrane is capable of separating selective components over a wide range of particle sizes and molecular weights while retarding one or more other components (Hilal, N. et al., 2012). The solution that enters the membrane is called the feed-solution whereas the fluid that passes through the membrane is known as permeate and the fluid that contains the retained components is the retentate. Notably, the membrane technology has two configurations namely the cross-flow and dead-end system as shown in Figure 2.1.

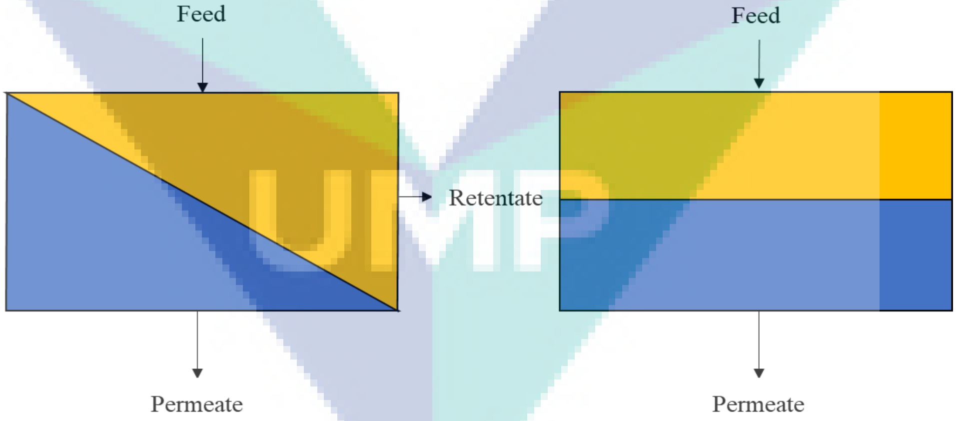

Figure 2.1 Passage in the membrane system (a) cross-flow and (b) dead-end system

Generally, the membrane may be classified based on two main factors namely the flux and selectivity (Scott, K. & Hughes R., 2012). Flux or permeation rate is defined as the volumetric (mass or molar) flow rate of fluid through the membrane per unit area of membrane per unit time as presented in Eq. 2.1. Selectivity, on the other hand, is defined as the selection of solute or particles to remain in the system or permeate through the system. Therefore, the membrane is often assembled according to the module of the separation process at the desired specification process. The transport mechanism on any membrane configuration can be either active or passive mode. Depending on the configuration, the membrane system can be driven by pressure, concentration and temperature difference (Mulder, J., 2012).

$$\text{Water flux} = \frac{\text{Volume}}{\text{Membrane area x Time}} \tag{2.1}$$

The membrane is being differentiated based on the pore size and porosity while physico-chemical properties such as the surface hydrophilicity and roughness, chemical, thermal and mechanical stability affect the performance and reliability of the membrane (Scott, K. & Hughes R., 2012). The pore of the membrane is measured based on the diameter of a particle or molecular weight of a molecule that is retained in an experiment which is known as the molecular weight cut-off (MWCO).

In the membrane system, every equipment is precisely tailored to the specific requirements of the finished product. Hence, the product from any of the membrane technology is very specific (Mulder, 2012). In fact, each of the membrane technology is built based on specific application and therefore have their distinctive properties.

In the pressure-driven membrane, there are four types of membrane technology namely the microfiltration (MF), ultrafiltration (UF), nanofiltration (NF) and reverse osmosis (RO). Table 2.1 presents a classification of membrane based on the driving force, separation mechanism, MWCO, pore size and operating pressure. Notably, the denser the membrane structure, the higher the resistance of the membrane mass transfer.

Thus, the applied pressure must be higher to get the same amount of flux through the membrane. As can be seen from the table, the FO technology relies on the pressure as the driving force. Moreover, the focus was placed on two commercial pressure-driven membranes namely the ultrafiltration (UF) and nanofiltration (NF) membranes.

Table 2.1 Classification of membrane based on pore size separation

Membrane	**Driving force**	**Separation mechanism**	**Molecular weight cut-off**	**Pore size**	**Operating pressure, bar**
Microfiltration	Pressure	Sieve	>100000	0.1-10	1-30
Ultrafiltration	Pressure	Sieve	>10000-100000	0.01-0.1	3-80
Nanofiltratin	Pressure	Sieve/diffusion/exclusion	300-1000	0.001-0.01	70-220
Reverse osmosis	Pressure	Diffusion/ exclusion	100-200	<0.001	800-1200
Forward osmosis	Concentratin	Diffusion/ exclusion	-	-	1-10
Pressure retard osmosis	Pressure	Diffusion/ exclusion	-	-	1-10

Source: Adapted from Stephenson, T. et al. (2000).

However, the advancement in water treatment technology has driven the usage of osmotically driven membrane processes (ODMPs) which comprises both forward osmosis (FO) and pressure retarded osmosis (PRO) which were included in Table 2.1. ODMPs offer a better efficiency, longer life-cycle, limited operating area, as well as low capital and operating expenditure (Bui et al., 2015).

There are two modes in the ODMPs, when an asymmetric membrane is used. The modes are dependent on the orientation of the membrane in the system. The process is called FO mode when the active layer is placed facing the feed solution (ALFS) while it is called PRO mode if the active layer is facing the draw solution (ALDS). For the purpose of this study, the only the ALFS configuration has been applied.

2.1.1 Ultrafiltration membrane

Ultrafiltration (UF) involves the pressure-driven separation of materials from water using a membrane pore size of approximately 0.002 to 0.1 μm, MWCO of approximately 10,000 to 100,000 Da and an operating pressure of approximately 3 to 8 bar. Table 2.2 presents the relation between UF membrane cut-off and pore size.

Table 2.2 Ultrafiltration membrane cut-off and pore size

Cut-off, Da	Pore diameter, nm
1,00,000	100
500,000	20
100,000	10
50,000	4
10,000	2.5

Source: Baker, R. W. (2012)

UF membranes can retain species in the range of 300-500,000 Da of molecular weight. Typical rejected species include sugars, bio-molecules, polymers and colloidal particles (Baker, R. W., 2004). The primary mechanism is size exclusion, but chemical interactions between solute and membrane as well as operating parameters can affect the process. Ultrafiltration membranes are anisotropic with a “skin” layer fused on top of a microporous support. The skin layer enhances the selectivity of the membrane while the role of the microporous backing layer is to provide mechanical support.

The thickness of the skin layer can range from 0.2 to 10 µm depending on the material and the application. UF membranes can be made from both organic (polymer) and inorganic materials. Among the potential organic materials, the most popular are cellulose, polysulfone (PS), polyethersulfone (PES), sulfonated polysulfone (SPS), polyvinylidene fluoride (PVDF), polyacrylonitrile (PAN), polyimide (PI), polyetherimide (PEI), aliphatic polyamides (PA), and polyetherketone (PEK) (Korbutowicz, M. K. & Nowak K. M., 2011).

2.1.2 Nanofiltration membrane

Nanofiltration (NF) is a pressure-driven membrane technology positioned between RO and UF membranes. NF refers to a membrane process that rejects solutes approximately 1 nm in size with a molecular weight above 300 Da. NF is a lower-pressure version of RO and is used where the high rejection of salts is not necessary. NF is capable of removing bacteria and viruses as well as organics related to water colour. It is also used to remove pesticides and other organic contaminants from surface and groundwater. NF membranes reject multivalent ions to a significantly greater degree than monovalent ions (Baker, R. W., 2004). The specific rejection of ions varies from one membrane manufacturer to another, but a multivalent ion rejection of 95 percent with a monovalent ion rejection of only 20 percent might be observed.

In the water treatment technology, NF is referred to as “membrane softening”, as it is an attractive alternative to chemical softening. However, hard water intended to be treated by NF will need pre-treatment to avoid precipitation of hardness ions on the membrane. Moreover, this membrane is usually charged using carboxylic groups and sulfonic groups which enhances its ion repulsion (Donnan exclusion), and it is the determinant factor for salt rejection (Ng, L. Y. et al., 2013c).

Because NF membranes also remove alkalinity, the product water can be corrosive. Hence, measures such as blending raw water and product water or adding alkalinity, may be needed to reduce corrosivity. However, more energy is required for NF than MF or UF due to the smaller pore size, denser and highly packed molecular arrangement on the active layer.

2.2 Forward osmosis

Since McCutcheon, J. R. et al. (2005) reported the use of FO technology for desalination, the publications on ODMPs especially FO have been expanding at an exponential rate. The applications based on FO have been extended to various water industries such as water treatment, wastewater reclamation and sea water desalination.

Without the requirement of draw solution (DS) separation, the stand-alone FO can be used to concentrate the feed water such as the concentration of anaerobic digester centrate (Holloway, R. W. et al., 2007), and concentration of waste water for energy and nutrients recovery or dilute the DS for fertigation (Phuntsho, S. et al., 2011), and osmotic dilution of sea water for desalination (Blandin, G. et al., 2015). The major advantage of the FO process over the pressure-driven RO and NF processes lies in the very low energy consumption.

Forward osmosis system works based on the natural process namely osmosis. This system exploits the use of osmotic pressure gradient ($\Delta\pi$). The main advantage of FO technology is that it operates under no hydraulic pressures which result in lower membrane fouling and lowler or no energy requirement (Cath, T. Y. et al., 2006). Given these merits, FO technology has been applied to a wide range of fields, such as seawater

water desalination (Akther, N. et al., 2015), wastewater treatment (Su, J. C. et al., 2012), and many other areas (Chekli, L. et al., 2016).

Although FO exhibits a great potential in alleviating the issues caused by freshwater shortage, challenges, such as relatively low water permeability, high reverse salt diffusion, severe concentration polarization, and membrane fouling, are still present in FO application. To eliminate these problems, exploration of FO membrane is urgently needed. Great efforts have been made in the development of FO technology in recent years, and a wide range of powerful FO membranes have been proposed to date.

In the FO system, there are three parameters which are commonly employed for measuring the performance of FO system, namely pure water permeability (A), solute permeability (B), and structural parameter (S) which governs the transport phenomena across the membrane support layer. Specifically, the structural parameter determines the extent of internal concentration polarization (ICP) in the ODMPs (T. Y. Cath et al., 2013). Two solutions of different concentrations namely feed solution (FS) and draw solution (DS) are used in order to drive the permeation of water across the membrane as shown in Figure 2.2.

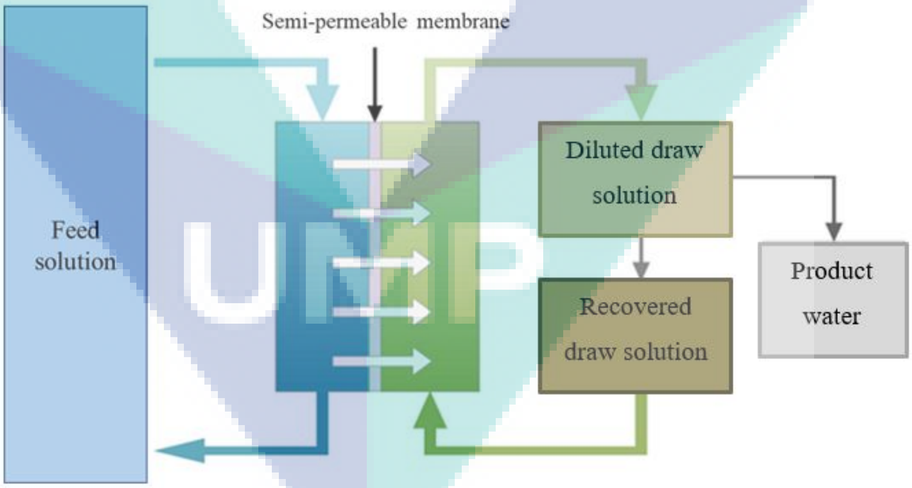

Figure 2.2 Forward osmosis configuration
Source: Jiao, Y. et al. (2015)

The process in Figure 2.2 starts when water molecules in the FS are transported naturally across the membrane into a concentrated DS by osmosis. Transferred water is called the permeate which dilutes the DS. The latter process is the elimination of permeates in the DS to maintain the osmotic pressure in the system. Usually, the DS may be recovered using the application of the mechanical protocol. It is used to drive pure water out of the system using the common desalination rate process namely the RO system (Akther, N. et al., 2015).

2.2.1 Mass transfer coefficient

The FO system utilizes the osmotic pressure gradient ($\Delta\pi$) as the driving force to facilitate the movement of water molecules across the membrane. The water is transported from low solute concentration across a membrane into a high solute concentration. The osmotic pressure (π) from the DS are measured using Van't Hoff equation shown in Eq. 2.1 (Qasim, M. et al., 2015).

$$\pi = \mathrm{MGT} \qquad 2.2$$

where M is the molar concentration of the solution, G is the universal gas constant and T is the absolute temperature.

By calculating the osmotic pressure gradient ($\Delta\pi$), it is then possible to determine the water flux of the osmosis process. The general equation describing the water transport in the FO system is given in Eq. 2.3:

$$J_w = A(\pi_D - \pi_F) \qquad 2.3$$

where J_w is the water flux, A, π_D, and π_F are the water permeability, osmotic pressure in DS and osmotic pressure in FS, respectively. It is worthy of note that standard symbols have been used in all the equations presented in this thesis.

2.2.2 Draw solution

Draw solution (DS) is a major component in the mass transport of an ODMPs. This system relies on the utilization of osmotic pressure differences across semi-permeable membranes to generate the water flux. The selection of suitable DS may vary from the osmotic pressure, diffusivity, density and dynamic viscosity (Tan, C. H. & Ng H. Y., 2013). Hence, it is crucial to select the appropriate membrane and DS.

The water flux through the FO membrane is directly proportional to the draw solution concentration. The greater the difference in osmotic potential, the faster water moves through the membrane (Cath, T. Y. et al., 2006). However, the osmotic pressure difference across the active layer of the membrane varies gradually during the system operation time. Specifically, as the dilution of the draw solution occurs, the difference in osmotic pressure gets lower, thereby decreasing the water flux through the membrane.

The selection of DS for the FO process involves several desired properties. The solute must have a high osmotic pressure, cheap, high solubility; low molecular weight, low reverse salt diffusion, low-toxicity, chemically stable and easy to recover upon operation (McCutcheon, J. R. et al., 2006). As illustrated in Figure 2.3, Shaffer, D. L. et al. (2015) in their review paper presents the relationship between osmotic and viscosity for 15 draw solutions.

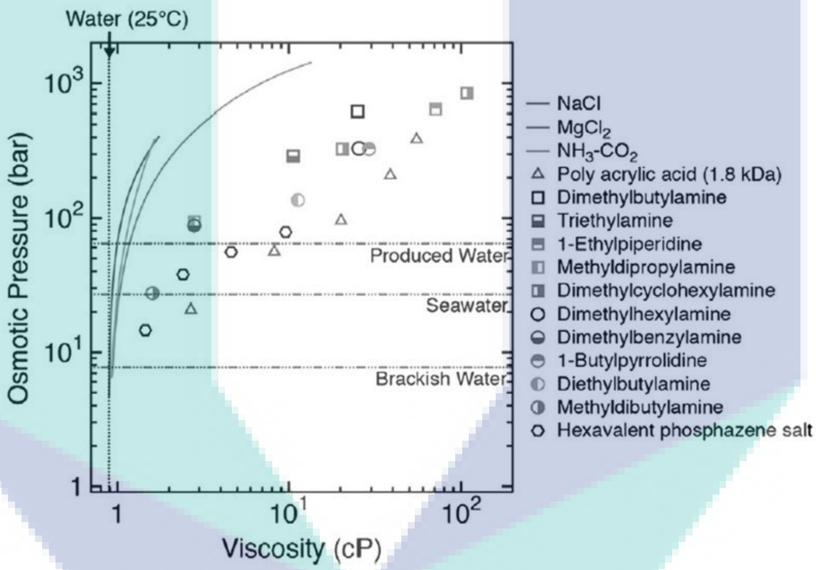

Figure 2.3 Osmotic pressure vs viscosity of the draw solution
Source: Shaffer, D. L. et al. (2015)

Numerous ideas in the selection of DS has been suggested ranging from polyelectrolytes, hydrophilic magnetic nanoparticles, hydrogels and switchable polarity solvents such as an ionic liquid. Likewise, in another review paper by Cai, Y. F. and Hu X. (2016), the history and the development of draw solutions have been completely presented with the evolution process in desalination. In anither report, Achilli, A. et al. (2010) have developed a protocol for selecting an optimal DS for FO application. The protocol was developed based on the screening process, laboratory and modelling analysis.

The measurement of osmotic pressure of the DS using OLI Systems Inc software was highly cited. The system works on published experimental data and analysed by thermodynamic modelling. The results provide an insight view including the concentrations and temperature. However, the access to the system is limited to the assumptions that underlie the software. The software may not be able to project pressures associated with newly developed draw systems whose experimental properties have yet to be published or included in the software database. Thus, comparing the previously calculated values by the OLI Systems software to newly developed draw solution systems may be problematic (Wilson, A. D. & Stewart F. F., 2013).

During the last few years, most studies have investigated the used of inorganic salts as DS due to their low cost and high osmotic pressure potential, which creates a high water flux (Achilli, A. et al., 2010). However, the low-charge and small hydrated radius of monovalent and divalent ions in the DS can result in a high reverse flux of salts, when DI water was used as the feed solution (Kiriukhin, M. Y. & Collins K. D., 2002).

In addition, recovering these DS requires a high amount of energy as the pressure-driven RO membrane is still required to recover water from the salts (Zhao, S. et al., 2012) or the standard of the water obtained is not close to that of drinking water. This is caused by the leakage of a high amount of ammonium bicarbonate into water (Ge, Q. et al., 2013). To overcome these disadvantages of inorganic salts, magnetic nanoparticles (MNPs) were synthesized and used as a smart draw solution, and no reverse salt flux occurred.

However, particle agglomeration was observed during recycling through a magnetic separator, and the FO performance deteriorated accordingly (Ge, Q. et al., 2010). Moreover, the synthesis of MNPs is complicated and difficult.

Furthermore, other materials have been used for FO, such as the polyelectrolyte of polyacrylic acid sodium salts (Ge, Q. et al., 2012), 2-methylimidazole-based organic compounds (Yen, S. K. et al., 2010), switchable polarity solvents (Stone, M. L. et al., 2013), dimethyl ether solutions (Sato, N. et al., 2014), and poly (sodium 4-styrenesulfonate) (Tian, E. et al., 2015).

These DS showed justifiable water flux. Nevertheless, high reverse salt flux and relatively energy-intensive regeneration make them impractical in FO desalination.

Therefore, identifying novel draw solutes with characteristics of highwater flux, low reverse salt flux, and easy recovery is necessary.

In a particular study, sodium chloride (NaCl) was chosen as the draw solution as presented in Figure 2.4. NaCl was used as the draw solution due it is highly solubility and non-toxicity at low concentrations. In addition, it is relatively easy to re-concentrate using conventional desalination processes without risk of scaling (Achilli, A. et al., 2010).

Moreover, the selection of NaCl as the DS is due to low cost in recovering and replenishment process (Thelin, W. R. et al., 2013). This DS provides an average osmotic pressure of 49.53 atm at 1M (McCutcheon, J. R. & Elimelech M., 2006). The solute diffusivity and size of NaCl are 1.610 x $10^{-9}m^2s^{-1}$ and 0.152 nm, respectively (Lau, W. J. & Ismail A. F., 2009).

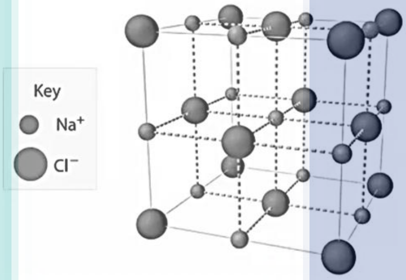

Figure 2.4 Sodium chloride molecular structure
Source: Physicsopenlab (2018)

2.3 Challenges in forward osmosis

Forward osmosis utilizes the osmotic pressure difference as its driving force. It uses lower energy and it is less susceptible to membrane fouling compared to conventional pressure-driven membrane processes. It allows for a higher removal of an extensive range of ion contaminants and higher water recovery over the conventional pressure-driven membrane processes (Ang, W. L. et al., 2015).

Notwithstanding, there are several challenges faced by FO applications which often limits its application in large-scale processes. The three notable challenges namely the concentration polarization, fouling and reverse salt diffusion which limits the wide range application of FO are discussed in the subsequent subsections.

2.3.1 Concentration polarization

Concentration polarization (CP) is a phenomenon which exists in all kinds of separation processes, either pressure driven or osmotic driven. CP is the inevitable effect of the increased solute concentration in the boundary layer close to the membrane surface. For example, salt may be accumulated at the boundary layer when they are rejected from crossing the membrane (Amini, M. et al., 2013). The formation of CP is one of the most important factors influencing a significant drop in water flux. CP is reversible and may be effectively reduced by increasing the shear rate and turbulence of the flow, pulsation or ultrasound (Su, J. C. et al., 2012).

CP occurs on the FS and DS of the membrane which defines as external concentration polarization (ECP). In the FO process, the system is configured in such a way where the FS is against the active layer of the membrane, while the DS is against the membrane support layer. Both concentrative and dilutive ECP reduces the effective osmotic driving force. However, both ECPs may be reduced by increasing the fluid flow and turbulence. The negative effect of ECP on osmotic-driven membrane processes can be minimized by adjustment of hydrodynamic conditions i.e., increasing cross-flow velocity and turbulence at the membrane surface.

Due to the no or low hydraulic pressure used in FO, membrane fouling induced by ECP has less effect on water flux compared to pressure-driven membrane processes. In fact, ECP has been shown to play only a minor role in osmosis-driven membrane processes and it is not the main cause of the lower-than-expected water flux in these processes. The osmotic pressure profile on the FO membrane is shown in Figure 2.5. The internal concentration polarization (ICP) is non-ideal flux behaviour that occurs in the porous support layer of the FO membrane. ICP refers to the occurrence of CP layer within the porous layer of the membrane due to the inability of the solute to penetrate the dense selective layer of the membrane easily.

As stated, the solutes from the draw solution tend to accumulate on the porous layer and some even diffuse through the rejection layer, thereby resulting in reduced effective driving force and lowering permeate flux. Hence, the ICP cannot be fully eliminated as it naturally exists in any porous layer (Yang, Q. et al., 2009).

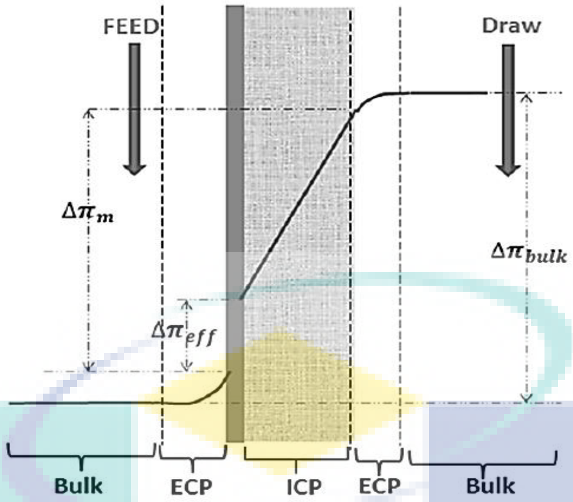

Figure 2.5 Osmotic pressure profile on ECP and ICP
Source:Yong, J. S. et al. (2012)

Experimental data proved that the reduction of water flux in FO is mainly caused by ICP (McCutcheon, J. R. et al., 2005). This is because the solutes are being retained in the porous layer and are unable to easily diffuse across the membrane. Hence, it will accumulate inside the porous layer which leads to the lowering of water flux. As this reaches the maximum accumulation inside the porous layer, the membrane will become fouled which is the major setback in FO commercialization (Boo, C. et al., 2013).

Several experiments have been performed to allow a better understanding of ICP and the various ways in which effects of ICP could be mitigated to boost FO performance. It has been observed that depending on the orientation of asymmetric membranes, two types of ICP can occur such as concentrative ICP and dilutive ICP. McCutcheon, J. R. and Elimelech M. (2006) in their research observed low water fluxes due to the occurrence of excessive ICP in the fabric layers and porous support of the RO membrane.

The concentration of ICP exists mainly in pressure retarded osmosis while dilutive ICP occurs in forward osmosis configuration. The term dilutive ICP arise when the permeate water dilutes the draw solution within the porous support of the membrane. In the mass transfer coefficient theory, this concept is referred to as the convection process (Chanukya, B. S. et al., 2013). The ICP effect exhibits a more severe impact on the reduction of water flux in the FO process than the ECP effect due to the fact that there is also an axial flow of a salt solution at the porous side of the asymmetric FO membrane (Chung, T.-S. et al., 2012).

2.3.2 Fouling

Fouling is a critical drawback for all membrane processes, as it causes a dramatic deterioration in membrane performance and subsequently increases operational and maintenance costs (Lee, J. et al., 2014). It is an inevitable phenomenon which results from deposition and adsorption of feed constituents such as organic and inorganic compounds, salts, colloids, and microorganisms on the membrane surface.

In general, membrane fouling is grouped into three categories: biofouling, organic fouling, and inorganic fouling (She, Q. H. et al., 2016). However, membrane fouling is less prominent in osmotically driven membrane processes compared to pressure-driven processes because the former processes operate with low or no hydraulic pressure (Lee, S. et al., 2010).

Biofouling is the result of biofilm formation through a series of fundamental steps, including reversible attachment of planktonic bacteria and ultimately the formation of a mature biofilm. Organic fouling is the adsorption of organic compounds from the feed stream onto the membrane surface. Organic fouling can be classified into, (1) rigid biopolymers such as large molecular weight polysaccharides, (2) fulvic compounds such as fulvic acid and humic acid and (3) flexible biopolymers such as proteins and organic molecules (molecular weight < 1000) (Boo, C. et al., 2013).

Organic contents are secreted by microorganisms in the membrane, which can adhere onto the membrane surfaces readily. These organic contents will then form extra–cellular polymeric substances and microbial cells matrix, fundamental structure of biofilms. Then biofilms will be formed and cause severe flux decline in the performance. Therefore, the elimination of organic fouling is fundamental to solve biofouling issues in the membrane technology.

On the other hand, inorganic fouling is the chemical or biological precipitation of inorganic solids onto the membrane surface. The mineral salts will be dragged towards the membrane surfaces and then accumulate in the concentration polarization layer of membranes.

Within the concentration polarization layer, the concentration of dissolved substance increases until it reaches labile region. Then nucleation on the membrane surface will occur spontaneously. Therefore, even with a relative low concentration of ions in the bulk feed solution, fouling will still occur in membrane filtration process.

2.3.3 Reverse salt diffusion

Reverse salt diffusion (RSD) is a situation whereby the material used as the draw solution diffuses back to the feed solution. The draw solution provides the required osmotic pressure but also becomes the key challenge in FO technology (Boo, C. et al., 2012). Reverse solute flux across the membrane from the draw to the feed solution seems to be unavoidable in FO due to the concentration gradient.

Hence, the selection of a draw solution is an important aspect of FO research. RSD is a significant component in any FO system because it can lead to the loss of draw solute, enhancement of concentration polarization, and the change of feedwater chemistry. All of these can significantly influence the membrane fouling behaviour (She, Q. H. et al., 2016).

In Figure 2.6, the movement of salt from the draw solution into the feed (J_s) leads to the loss of draw solutes which requires additional cost for replenishment of the draw solution (She, Q. H. et al., 2012a). The accumulation of draw solutes in the feed can change the feed solution composition. Unfortunately, this can have a detrimental effect on membrane fouling (Jamalludin, M. R. et al., 2016).

The water flux was (J_w) increased with the driving pressure nonlinearly before approaching a linear relation with the pressure. In addition, salt transport was highly dependent on the feed salt concentration.

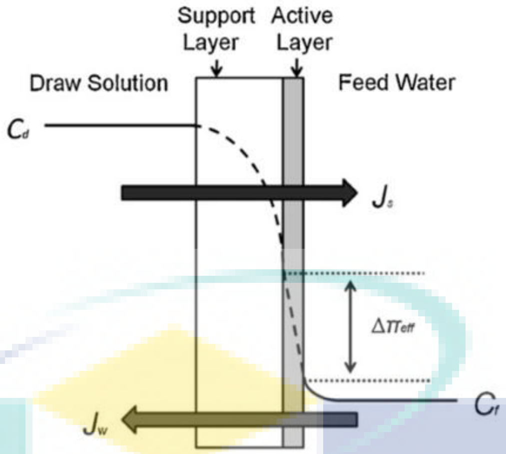

Figure 2.6 Salt concentration profile
Source: Xiao, D. et al. (2011)

In FO, the energy required to transport water across the membrane is negligible because of the absence of hydraulic pressure. Typically, selecting a semipermeable membrane and a suitable draw solution are crucial for attaining high FO system performance (Ge, Q. et al., 2013).

Recently, considerable efforts have focused on developing a novel draw solution to meet the following requirements: (1) high water flux; (2) low reverse salt diffusion; and (3) easy recovery of the diluted draw solution. However, the high reverse salt diffusion and high energy consumption involved in recovering the diluted draw solution are major challenges that restrict the development of FO (Chekli, L. et al., 2016).

2.4 FO membrane development

In the development of the FO membrane, there are various methods to make them an ideal candidate for designated separation processes. Researchers are focusing on improving transport properties as well as their chemical resistant. In general, the development of the FO membrane is oriented in reducing the internal concentration polarization and reverse solute diffusion as well as obtaining a highly selective active layer (Qasim, M. et al., 2015).

There are two routes to develop high-performance membrane namely bulk modification and surface modification (Zhao, C. et al., 2013). The bulk modification is often more straightforward because they can be applied in the preparation of polymer solution which is referred as the membrane fabrication.

The membrane development via bulk modification is not limited to phase inversion in fabricating the flat-sheet membrane and dry-wet spinning to produce hollow-fibre membrane. The latter modification only focuses on the surface of the membrane only. However, this type of membrane development is not limited to the active layer only. The research was also conducted on the support layer as well as a post-treatment method.

2.5 Bulk modification

2.5.1 Phase inversion

In a particular research, flat sheet membrane was fabricated using the phase inversion technique. This technique starts with the preparation of the dope solution. It is a combination of main polymer, additives and solvent. The dope formulation determines the intrinsic properties of the developed membrane (Ahmad, A. et al., 2005).

The polymer, additives and solvent were stirred until a homogeneous solution was formed. Normally, the additional material such as nanoparticles was added during the dope preparation. Then, the dope solution was poured into the glass plate and cast using pneumatic knife as shown in Figure 2.7.

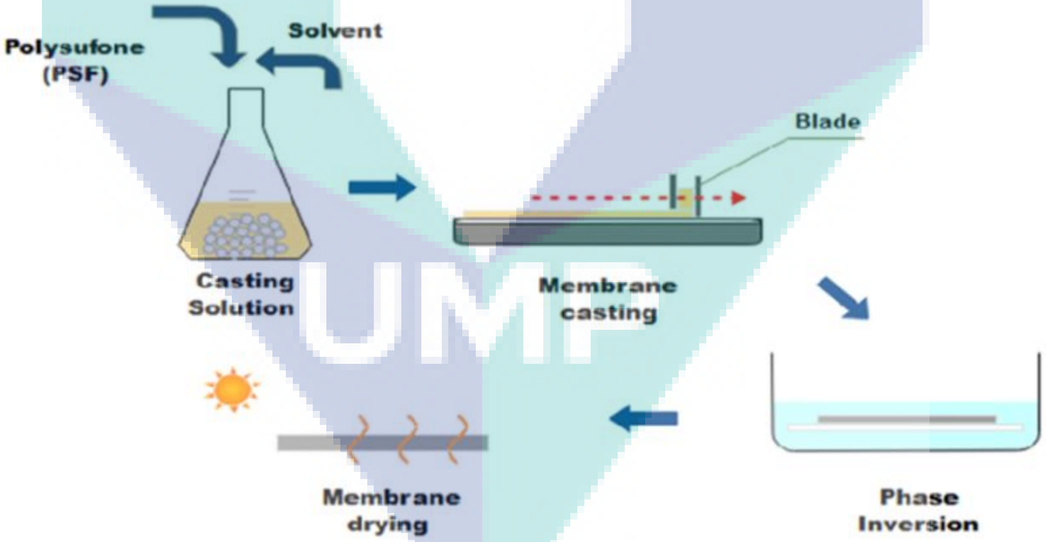

Figure 2.7 Membrane preparation via phase inversion
Source: Shaari, N. Z. K. et al. (2017)

The morphology of the fabricated membrane was affected by the thickness of the knife, the casting speed, time and temperature of the curing environment. At this stage, the nascent membrane was left for few second for evaporation process before immersed in the coagulation bath (curing process) to complete the phase inversion process. In the phase inversion technique, the backing layer can be varied from no backing layer, woven layer and a non-woven layer.

Phase inversion has been introduced in the year 1973 to form an asymmetrical membrane (So, M. et al., 1973). The membrane structure contains a dense skin or active layer on top of a thick porous support layer shown in Figure 2.8. The active layer was attributed to rapid solvent evaporation during the cast and subsequent solvent outflow to surrounding water when immersing the nascent membrane to coagulant bath (Zhang, S. et al., 2010).

The porous layer or the bottom layer is formed due to the delayed de-mixing dominates in the membrane bulk and results in a fully porous inner structure. Currently, this fabrication technique has dominated most of the production of flat sheet membrane.

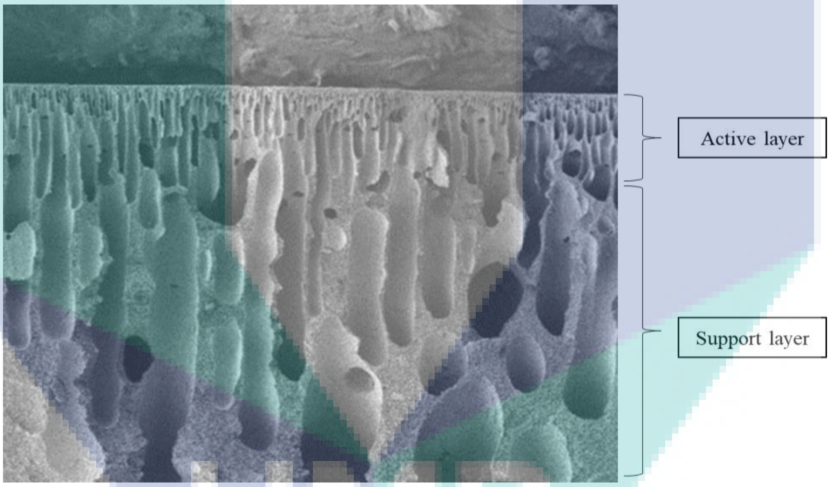

Figure 2.8 Asymmetric membrane structure of asymmetric flat sheet membrane.
Source: Liu, Y. A. et al. (2016)

2.5.2 Dry-wet spinning

Fabrication of hollow fibre (HF) membrane has been conducted using the dry-wet spinning technique. Usually, the dope solution in this membrane fabrication utilizes the same protocol as in phase inversion. A key component in selecting the HF membrane is the high packing density per unit of the membrane module and no spacer is required compared to flat sheet (Wang, R. et al., 2010).

Moreover, it is built with a self-mechanical support which allows the membrane to be back-flushed for liquid separation and it has a good flexibility and ease of handling during module fabrication and system operation (Baker, R. W., 2004). The process of fabricating the HF membrane is shown in Figure 2.9.

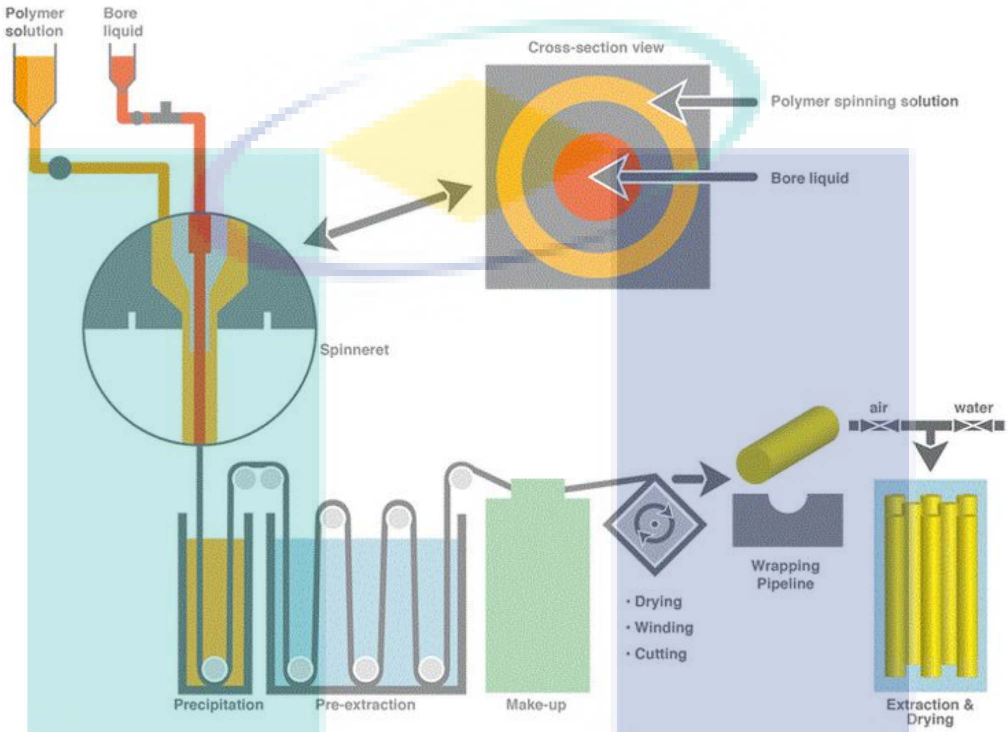

Figure 2.9 Fabrication of hollow fibre membrane

Source: Membrana GmbH (2015)

Although both the flat sheet membrane and hollow fibre membrane configurations have been used commercially, HF membrane has more advantages owing to their large specific membrane area and easy module construction (Shibuya, M. et al., 2015). HF membranes with a smaller diameter can enable the fabrication of modules with larger effective membrane area.

However, the development of HF membrane is very tricky because there are strict rules and regulation to be followed in order to fabricate the state-of-the-art membrane. Specifically, fabricating the hollow fibre requires specific figures in the outer channel, inner dope composition, bore fluid, outer flowrate, inner dope flowrate, air gap, take-up speed, external coagulant and dimension of spinneret (Zhu, W. P. et al., 2015).

2.6 Surface modification

2.6.1 Interfacial polymerization

Interfacial polymerization (IP) is a process of adding a new layer of a functional group onto the membrane, surface using at least two (2) different types of homopolymer or polymer. Normally, the product of IP is called the thin film composite (TFC) membrane. Hence, thin film composite (TFC) membrane is generally developed via polymerization which takes place at the interface of the two liquids which are insoluble in each other. The process of IP consists of a sequence of steps shown in Figure 2.10.

The first step is the preparation of the support layer or substrate via immersing it into an aqueous solution containing the first monomer namely the polyethylemine (PEI). The substrate is then immersed in the second solution either the cyanuric chloride (CC) or trimesoyl chloride (TMC) according to the pre-determined time. The interface is created between two immiscible solutions. During the IP process, the monomer travels through the interface and react with the other monomer to form a new polymer on the substrate's surface.

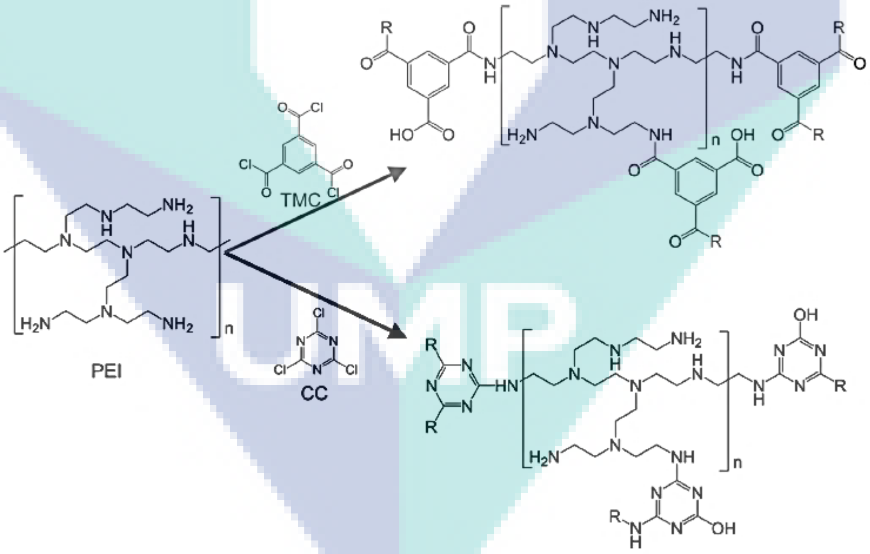

Figure 2.10 The development of polyamine via interfacial polymerization
Source: Lee, K. P. et al. (2015)

To produce a high-performance membrane, there are several parameters that can be manipulated during IP processes such as monomer selection, monomer concentration and reaction time (Lau, W. J. & Ismail A. F., 2011). In general, high monomer concentration, high reaction rates, as well as longer polymerization time often results in thicker layers with high rejection rates, but with a lower flux. Abu Seman, M. N. et al. (2010b) have developed a polyamide (PA) layer using trimesoyl chloride (TMC) and bisphenol A (BPA). They observed that water flux decreased as the reaction time and monomer concentration were both increased. They concluded that formation of a dense layer of polyester on the NFPES10 membrane surface affects the membrane rejection towards humic acid.

Likewise, Wei, J. et al. (2011a) have developed a polyamide layer from m-phenylenediamine (MPD) and trimesoyl chloride (TMC) using the IP method for FO application. The result of their study showed that a strong trade-off between water permeability and solute permeability was observed by the increase in monomer concentration.

Another interesting research has been conducted by Han, G. et al. (2012) in the modification of the membrane using interfacial polymerization method. The active layer of the polysulfone was pre-treated with a novel bio-inspired polymer polydopamine (PDA) through the oxidant-induced dopamine polymerization. Then, the polyamide layer was added via interfacial polymerization on top of the pre-treated membrane.

Specifically, PDA was added to improve the fouling resistance by increasing the hydrophilicity of the modified membrane. The result of their study revealed that the fabricated membranes possesses high hydrophilic tendency despite having smaller pore sizes and a narrower pore-wall inside the substrate layer. This resulted into an increase in water permeability, and salt rejection.

As can be seen from Table 2.3, the development of the FO membrane via IP is applicable in various applications. In conclusion, the surface modification via IP process is an effective to modify the membrane performance as the monomers needs to be carefully selected. The product of IP process will have significant changes including outstanding permeability, selectivity and high fouling resistance (Wang, Y. Q. et al., 2016).

Table 2.3 Development of FO membrane via interfacial polymerization

No	Method	Material	Findings	References
1	Phase inversion and dual interfacial polymerization	Jeffamine into nascent polyamide on polysulfone (PS)	Fabrication of FO membranes whose enhanced fouling resistance permits operation at high water fluxes over extended periods of time.	(Lu, X. et al., 2013)
2	Phase inversion and interfacial polymerization	Silica nanoparticle into polyamide on polysulfone (PS)	The silica loading improves the water flux and salt rejection	(Niksefat, N. et al., 2014)
3	Phase inversion and interfacial polymerization	Polyamide on blended polyethersulfone (PES)/polysulfone (PS)	Slow-fast phase separation improves the morphology, pore structure, hydrophilicity and mechanical strength of the substrate	(Sun, Y. N. et al., 2014)
4	Phase inversion and interfacial polymerization	Polyamide on blended polysulfone (PS)/sulfonated polyphenylene oxide (SPPO)	Enhancing the internal osmotic pressure (IOP) to reduce internal concentration polarization (ICP)	(Zhou, Z. Z. et al., 2014)
5	Interfacial polymerization and post surface treatment	Trimesoyl chloride (TMC)/oxalic acid on polyamide/polyethersulfone (PES)	Hydrophilic solvent and oxidation resistance improve the water flux, salt rejection and reverse salt diffusion.	(Jia, Q. B. et al., 2015)
6	Phase inversion and interfacial polymerization	Halloysite nanotubes (HNTs) into polysulfone (PS)	Addition of HNTs improves the porosity, mean pore size, and hydrophilicity of the composite substrate	(Ghanbari, M. et al., 2016)
7	Phase inversion of electrospun nanofiber support and interfacial polymerization	Polyamide of Nylon 6,6 electrospun PVDF fibre	Non-swelling hydrophobic fiber without negatively impacting the mechanical properties of the material	(Huang, L. W. et al., 2016)

2.6.2 Layer-by-layer technique

Layer-by-layer (LbL) technique is a chemical modification technique of adding a thin layer of water-soluble polymers, surfactants, or polyelectrolytes from solution by physical adsorption to the membrane surface (Xu, G. R. et al., 2015). Hence, the LbL assembly involves the sequential deposition of cationic and anionic nanostructures on the support, to fabricate thin layered membranes in the nanoscale range as shown in Figure 2.11. The dried hollow fibres are usually immersed in the polyanion (PSS) and polycation (PAH) solutions alternatively to achieve the desired number of layers. Thus, this technique offers an easy, facile, robust reproducibility and flexibility for modifying modification (Ng, L. Y. et al., 2013c).

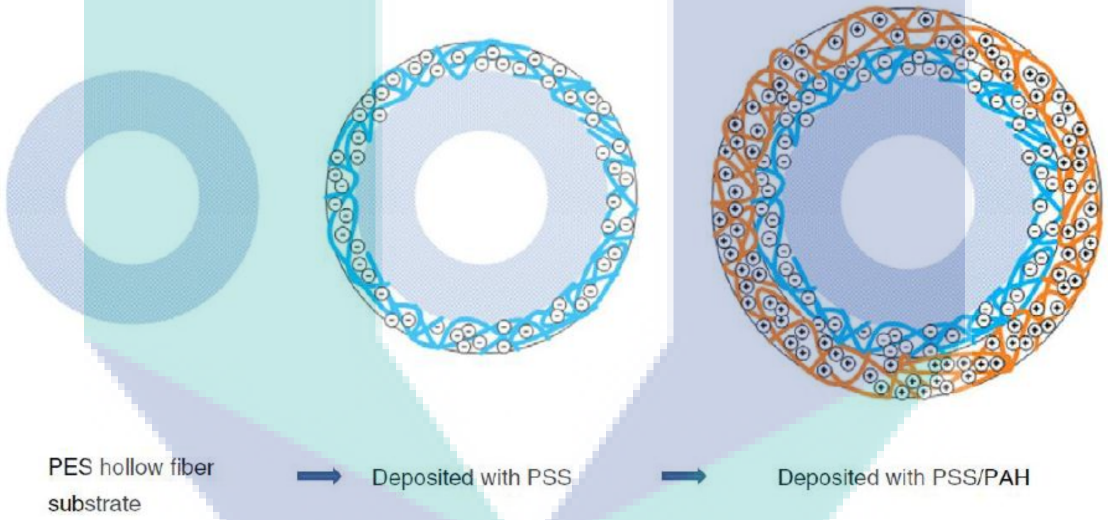

Figure 2.11 Schematic drawing of LbL deposition on hollow fibre membrane
Source: Liu, C. et al. (2013)

Shi, H. Y. et al. (2016) have developed a dual layer of hollow fibre membrane by coating polyvinylidene fluoride (PVDF) membrane with dopamine, with a subsequent grafting with polyethyleneimine under quaternization processes. The modification improved hydrophilicity despite narrowing the average pore sizes.

Unsurprisingly, Sanyal, O. et al. (2015) have identified that the thickness of the coating directly affects the permeability but is subjected to the selection of coating materials used. In his research, the addition of polyallylamine hydrochloride (PAH) and polyacrylic acid (PAA) into NF membrane was observed to provide a better anti-fouling only under alkaline conditions, but revealed severe fouling at the acidic conditions.

Notwithstanding, the main problem associated with the surface coating using a coating technique is the instability of the coated layer (Li, X. F. et al., 2010). Specifically, the fabricated layer could be washed away along the operation and cleaning processes because of the relatively weak physical adsorption interaction between the membrane and the coated layer.

In an attempt to proffer a solution to this, chemical treatments or redox graftings such as sulfonation or crosslinking have been performed on the membrane surface to anchor the coated layer (Liu, F. et al., 2011). The grafting method was used to immobilize the functional chains, brushes or layers on the membrane surface through covalent bonding interaction.

In general, membranes fabricated via LbL offers a wide range of fabrication options. However, it has been observed that an increase in polyelectrolytes layers enhances the LbL membranes selectivity but decreases their water permeability and reverse salt flux (Qiu, C. Q. et al., 2011). Hence, it may be inferred that LbL assembly of polyelectrolytes is a flexible technique which can be used to fabricate FO membranes dependent on applications (Duong, P. H. H. et al., 2013).

Table 2.4 shows the development of the FO membrane via layer-by-layer technique with the key findings in the respective study. In conclusion, the utilization of this LbL technique improve the permeability of the membranes, essentially creating molecular, hydrophilic tunnels across the membrane matrix which water preferentially passes through, while the greater negative charge on the nanoparticle pore walls enhance ion exclusion, and thus maintain salt rejection (Liu, C. et al., 2015b).

Table 2.4 Development of FO membrane via layer by layer

No	Monomers	Support	Findings	References
1	Polyallylamine hydrochloride (PAH) and polysodium 4-styrene-sulfonate (PSS) with glutaraldehyde (GA)	Polyacrylonitrile (PAN)	Increasing LbL layers and introducing crosslinking enhanced the membrane rejection but reduced the water permeability of the rejection layer	(Qiu, C. Q. et al., 2011)
2	Polyallylamine hydrochloride (PAH) and polysodium 4-styrene-sulfonate (PSS)	Polyacrylonitrile (PAN)	Double-skinned xLbL performs better than single skinned for antifouling performance	(Qi, S. et al., 2012)
3	Poly-diallyl-dimethylammonium chloride (PDADMAC) and polystyrene sulfonate (PSS)	Polysulfone (PS)	The deposition of the first and second bilayer was crucial to the membrane integrity	(Su, B. W. et al., 2012)
4	Polyallylamine hydrochloride (PAH) and polysodium 4-styrene-sulfonate (PSS) with glutaraldehyde (GA)	Polyacrylonitrile (PAN)	Fabrication and deposition of LBL influenced by the salt concentration and deposition time	(Duong, P. H. H. et al., 2013)
5	Sodium carboxymethyl cellulose (CMCNa) and polyethylenimine (PEI)	Polypropylene	At neutral pH, modified membrane exhibit salt rejection order of $MgCl_2$> $CaCl_2$> KCl > NaCl >$MgSO_4$>Na_2SO_4	(Chen, Q. et al., 2015)
6	Polyethyleneimine (PEI) and polyacrylic acid (PAA)	Polyacrylonitrile (PAN)	The stability and membrane performance is depending on the ionic strength and environment	(Kwon, S. B. et al., 2015)
7	Polyallylamine hydrochloride (PAH) and polysodium 4-styrene-sulfonate (PSS) with glutaraldehyde (GA)	Polyethersulfone (PES)	Crosslinking agent tighten the membrane surface pores with increased hydrophilicity while the membrane surface charge was reduced	(Liu, C. et al., 2015a)
8	Polyallylamine hydrochloride (PAH) and polysodium 4-styrene-sulfonate (PSS)	Polyethersulfone (PES)	In the hollow fibre membrane, the inner surface is more suitable for the formation of the selective layer compared to the outer surface	(Liu, C. et al., 2015b)

2.6.3 Incorporating nanoparticle

Incorporation of various nanoscale materials into polymer matrices is known to affect membrane structure and properties. Most studies found that the membrane surface hydrophilicity was enhanced by incorporating hydrophilic nanomaterial that was partially exposed on the membrane surface (Zhu, W. P. et al., 2015). However, in the membrane development, the incorporation of the nanoparticle can be either through bulk modification or surface modification.

The idea of incorporating a nanoparticle into the membrane is to increase the performance of membrane technology. The additions of nano-scale material have gained a momentum in many areas of science and technology due to their remarkable changes in membrane properties (Ng, L. Y. et al., 2013b).

Various materials can be added such as polysulfobetaine methacrylate (polySBMA), polymerization of oligo ethylene glycol methacrylates (polyOEGMA) and carbon nanofiber (CNF). These have been observed to result into significant changes in the membrane properties such as morphology, hydrophilicity and FO performance as well as antifouling properties (Ren, P. F. et al., 2015).

Apart from hydrophilic nanomaterial, inorganic nanoparticles such as boehmite have also been reported to affect the physical and chemical properties of the membrane matrix (Zirehpour, A. et al., 2015).

The nanoparticles were added during the dope preparation process. The addition affects the porosity and pore size of membranes, and subsequently, change their water permeability and solute rejection. Moghimifar, V. et al. (2014) have discovered that following the addition of titanium dioxide (TiO_2), the surface pore size increased initially, but decreased with further loading. Ng, L. Y. et al. (2013b) have produced an excellent review paper on polymeric membranes incorporated with metal and metal oxide nanoparticles.

Based on information gathered from these literatures, it can be inferred that incorporating Nano-scale material into the polymeric membrane is an endless journey. The suitability of material and polymeric membrane will therefore depend on the manipulated parameter as the application will be the benefactor.

2.6.4 Plasma treatment

Plasma is the fourth state of matter after solid, liquid, and gaseous states. It is the gaseous cloud of charged particles. As such, plasma treatment works by the ionization process to create free electrons and ions which are carried via a gaseous medium. Thus, it requires the use of non-polymerizable gases such as argon (AR), helium (He) and oxygen (O_2) (Xu, W.-T. et al., 2015). As illustrated in Figure 2.12 plasma t plasma induced vapor phase graft polymerization (PIVPGP) consists of highly excited species that can alter the physicochemical properties of polymeric membrane surfaces. It can modify the surface layer between 1-10 nm of the material (Liu, L. X. et al., 2016).

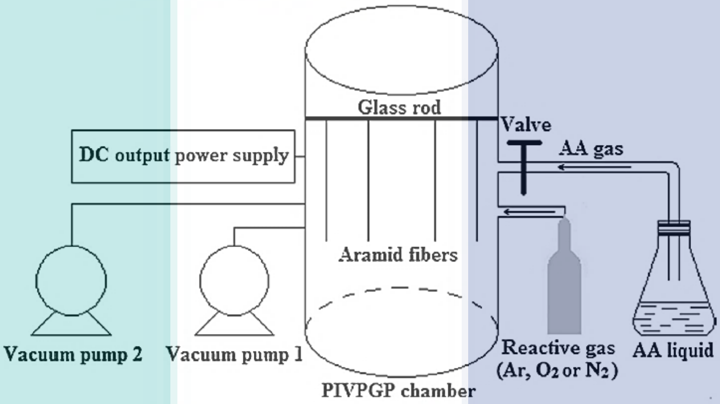

Figure 2.12 Schematic diagram of PIVPGP acrylic acid system
Source: Wang, C. X. et al. (2015)

Due to its low penetration depth, plasma can be used to improve polymer surface properties such as wettability, permeability, conductivity, adhesion or biocompatibility while preserving bulk properties of the material. However, the morphology and chemical changes on the modified sample may be affected by the type of precursor gas, applied microwave or radiofrequency (RF) power, treatment time, the distance between the plasma source and the surface, as well as the system pressure (Torres, J. G. et al., 2014).

Plasma treatment is conducted using a plasma generator in a vacuum chamber. A piece of sample is placed in a plasma chamber with a fixed distance from the electrode. The fluorochemicals are often used as hydrophobic monomers because of their low surface energy. Previously, tetrafluoromethane (CF_4) was mainly in the plasma technique. However, further investigation has impacted the plasma treatment as it was observed that the gas is not only expensive but also harmful to the environment (Xu, W.-T. et al., 2015).

The major limitation to plasma treatment is the temporal nature of the modified surface. It has been hypothesized that polar functional groups at the surface can reorient from the topmost layer or migrate due to segmental diffusion toward the underlying subsurface region (Xu, W.-T. et al., 2015). This can then result in the gradual deterioration of surface hydrophilicity. This process, called “ageing” or “hydrophobic recovery”, is driven by minimization of the free energy of the interface between the polymer surface and surrounding medium.

This is further favoured by the flexibility of polymer chains, which allows for rearrangement. To date, no surface modification via plasma treatment has been reported in the FO application. In fact, the number of publications of this membrane technology are limited as presented in Table 2.5.

Table 2.5 Plasma treatment

No	Chemical	Material	Technique	References
1	Perfluorodecyl methacrylate (F8)	Polyacrylonitrile (PAN)	Surface coating induces Ar gas in a plasma chamber	(Liu, L. X. et al., 2016)
2	Silane coupling agent	Polyvinylidene fluoride (PVDF)	Grafting of silane coupling agent after plasma flow irradiation	(Xu, W.-T. et al., 2015)
3	Acrylic acid	Aramid fibre	Plasma-induced vapour phase graft polymerization	(Wang, C. X. et al., 2015)
4	Acrylic acid	Cellulosic substrate	Atmospheric pressure plasma enhanced chemical vapor deposition	(Torres, J. G. et al., 2014)
5	Titanium oxide (TiO_2)	Polyethersulfone (PES)	Corona air plasma and coating	(Moghimifar, V. et al., 2014)
6	Polymethacrylic acid (PMAA)	Polysulfone (PS)	Atmospheric pressure plasma-induced graft polymerization	(Kim, S. M., 2013)
7	Acrylic acid (AA)	Poly p-phenylene benzobisoxazole (PBO) fibre	Oxygen plasma induced vapour phase grafting	(Song, B. et al., 2012)

2.7 Ultraviolet photografting

Ultraviolet (UV) photografting has attracted various researchers as it provides advantages in simplicity, cost, and breadth of application (X, W. et al., 2006). Details of previous reports on surface modification via UV-photografting is presented in Table 2.6. As can be seen, this grafting technology has been widely used in various industries. In the coating industry, the UV-light provides low energy consumption, low emission, low capital investment, low space consumption and marginal substrate heating (Ng, L. Y. et al., 2013a). In addition, the fabrication via UV photografting produces an integral selective layer due to a strong chemical bond to the substrate.

This helps to provide sufficient mechanical stability under relatively high operating pressure and also helps to guide against delamination or leaching of the grafted chains (Zhong, P. S. et al., 2012). However, there is no report on the incorporation of this technique into FO technology.

Grafting itself is a process of adding new properties of functionalities into a polymer. Hence, the term grafting may be simply put as the developed covalent bond between the carbon-carbon bond between a monomer, or a polymer and a substrate (Ng, L. T. et al., 2001).

As stated, it provides long-term stability and avoidance of delamination or leaching of the grafted chains as in physically coated polymer chains. In general, grafting can be classified into 'grafting-to' and 'grafting-from' as illustrated in Figure 2.13.

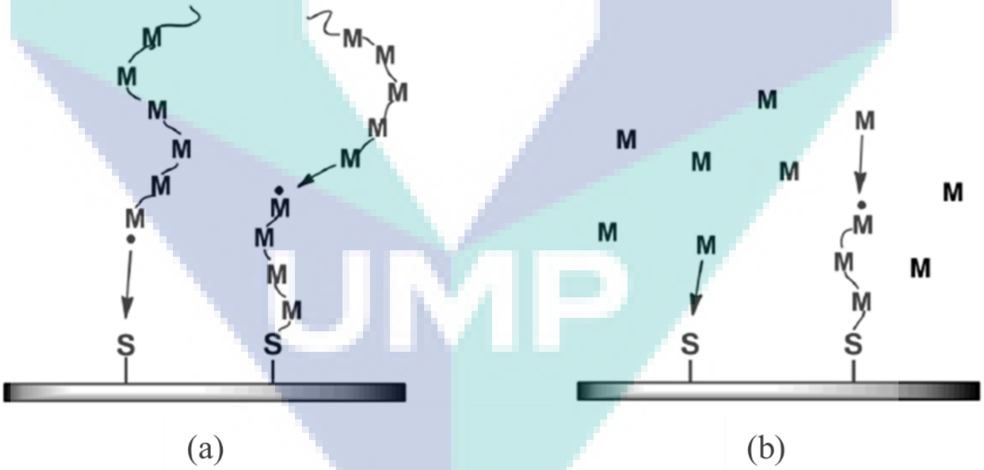

Figure 2.13 Routes to modify a polymer (a) "Grafting to" and (b) "Grafting from"
Source: Zhao, B. and Brittain W. J. (2000)

In the 'grafting-to' methods, polymer chains that have reactive groups at the end or on the side chains are covalently coupled to the membrane surface. On the other hand, 'grafting-from' has to do with monomers which are polymerized using an active site at the membrane surface, followed by propagation, and then chain termination. As such, this often involves the use of an initiator (Van der Bruggen, B., 2009b). In this study, no initiator was used as the PES membrane can form graft polymerization via “grafting from” method. Detailed property of the PES is provided in the subsequent sections of this thesis.

Generally, surface modification via UV-photografting has four factors that may affect the performance of the modified membrane. The first factor is grafting time, which is the time required for a membrane to absorb the energy from UV light to form free radicals (Abuhabib, A. A. et al., 2012; Garcia-Ivars, J. et al., 2016).

The second factor is monomer concentration, where the strength of the functional group of selected monomers dictate the operating conditions including pH, reactivity, and valence (Abu Seman, M. N. et al., 2010a; Abu Seman, M. N. et al., 2012).

The third factor is UV intensity, which is the energy required to initiate the grafting process by opening polymer chains towards the monomer solution (Peeva, P. D. et al., 2010; Pieracci, J. et al., 2002). The fourth factor is monomer selection, which has to do with monomer suitability for the selected application (Rahimpour, A., 2011; Taniguchi, M. & Belfort G., 2004).

In conclusion, the surface modification via UV-photografting has distinct advantages in simplicity, cost and breadth of application. This simple method increases membrane surface wettability and shifts the membrane pore size distribution to smaller sizes.

The results of previous studies suggested that the selective UV excitation of a photo-initiator adsorbed onto the polymer surface causes a heterogeneous hydrogen abstraction and subsequent initiation by polymer mechanisms for polymer surface modification (Wei, X. et al., 2006).

Table 2.6 Development of membrane via UV-photografting

No	Material	Monomer	UV-intensity	Findings	References
1	Polyethersulfone (PES)	N-vinyl-2-pyrrolidine (NVP), 2-acrylamidoglycolic acid monohydrate (AAG) and 2-acrylamido-2-methyl-propane sulfonic acid (AAP).	254 nm	UV irradiation of PES membranes results in competition between crosslinking and chain scission processes.	(Kaeselev, B. et al., 2002)
2	Polysulfone (PS)	Methacrylatoethyl trimethyl ammonium chloride (DMC)	300 nm	The grafting degree (DG) increased with increasing the monomer concentration, prolonging the irradiation time and reducing the irradiation distance.	(Deng, H. Y. et al., 2011)
3	Polyethersulfone (PES)	Acrylic acid (AA), 2-hydroxyethylmethacrylate (HEMA), 1,3-phenylenediamine (mPDA) and ethylene diamine (EDA)	259 nm	The pure water flux and milk water permeation of the membranes were declined by UV photografting, but the protein rejection was improved.	(Rahimpour, A., 2011)
4	Polyether ether-ketone (PEEK)	Acrylamide(AAm)	365 nm	The increases in irradiation time and monomer concentration, contact angles decrease to as low as 30°, demonstrating a significant improvement of surface hydrophilicity.	(Chen, R. C. et al., 2012)
5	Polyethersulfone (PES)	Acrylic acid (AA) and N-vinylpyrrolidone (NVP)	365 nm	The selection of a monomer concentration and UV-irradiation time are crucial parts for modification because monomer cross-linking and chain scission of polymer backbone are two parallel competitive processes in UV-irradiation technique.	(Abu Seman, M. N. et al., 2012)

Table 2.6 Continued

No	**Material**	**Monomer**	**UV-intensity**	**Findings**	**References**
6	Sulfonated polyphenylenesulfone (sPPSU)	2-methacryloyloxy ethyl trimethyl ammonium chloride and diallyl dimethyl ammonium chloride	254 nm	The gradual transition from a dense to porous substructure with no sign of delamination shows the strong covalent chemical bonding between the polymer of the substrate and the vinyl monomers.	(Zhong, P. S. et al., 2012)
7	Polyethersulfone (PES)	Acrylic acid (AA) on polyamide layer	300 nm	Denser and compressed skin layer forms on the thin layer surface by increasing of AA concentration and UV irradiation time.	(Mansourpanah, Y. & Habili E. M., 2013)
8	Sulfonated-polysulfone (SPS)	Methacrylic acid (MAA)	365 nm	Optimized membrane using response surface methodology (RSM) with monomer concentration and grafting time as factors. Responses were water permeability and rejection for humic acid	(Chung, Y. T. et al., 2014)
9	Polyethersulfone (PES)	Polyethyleneglycol/ aluminium oxide nanoparticles	300 nm	Two nanosized hydrophilic compounds displayed superior antifouling properties and desirable performance	(Garcia-Ivars, J. et al., 2014)
10	Polyethersulfone (PES)	Aluminium oxide (Al_2O_3) nanoparticles and organic polyethene glycol (PEG).	300 nm	Modified membrane influenced by the concentration, irradiation time and the pH of the additive solution	(Garcia-Ivars, J. et al., 2016)

2.7.1 Dip method

In the modification of polymer via UV-photografting, there are two notable approaches namely the dip method and immersion method. Both methods have their distinctive advantages and disadvantages. Pieracci, J. et al. (2000) have conducted a research, comparing both modification techniques. It was reported that both modification techniques sharply decreased membrane permeability at high monomer concentrations due to pore blockage by grafted polymer chains.

Dip method is a process of modifying the membrane via UV-photografting in an open air. In this method, the membrane is initially immersed in the monomer solution under gentle stirring. The whole membrane layer is ensured to soak in the monomer solution at a pre-determined time such as 15 minutes, to ensure that the membrane is fully wet upon modification.

After this, the membrane will be kept in a vertical position so as to remove any excess monomer solution on the membrane surface. Subsequently, UV-light is allowed to illuminate the membrane samples at a predetermined time, after which the membranes are taken out and rinsed with deionized water to remove the unreacted compounds. Finally, the modified membranes may be stored for at least one-day, prior to its usage. Table 2.7 presents some of the reported surface modifications via the dip method.

Table 2.7 Membrane grafting using the dip method

No	Membrane material	Monomer (s)	Wavelength	Configuration	References
1	Polypropylene (PP)	Methyl methacrylate (MMA), hydroxyethyl methacrylate (HEMA), glycidyl methacrylate (GMA), and polyethylene glycol methacrylate (OEGMA)	50 W (Lamp)	Three-cycle dead-end filter cell	(Meng, J. Q. et al., 2014)
2	Sulfonated polyphenylenesulfone (sPPSU)	2-(methacryloyloxy)ethyl trimethyl ammonium chloride and diallyldimethylammonium chloride	254 nm (UV)	Dead-end filtration cell	(Zhong, P. S. et al., 2012)
3	Polyethersulfone (PES)	Acrylic acid (AA) & hydroxyethyl methacrylate (HEMA)	259 nm (UV)	Cross-flow filtration rig	(Rahimpour, A., 2011)
4	Polypropylene (PP)	Polysulfobetaine methacrylate (polySBMA)	300 W (UV)	Dead-end stirred-cell	(Yang, Y. F. et al., 2010)
5	Polyethersulfone (PES)	N-vinyl-2-pyrrolidine (NVP)	365 nm (UV)	Cross-flow filtration cell	(Khayet, M. et al., 2010)
6	Polyvinylidene fluoride (PVDF)	Acrylic acid (AA) & hydroxyethyl methacrylate (HEMA), 2,4-phenylenediamine (PDA) and ethylene diamine (EDA)	160 W (UV)	Cross-flow filtration cell	(Rahimpour, A. et al., 2009)
7	Polysulfone (PS)	Acrylic acid (AA)	295 nm (UV)	Cross-flow filtration cell	(Bequet, S. et al., 2002)

2.7.2 Immersion method

The immerse method is a process of modifying the membrane while it is immersed in the monomer solution. This immersion technique is applied to ensure the monomer is fully in-contact or to ensure wettability of the membrane. In order to reduce the time consumption during membrane fabrication, this study applies the procedure taken by Zhong, P. S. et al. (2012) which takes about 15 min.

However, the shorter immersion time (5 min) recorded by Garcia-Ivars, J. et al. (2016) for flat sheet ultrafiltration polyethersulfone membrane was used. It is worthy of note that the immersion method requires a larger amount of monomer and might be less adaptable in a continuous process or on an industrial scale (Hilal, N. et al., 2015). Table 2.8 highlights some of the surface modifications via the immersion method.

Table 2.8 Membrane grafting using the immerse method

No	Membrane material	Monomer (s)	Wavelength	Mode of operation	References
1	Polypropylene (PP)	Polysulfobetaine methacrylate (polySBMA) & polyethylene glycol methacrylate (OEGMA)	300 nm (UV)	Dead end filtration system	(Ren, P. F. et al., 2015)
2	Polyethersulfone (PES)	Aluminium oxide (Al_2O_3) nanoparticles and organic polyethylene glycol (PEG)	300 nm (UV)	Cross-flow filtration cell	(Garcia-Ivars, J. et al., 2016)
3	Polyethersulfone (PES)	Polyethylene glycol diglycidyl ether (PEGDE), 1,3,5-benzene tricarbonyl trichloride (TMC) & m-phenylene diamine (MPD)	300 nm (UV)	Cross-flow filtration cell	(Castrillon, S. R. V. et al., 2014)
4	Polyethersulfone (PES)	Acrylic acid (AA)	160 W (UV)	Cross-flow filtration cell	(Mansourpanah, Y. & Habili E. M., 2013)
5	Polyethersulfone (PES)	Acrylic acid (AA) & N-vinyl-2-pyrrolidine (NVP)	365 nm (UV)	Cross-flow filtration cell	(Abu Seman, M. N. et al., 2012)
6	Polysulfone (PS)	Methacrylatoethyl trimethyl ammonium chloride (DMC)	300 nm (UV)	Cross-flow filtration cell	(Deng, H. Y. et al., 2011)
7	Polyacrylonitrile (PAN)	1,3,5-benzene tricarbonyl trichloride (TMC) & m-phenylene diamine (MPD)	300 nm (UV)	Stirred-cell filtration system	(Klaysom, C. et al., 2013)

2.8 Polyethersulfone

Polyethersulfone (PES) is one of the commonly used polymers in the fabrication of microfiltration (MF), ultrafiltration (UF) and nanofiltration (NF) membranes. The main advantages of this hydrophobic material includes its high mechanical, chemical and thermal stability due to the existence of aromatic hydrocarbon groups in its structure (Ng, L. Y. et al., 2013a).

The molecular structure of PES is shown in Figure 2.14. Generally, PES has a good oxidative, thermal, and hydrolytic stability, as well as good mechanical and film-forming properties. As such, it has been widely applied in the fields of artificial organs and medical devices.

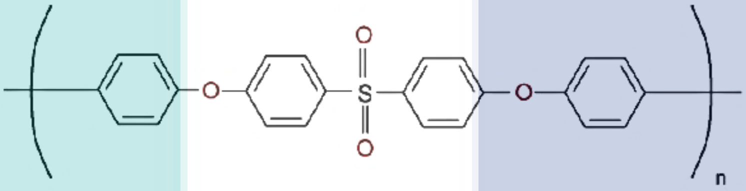

Figure 2.14 Molecular structure of polyethersulfone
Source: Abu Seman, M. N. et al. (2010a)

Notably, this polymer can generate several sites on the surface and on the pore walls because it is a photosensitive material (Li, S.-S. et al., 2016). However, besides PES, polyarylsulfone (PAS) also has the photosensitive characteristic as reported by Yamagishi et al. (1995). Therefore, it is expected that the same modification method can be applied to this polymer without requiring any photoinitiator to form active sites.

Since the PES polymer is a thermoplastic polymer and typically amorphous in nature, the modification can be carried out in several ways ranging from physical to chemical modification processes (Nair et al., 2001). In fact, it has been used in numerous applications such as in biomedical fields for blood purification specifically in hemodialysis and plasma collection (Barzin, J. et al., 2004). Reports have shown that PES presents outstanding oxidative, thermal and hydrolytic stability as well as good mechanical property. Notwithstanding, despite its wide use and its outstanding properties, it has been observed that the hydrophobic nature of the membrane tends to contribute to the membrane fouling as reviewed by Van Der Bruggen, B. (2009a).

Table 2.9 presents some of the notable application of PES polymer in various membrane applications. As can be seen from the table, all range of PES membrane namely the MF, UF and NF membranes were subjected to different modification technique and applications. However, it is interesting to note that the development of PES material in FO technology is on the increase.

Most of the current research focuses on conventional fabrication methods such as phase inversion, interfacial polymerization and dry-wet spinning technology. In fact, recently, PES has been highly cited in the literature with various modification processes. This is evidenced by the different reviews on this material such as the ones by Ng, L. Y. et al. (2017) and Zhao, C. et al. (2013) In general, PES has been fabricated, applied and modified for microfiltration, ultrafiltration, nanofiltration as well as forward osmosis purposes as presented in Table 2.9.

Table 2.9 The application of polyethersulfone in membrane technology

No	Type of membrane	Modification technique	Application	References
1	Microfiltration	Phase inversion	pH sensitivity and ion-exchange capacity	(Wei, Q. et al., 2009)
2	Microfiltration	Corona irradiation	Microfiltration	(Zhu, L. P. et al., 2007)
3	Microfiltration	γ-ray irradiation	pH dependant membrane	(Deng, B. et al., 2009)
4	Ultrafiltration	Electrophoresis-UV	Natural organic matter (NOM) removal	(X, W. et al., 2006)
5	Ultrafiltration	Corona-plasma	Ultrafiltration	(Moghimifar, V. et al., 2014)
6	Ultrafiltration	Interfacial polymerization	Ion exchange capacity (IEC)	(Wei, Q. et al., 2009)
7	Nanofiltration	Interfacial polymerization	Nanofiltration	(Vatanpour, V. et al., 2011)
8	Nanofiltration	Redox and sulfonation	Nanofiltration	(Van der Bruggen, B., 2009b)
9	Nanofiltration	Polyelectrolyte	Nanofiltration	(Ng, L. Y. et al., 2014)
10	Dual hollow fibre	Triple orifice spinneret	Forward osmosis	(Setiawan, L. et al., 2012)
11	Nanoporous	Interfacial polymerization	Forward osmosis	(Yu, Y. et al., 2011)
12	Nanocomposite FO	Electrospinning	Forward osmosis	(Song, X. et al., 2011)
13	PES/carbon nanotube	Phase inversion	Forward osmosis	(Wang, Y. Q. et al., 2013)
14	Thin film composite	Interfacial polymerization	Forward osmosis	(Widjojo, N. et al., 2011)
15	Thin film composite	Interfacial polymerization	Forward osmosis	(Jia, Q. et al., 2014)
16	Hollow fibre	Interfacial polymerization	Forward osmosis	(Chou, S. R. et al., 2010)
17	Hollow fibre	Polyelectrolyte	Forward osmosis	(Setiawan, L. et al., 2013)
18	TFC-Hollow fibre	Interfacial polymerization	Forward osmosis	(Wang, R. et al., 2010)

2.9 Monomer selection

It is well known that the selected monomer can affect the whole membrane properties such as hydrophilicity and hydrophobic. Also, the reactivity of monomers depends on various factors, viz. polar and steric nature, swell ability of backbone in the presence of the monomers and concentration of monomers (Bhattacharya, A., 2004). To obtain a high-performance PES membrane, monomer or/and polymer are often incorporated into the modification via UV-photografting.

Be as it may, the selectivity of the monomer has been classified into anionic, neutral and cationic monomers (Wei, X. et al., 2006). The functional group of the monomer may be measured using the isoelectric point, the dissociation constant, surface charge density and the acid-base ratio (Xu, Z. K. et al., 2009).

In this research, acrylic acid has been used as the sole monomer, hence the effect of monomer size, chemical group, the degree of polymerization and surface coverage are kept constant (Kato, K. et al., 2003). Moreover, this monomer has a high hydrophilicity and water solubility (Abu Seman, M. N. et al., 2010a).

In fact, it has been found that acrylic acid grafted membranes exhibit higher water flux compared to unmodified membranes. However, the modified membranes have smaller pore sizes than the unmodified one. In a particular study, Doo Hyun, L. et al. (2004) conducted a surface modification by using acrylic acid on polypropylene and polysulfone. The research reports an increase in membrane hydrophilicity, with water flux increase of up to 4 times.

Acrylic monomers are an ester of acrylic and methacrylic acid. The ester can contain various functional groups such as hydroxyl group, amino groups, and an amide group (Rana, D. & Matsuura T., 2010). In the polymer technology, the monomer is measured in terms of glass transition temperature. The acrylic acid has a glass transition temperature of 112 T_g (^oC).

This is a simple average value in degree Celsius representing a range of temperatures through which the polymer changes from a hard and often brittle material into one with soft, rubber-like properties (Tracton, A. A., 2006). The molecular structure of acrylic acid is shown in Figure 2.15. As can be seen from the figure, the molecular structure of AA has two double bonds on its molecular structure. This double bond provides the polymer network structure by connecting the long, linear chains in the polymerization process (Elliott, J. E. et al., 2004).

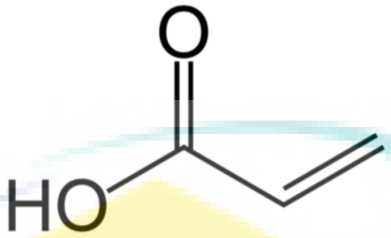

Figure 2.15 Acrylic acid molecular structure
Source: Elliott, J. E. et al. (2004)

2.10 Mathematical modelling

The modelling process in FO system is a very important tool for process design and performance projection. The concept of modelling allows researchers to predict the water flux from the FO operation at different FO membrane, feed and draw solutions, and operating condition without actually conducting any physical experiment (Xiao, D. et al., 2011).

In the FO technology, both external concentration polarization (ECP) and internal concentration polarization (ICP) as well as the membrane permeability have to be considered and their models have to be developed separately before combining them to allow for accurate flux prediction in an FO process. The water flux (J_w) which is previously shown in Eq. 2.3 is based on the differential flux across the membrane selective layer and it is typically represented by the osmotic-pressure model.

To calculate the concentration of the solute at the membrane interface, film theory is widely used to describe the ECP in the membrane system. During the FO operation, dilutive ECP occurs at the DS due to the movement of water flux across the membrane. The film theory is given as Eq. 2.5.

$$J_w = -D\frac{dC}{dx} \qquad 2.5$$

where D is the solute diffusivity, dC is the concentration gradient and dx is the draw solution direction. However, Eq. 2.5 can be integrated into Eq. 2.6.

$$J_w = -k\ln\frac{C_{d,w}}{C_{d,b}} \qquad 2.6$$

Since k depends strongly on the hydrodynamics of the system, it can be related to the Sherwood number as presented in Eq. 2.7.

$$k=\frac{ShD}{d_h} \qquad 2.7$$

However, the Sherwood relation which is commonly used to model ECP effects for pressure-driven processes is illustrated as in Eq. 2.8.

$$\text{Laminar flow } (Re\leq 2100): \qquad Sh=1.85\left(ReSc\frac{d_h}{L}\right)^{0.33} \qquad 2.8$$

For a fluid flowing through a rectangular channel, a thin layer of fluid close to the fluid-channel interface will be in laminar flow regardless of the nature of the free stream (Welty, J. R. et al., 2009). In this study, the mathematical modelling is only focused on the FO configuration. Thus, the concentration polarization in the FO process can be separated into dilutive ICP (Eq. 2.9) and concentrative ECP (Eq. 2.10).

The purpose of using the mathematical modelling is to predict the water flux through the asymmetric commercial NFPES membrane for the FO application at a different applied pressure (π).

$$K=\left(\frac{1}{J_w}\right)\ln\frac{B+A\pi_D}{B+J_w+A\pi_{F,w}} \qquad 2.9$$

$$K=\left(\frac{1}{J_w}\right)\ln\frac{B+A\pi_{D,w}-J_w}{B+A\pi_{F,w}} \qquad 2.10$$

where K is the solute resistivity for diffusion within the porous support layer, J_w is the water flux, A is the water permeability and B is the solute permeability, π_D is the bulk osmotic pressure of the draw solution, and π_F is the bulk osmotic pressure of the feed solution. The value of K can also be calculated as shown in Eq. 2.11;

$$K=\frac{S}{D} \qquad 2.11$$

where S is the structural parameter of the support layer and D is the diffusion coefficient of the solute (NaCl). The solute resistivity coefficient K is related to the structural parameter of the support layer, and the draw solute diffusion affects ICP in the support layer. This is an indication that it must be a significant parameter in the FO model (Suh, C. & Lee S., 2013).

McCutcheon, J. R. and Elimelech M. (2006) have incorporated the dilutive ICP and concentrative ECP models using the experimental data. The forward osmosis configuration was accurately described for water flux (J_v) as shown in Eqs. 2.12. This equation could work as a standalone predictor of flux under a variety of experimental conditions. In addition, these combined models may be used to predict the generate water flux and reverse solute flux under a different range of draw solution (DS) concentration and osmotic pressure.

$$J_v = A\left[\frac{\pi_{D,b}\exp\left(-\frac{J_v S}{D}\right) - \pi_{F,b}\exp\left(\frac{J_v}{k}\right)}{1+\frac{B}{J_v}\left[\exp\left(\frac{J_v}{k}\right) - \exp\left(-\frac{J_v S}{D}\right)\right]}\right] \qquad 2.12$$

where A is the water permeability, B is the solute permeability, $\pi_{D,b}$ is the bulk osmotic pressure of the draw solution, $\pi_{F,b}$ is the bulk osmotic pressure of the feed solution. Both terms $\left(\frac{J_v S}{D}\right)$ and $\left(\frac{J_v}{k}\right)$ depict the internal concentration polarization (ICP) and external concentration polarization (ECP) respectively, D is the diffusion coefficient value and *k* is the mass transfer coefficient. The negative and positive exponents indicate the concentrative and dilutive portions at that particular time respectively.

2.11 Membrane optimization using response surface methodology

In mathematical concept, optimization is mainly conducted to determine the optimal condition from a given set of factors. It involves statistical analysis and a mathematical algorithm to analyse several independent variables which influences a dependent variable or response.

In this study, the optimization was conducted using response surface methodology (RSM). In fact, the optimization process can be used to evaluate the relative significance of several affecting factors even in the presence of complex interactions (Witek-Krowiak, A. et al., 2014). Using the optimization, the relationship between the input parameters and output responses is defined using regression analysis in form of a polynomial equation.

A regression is performed to describe the data collected based on an estimated response variable, *y*, and one or more input variables x_1, x_2, . . ., xi. Depending on the behaviour of the model, the polynomial equation can be of a linear or non-linear form. Eq. 2.13 and Eq. 2.14 are examples of first-order and second-order polynomial equations respectively.

$$y=b_0+b_1x_1+b_2x_2+\ldots+b_kx_k+\varepsilon \qquad 2.13$$

$$y=b_0+\sum_{i=1}^{k} b_1x_1+\sum b_2x_1^2+\sum_{i<j}\sum b_{12}x_1x_2+\varepsilon \qquad 2.14$$

To ensure that the selected polynomial equation best represents the model, a least squares technique is used to minimize the residual error measured by the sum of squared deviations between the actual and the estimated responses (Cojocaru, C. & Trznadel G. Z., 2007). This involves the calculation of estimates for the regression coefficients such as the coefficients of the model variables including the intercept or constant terms. The calculated coefficients of the model equation can then be tested using an analysis of variance approach (ANOVA). This helps to measure the significance of the regression model, significance of individual model coefficient, and the lack of fit.

2.11.1 Design of experiment

The choice of the design of experiments (DOE) can have a large influence on the accuracy of the approximation and the cost of constructing the response surface (Khayet, M. et al., 2010). The origin strategy was to develop the model that fit the physical experiments and applicable to numerical experiments. The objective of DOE is the selection of the points where the response should be evaluated. Most of the criteria for the optimal design of experiments are associated with the mathematical model of the process.

The optimization process is simplified as it suggests an outline of important experimental design as stated in the literature (Solouk, A. et al., 2011; Xiarchos, I. et al., 2008). Generally, these mathematical models are polynomials with an unknown structure, so the corresponding experiments are designed only for every particular problem (Xiangli, F. et al., 2008). The purpose is to identify the design variables that have large effects for further investigation.

2.11.2 Central composite design

The central composite design (CCD) is used to build a second order experimental model. CCD is composed of a factorial design, a set of central points, and axial points equidistant to the centre point (Witek-Krowiak, A. et al., 2014). The factorial design component of CCD is of the class 2^k factorial where k represents the number of relevant factors or variables. Each of the variables is taken at two levels meaning that each variable has a low and high numeric value. A coded numeric value of -1 and +1 is assigned to represent the variable's low and high values as illustrated in Figure 2.16. The design involves 2^k factorial points, 2^k axial points and 1 central point.

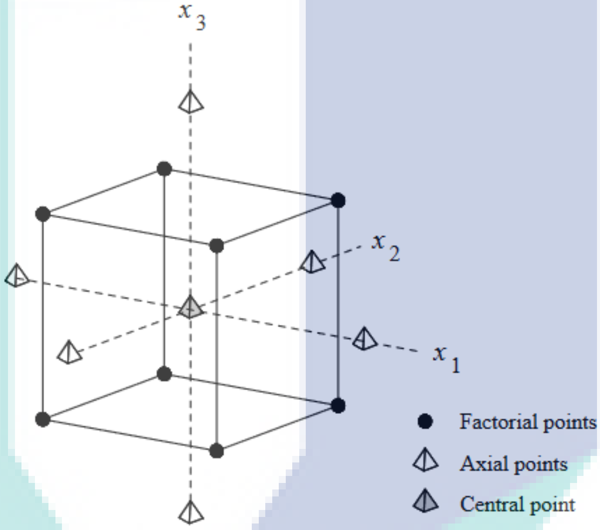

Figure 2.16 Central composite design
Source: Witek-Krowiak, A. et al. (2014)

Notably, the geometric representation of a factorial is a cube in which each corner represents an interaction of the factors. In this perspective, 8 interactions are to be evaluated when 3 processing variables are selected to determine their significance in the final response. Normally, the model verification is often conducted by statistical technique to validate the accuracy of the model. The accuracy of the developed model covers the space of the process or independent variables. Thus, the empirical statistical modelling was used to develop an appropriate approximating relationship between the yield and the process variables, and optimization methods for finding the values of the process variables that produce desirable values of the response (Banerjee, A. & Ray S. K., 2018).

CHAPTER 3

METHODOLOGY

3.1 Introduction

This chapter is outlined as illustrated in Figure 3.1. It describes the experimental procedures adopted in this study. The flowchart starts with the membrane pre-treatment, selection of membrane support namely the UFPES and NFPES membranes followed by the modification of the membrane using the UV-photografting. Herein, the unmodified and modified membranes were measured in RO mode and FO mode.

Furthermore, UFPES and NFPES membrane supports were compared in terms of their performances and reliability in the FO system following the standard operating procedures. Moreover, mathematical modelling was performed on the selected membrane support which has been initially compared for its performance and intrinsic properties. The model was used to predict the water flux at different osmotic pressure.

Finally, the optimization process was conducted to produce the high-performance FO membrane. In the design of the experiment, grafting time and monomer concentration were selected as factors while water flux and reverse salt diffusion are considered as the responses. The optimization ends with the validation process to confirm the reliability of the developed regression coefficient.

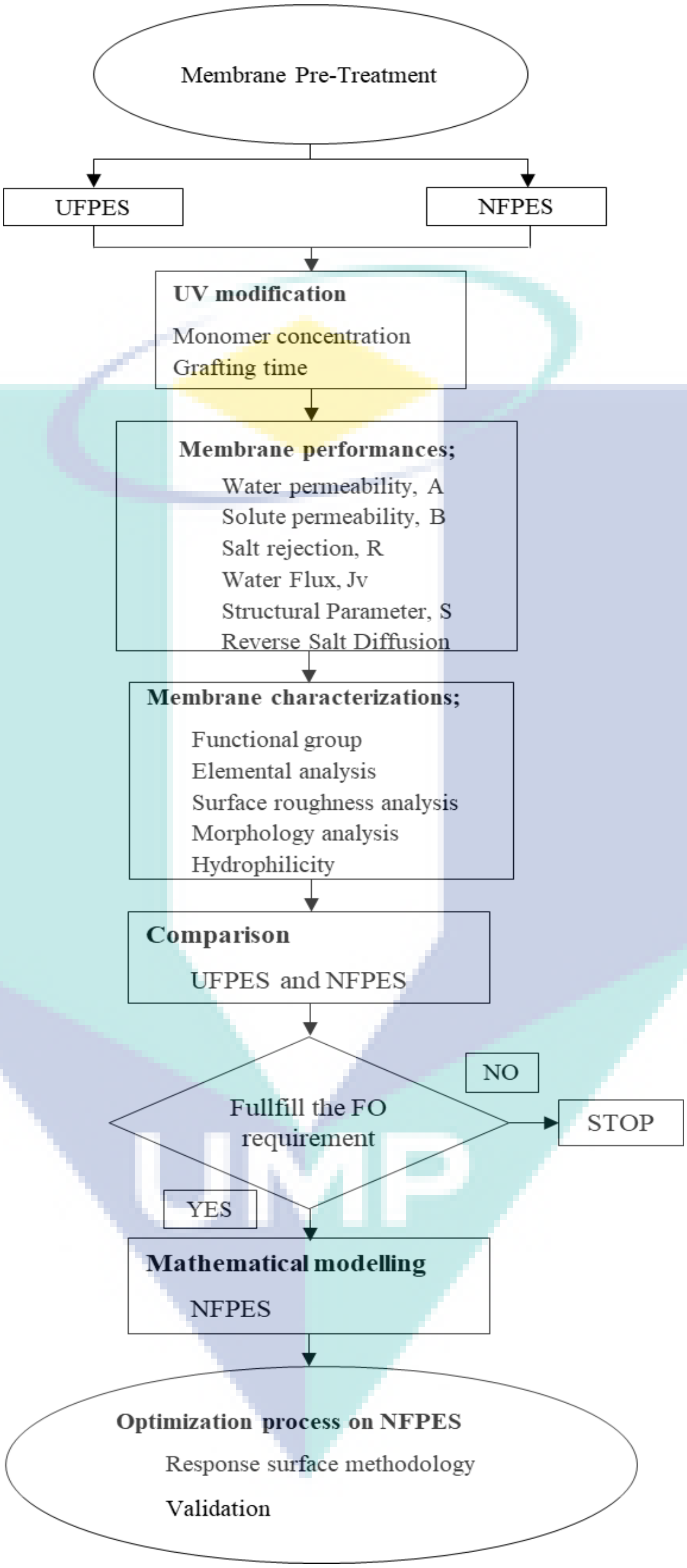

Figure 3.1 Flowchart of the experimental work

3.2 Materials

3.2.1 Chemicals

Sodium chloride (NaCl) with the CAS No of 7646-14-5 and acrylic acid (AA) were obtained from Merck Chemicals. Typical properties of acrylic acid are presented in Table 3.1. The chemical used for this study is laboratory grade. Hence, it was used without further purification.

Table 3.1 Chemical properties of acrylic acid

Chemical Properties	**Value**
CAS-No	79-10-7
Formula	CH_3=CHCOOH
EC-No.	201-177-9
Molecular weight (g/mol)	72.06
Solubility in water at 25°C (%)	1,000 g/l
Density at 20°C	1.05 g/cm^3
Viscosity, dynamic at 20°C	1.22mPa.s

3.2.2 Membrane

The commercial ultrafiltration polyethersulfone (UFPES) and nanofiltration polyethersulfone (NFPES) membranes were obtained from Amfor Inc. Detail of the UFPES and NFPES membrane properties are presented in Table 3.2. It has the commercial name, water flux, molecular weight cut-off and the rejection properties.

Table 3.2 Properties of UFPES and NFPES membranes

Membrane	**UFPES**	**NFPES**
Commercial name	UFPES50	NF2
Water flux	260 L.m^{-2}h^{-1} at 25°C and 50 psi.	100 L.m^{-2}.h^{-1} at 25°C and 150 psi.
Molecular weight cut-off	50 kDa	Not provided
Rejection	Not provided	Rejection of 95% of magnesium sulphate ($MgSO_4$)

3.3 Experimental procedures

3.3.1 Pre-treatment and sample preparation

It is well known that different types of the membrane will require different type of pre-treatment. Generally, pre-treatment is basically used to remove any protective layer from the manufacturer. Herein, the manufacturer coats the membrane with glycerine to prevent the membrane from drying out. Prior to surface modification, the membrane was immersed overnight in deionized water to remove its protective layer.

The samples were then prepared to fit the dead-end stirred cell for RO system and crossflow for FO system. In the RO system, the sample was cut in circular shape with a 50 mm Ø. On the other hand, for the FO system, the sample was cut in a rectangular shape with a dimension of 50 mm x 100 mm. The samples were carefully prepared with minimum contact on the active layer to prevent disturbance of the pore structure.

3.3.2 Ultraviolet-photografting

The surface modification was conducted using a Blak-Ray B-100 Series from UVP as shown in Figure 3.2. The photoreactor was a square stainless-steel black chamber with (15cm × 15cm) in dimension. The membrane was fixed at the bottom, while the ultraviolet (UV) lamp was placed at the top centre of the chamber which installed vertically down light.

The UV-light (λ = 365 nm) was a medium skirted mercury spot lamp. A fixed distance of 10 cm between the UV lamp and the membrane was chosen to provide UV irradiation energy of 15 $W.m.cm^{-2}$. Before any experimental work being conducted, the light must be turn on for 15min to allow a stable intensity. Moreover, it should be noted that the light will produce a significant heat while operating. Thus, proper ventilation is a must to ensure the UV-light has a longer operating hours.

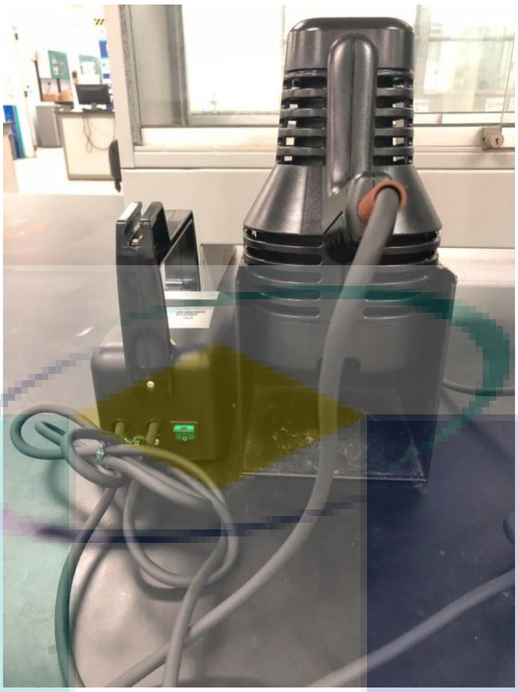

Figure 3.2 UVP photoreactor

In the UV-photografting process, the membrane was immersed initially in 50 mL of different concentrations (5–50 g/L) of AA which represents the monomer concentration and left for 15 min. Details of the grafting parameter as shown in Table 3.3. Then, the membrane was exposed to surface modification at a predetermined time (1-60 min) using the immersion method. After this, the membrane was rinsed with deionized water to remove unreacted compounds. The modified membrane was stored in deionized water at 4 °C for one day before use.

Table 3.3 Grafting parameter of the membrane

Membrane	**Monomer concentration (g/L)**	**Grafting time (min)**
5-1	5	1
5-3	5	3
5-5	5	5
15-1	15	1
15-3	15	3
15-5	15	5
30-1	30	1
30-3	30	3
30-5	30	5

Table 3.3 Continued

Membrane	Monomer concentration (g/L)	Grafting time (min)
50-1	50	1
50-3	50	3
50-5	50	5

3.4 Evaluation of membrane performance in RO mode

The water flux (J_w), water permeability (A), salt rejection (R) and solute permeability (B) were determined using a stirred cell (Sterlitech, HP4750) as shown in Figure 3.3. It has a volume capacity of 200 mL and a flat sheet membrane with an active area of 14.2 cm^2. Different pressures were tested ranging from 1-10 bar.

Figure 3.3 HP4730 Sterlitech stirred cell

3.4.1 Water flux

Water flux (J_w), is defined as the volume of water that passes through a membrane per unit time, per unit area as shown in Eq. 3.1.

$$J_w = \frac{\Delta L}{A_m(\Delta T)} \tag{3.1}$$

where J_w is the water flux ($L.m^{-2}.s^{-1}$), ΔL is the volume of permeate, A_m is the surface-active area, and ΔT is the time.

3.4.2 Water permeability

Water permeability (A), is the intrinsic properties of a membrane. It is determined using the water flux (J_w) over pressure (ΔP) as shown in Eq. 3.2. In this method, both UFPES and NFPES membranes were tested with different pressure ranging from 1-10 bars.

$$A=\frac{J_w}{\Delta P} \qquad 3.2$$

where A is the water permeability ($L.m^{-2}.s^{-1}.atm^{-1}$), Jw is water flux and ΔP is pressure.

3.4.3 Salt rejection

The salt rejections (R), was conducted using HP 4730 Sterlite stirred cell using 200 ppm of sodium chloride (NaCl) as the feed solution (Kwon, S. B. et al., 2015). The solute rejection was calculated based on Eq. 3.3. The value of salt rejection was calculated from the difference between bulk feed (C_b) and permeate (C_p) salt concentrations. The stirring rate was fixed at 100 rpm. The salt rejection was measured using the conductivity meter (PC 2700, Eutech Instruments). The obtained conductivity value was then converted into concentration (M) using the correlation as shown in Appendix A.

$$R=\left(1-\frac{C_p}{C_b}\right) \qquad 3.3$$

where R is the salt rejection, Cb is feed and Cp is permeated of salt concentrations.

3.4.4 Solute permeability

The solute permeability (B), is also an intrinsic property of a membrane. It is determined using Eq. 3.4;

$$B=J_w\left(\frac{1-R}{R}\right)\exp\left(-\frac{J_w}{k}\right) \qquad 3.4$$

where J_w is the water flux, R is the salt rejection, and k is the mass transfer coefficient for the crossflow channel of the reverse osmosis. The value of k and D_∞ was taken from Bowen, W. R. et al. (1997) where the stirring effect was included in the stirred cell. The value of k and ω are as follows:

$$k = k'\omega^{0.567} \qquad 3.5$$

where k is the mass transfer constant, k’ is the mass transfer by calculated equation and ω is the stirring speed.

$$k' = 0.23\left(\frac{r^2}{\upsilon}\right)^{0.567}\left(\frac{\upsilon}{D_\infty}\right)^{0.33}\frac{D_\infty}{r} \qquad 3.6$$

where r is the radius of the stirrer, υ is the kinematic viscosity of NaCl, and D_∞ is the bulk diffusivity.

3.5 Evaluation of membrane performance in FO mode

The performance of the FO membrane for water flux (J_v), the structural parameter (S), and reverse salt diffusion (RSD) are measured using the lab-scale FO cross-flow filtration system unit illustrated in Figure 3.4. The system has a cross-flow FO cell with an effective area of 0.0042 m^2 (Sterlitech CF042 Cell), peristaltic pump with two heads (BT600-2J, Longer-Pump), 2 tanks with a capacity of 1000 mL and weighing balance (FX-3000i, A&D Company Limited) with data logging to record the mass changes.

Figure 3.4 Laboratory scale of forward osmosis unit

A silicone tube was used to connect the FS, DS and FO cells in a closed-loop system. The flow rate of both solutions was maintained at 167 ml/min. Water flux was determined by the variation in weight of FS using a weighing balance. The initial mass of FS was recorded, and further reading was determined at the intervals of 5 minutes until the process was completed after one hour.

3.5.1 Water flux

Water flux (J_v) is measured using Eq. 3.7. The FO system was configured with the deionized water in the FS and 1 M of NaCl in the DS. The permeate water flux was determined by the variation in the weight of the feed solution using a weighing balance. The obtained weight was then converted into a volume using the following water density correlation;

$$J_v = \frac{\Delta L}{A_m . \Delta t} \qquad 3.7$$

where J_v is the water flux ($L.m^{-2}.s^{-1}$), ΔL is the volume of permeate, A_m is the surface-active area and Δt is the time.

3.5.2 Structural parameter

The structural parameter is used to determine the average distance for a solute molecule to travel across the semi-permeable membrane. It is measured using 1M of NaCl as the DS and deionized water as the FS. In general, small S values improves the membrane water permeability and enhances the support layer's performance by reducing the ICP effect during the FO process. The membrane support structural parameter was determined using Eq. 3.8.

$$S = \frac{D_s}{J_v} \ln\left(\frac{B + A\pi_{D,b}}{B + J_v + A\pi_{F,m}}\right) \qquad 3.8$$

where D_s is the diffusivity of the draw solute, J_v is the water flux in FO mode, $\pi_{D,b}$ is the bulk osmotic pressure of the draw solution and $\pi_{F,m}$ is the osmotic pressure at the membrane surface on the feed side. D_s is the diffusivity of the draw solute.

3.5.3 Reverse salt diffusion

Reverse salt diffusion (J_s) was measured via FO configuration. The RSD was calculated by multiplying the rate of change of feed concentration with time by the volume of the feed solution and then dividing it by the area of the membrane, expressed in units of $g.m^{-2}h^{-1}$ as shown in Eq. 3.9.

$$J_S=\frac{C_tV_t\text{-}C_0V_0}{A\Delta t} \quad 3.9$$

where C_o(g/L) and V_o(L) is the intial concentration and initial volume of the feed solution, respectively and C_t (g/L) and V_t (L) are the solutes concentration and the volume of the feed solution measured at the time of t, respectively. Accordingly, the conductivity value was converted into concentration (M) using the correlation in Appendix A.

3.6 Membrane characterization

3.6.1 Functional group analysis

The functional group analysis was measured using attenuated total reflection-Fourier transform infrared spectroscopy (ATR-FTIR), model Nicolet iS5 FTIR spectrometer from Thermo Fisher Scientific. The equipment used diamond crystal at an incident angle of 42^o.

The functional group of the samples was characterized using the vibration of molecules. Infrared beam travels through the diamond crystal to form an evanescent wave to penetrate the sample and reflects off the sample. Infrared light will be absorbed or emitted depending upon the chemical bonding within the material and the subsequent spectral fingerprints is generated to determine the functional group.

3.6.2 Elemental analysis

The elemental analysis was measured using x-ray photoelectron spectroscopy (XPS) with a PHI-5000 VersaProbe II spectrometer. It is equipped with a monochromated AI Kα as the radiation source to determine the binding energy. The pressure of the analysis chamber was fixed at 2.7 x 10^{-4} Pa and was operated with pass energy at 29.35eV.

The XPS measures at three different levels of penetration namely the survey scan, narrow scan and mapping scan. Survey scan is the basic scan in XPS where the element composition is measured via the tilting process. Narrow scan utilizes ion beam etching while mapping scan measures the elemental composition across the top surface of the sample. Photons (monoenergetic) from soft x-ray radiation are directed on the membrane and the photoelectrons are emitted from the sample by the photoelectric effect. Ejected photoelectrons are then identified by the generated kinetic energy.

3.6.3 Surface roughness analysis

The multimode atomic force microscope (AFM) from Scanning Probe Microscope (NTEGRA Prima) was used to analyse the surface roughness. It characterized the surface of both unmodified and modified membranes. The image was obtained over different square areas of each membrane sample based on a scan area of around 5 µm x 5 µm. The roughness value was determined by averaging the values measured over 1 µm x 1 µm in three different locations chosen arbitrarily for each membrane sample.

The average roughness (Sa) represents the mean value of the surface height relative to the calculated centre plane, for which the volumes enclosed by the image above and below the plane are the same. It was calculated using Eq. 3.10, in which the number of points within the given area (Np) considered was 512 data points:

$$S_a = \frac{1}{N_p}\sum_{i=0}^{N_p}\left|Z_i - Z_{avg}\right| \qquad 3.10$$

where Z_i is the current height value measured, while Z_{avg} is the average of the height values within the given area.

3.6.4 Morphology analysis

The field emission scanning electron microscopy (FESEM) was conducted using JSM7800F Schottky Field Emission Scanning Electron Microscope from JEOL. The analysis was conducted to examine the morphology, or specifically the membrane structure, pore distribution, defects and presence of impurities. The cross-section of the grafted film was obtained by breaking the films under liquid nitrogen.

The selected cross-section of control and grafted samples were deposited on the metal grid using double-sided adhesive tape and coated with platinum under vacuum to avoid electrostatic charging during the examination. After this, the surface characteristics were studied and photographed within a working distance at 15 kV operating voltage and 2000x magnifications.

3.6.5 Hydrophilicity

The hydrophilicity of the membrane was measured using a contact angle instrument by employing the static sessile drop method. It was conducted using direct measurement by a goniometer telescope (Rame-Hart, Model 290). It is well known that water contact angle is usually used to measure the hydrophilicity/hydrophobicity of a material surface. Normally, the medium used is deionized water. When a water droplet is placed on the surface of a membrane sample, the shape of the droplet is determined by balance from the three forces of water, membrane surface and air. The line tangent drawn at the curve of the droplet to the point where it intersects the membrane surface forms the contact angle.

3.7 Theoretical modelling

Theoretical modelling was used to predict the water flux at different osmotic pressure using different concentration of draw solution as shown in Eq. 3.11.

$$J_v = A\left[\frac{\pi_D \exp\left(-\frac{J_v K}{D}\right) - \pi_F \exp\left(\frac{J_v}{k}\right)}{1+\frac{B}{J_v}\left[\exp\left(\frac{J_v}{k}\right) - \exp\left(-\frac{J_v S}{D}\right)\right]}\right] \qquad 3.11$$

where details of the abbreviation are as presented in Table 3.4. The k value was taken from our previous study using this membrane (Aziz, S. N. S. A. et al., 2018).

Table 3.4 Parameters for forward osmosis mathematical modelling

Parameter	Symbol	Units	Value/Range
Solute diffusivity	D	m^2s^{-1}	$1.68x10^{-9}$
Bulk draw osmotic pressure	π_D	bar	0-70
Bulk feed osmotic pressure	π_F	bar	0-65.4
Water permeability	A	$L.m^{-2}hr^{-1}.bar^{-1}$	0.75-2.2
Solute permeability	B	$L.m^{-2}hr^{-1}$	15-117
Solute resistance to diffusion	k	ms^{-1}	9.56×10^6
Temperature	K	^oC	20
Crossflow velocity		$cm.s^{-1}$	21.3

Initially, the comparison between these two support membranes UFPES and NFPES was made by differentiating between the predicted flux at different monomer concentration and grafting time. The selected parameters for the comparison are water permeability (A), solute permeability (B), salt rejection (R), water flux (Jv) and reverse salt diffusion (Js). The selected membrane support was further subjected to prediction of water flux at different osmotic pressure and feed solution. Detail of the theoretical modelling is illustrated in Figure 3.5. In here, data for the value of A, B, R, Jv and Js were discussed thoroughly in the application of FO system. Either UFPES or NFPES membrane support will be selected for the mathematical modelling. No further analysis to the unselected membrane support.

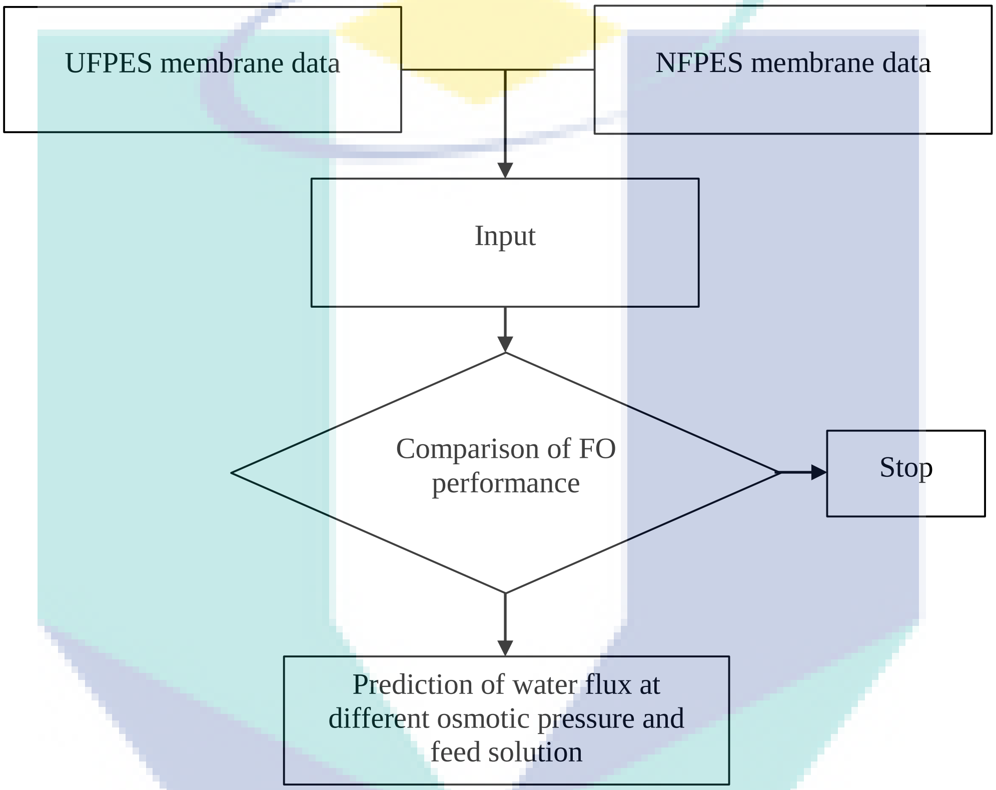

Figure 3.5 Flow chart of the theoretical modelling

3.8 Membrane optimization

3.8.1 Response surface methodology

The experimental design and optimized regression equations were developed using Design-Expert (version 7.0). The experimental design was developed using a central composite design (CCD) based on response surface methodology (RSM). The investigated processing variables are the grafting time (x_1) and the monomer concentration (x_2). On the other hand, the measured response variables are the water permeate flux and the reverse salt diffusion (RSD). The response was analyzed using analysis of variance (ANOVA) based on the *p* value with 95% confidence level.

3.8.2 Screening process

Previously in Section 2.7, we have discussed that the surface modification via UV-photografting has four factors that affect the performance of the modified membrane. The grafting time, monomer concentration, UV intensity, and the monomer selection plays a vital role on the outcome of the modified product. In this research, we have pre-determine the selection of monomer selection (acrylic acid) and monomer concentrations (5, 15, 30 and 50 g/L). Thus, we apply only three factors into our screening process of optimization processes that was in Table 3.5

Table 3.5 Design of experiment for the screening process

Run	Membrane	Input variables		
N		Grafting time (min) x_1	Monomer concentration (g/L) x_2	UV-Intensity mWcm^{-2} x_3
1	16.25NF-2-15UV	2	16.25	15
2	38.75NF-2-25UV	2	38.75	25
3	27.5NF-3-10UV	3	27.5	10
4	27.5NF-5-20UV	5	27.5	20
5	27.5NF-3-30UV	3	27.5	30
6	27.5NF-1-20UV	1	27.5	20
7	27.5NF-3-20UV	3	27.5	20
8	27.5NF-3-20UV	3	27.5	20
9	27.5NF-3-20UV	3	27.5	20
10	16.25NF-4-15UV	4	16.25	15
11	27.5NF-3-20UV	3	27.5	20
12	27.5NF-3-20UV	3	27.5	20
13	27.5NF-3-20UV	3	27.5	20
14	38.75NF-4-25UV	4	38.75	25
15	38.75NF-4-15UV	4	38.75	15
16	5NF-3-20UV	3	20	20
17	16.25NF-2-25UV	2	16.25	25
18	16.25NF-4-25UV	4	16.25	25
19	38.75NF-2-15UV	2	38.75	15
20	50NF-3-20UV	3	50	20

3.8.3 Central composite design

The CCD consists of 5 levels of plus and minus alpha (axial points), plus and minus one (factorial points), and the centre point. The axial design points (α) for this certain design was set to 2. In the process of optimizing the performance of the modified membrane, the factor levels for grafting time is (1-5 min) and the monomer concentration is (7.5-37.5 g/L) as shown in Table 3.6.

Table 3.6 An experimental design using actual and coded variables

Variables	**Unit**	**Real values of coded levels**				
		-α	**-1**	**0**	**+1**	**+α**
Grafting time	min	1	2	3	4	5
Monomer concentration	g/L	7.5	15	22.5	30	37.5

The design involved 13 sets of experiments which consist of six centre points as presented in Table 3.7. The experiments were conducted in the same run order as suggested by the software.

Table 3.7 Design of experiment for the optimization process

Run	**Membrane**	**Input variables**	
		Grafting time (min)	Monomer concentration (g/L)
N		x_1	x_2
1	22.5NF-3	3	22.5
2	22.5NF-1	1	22.5
3	30NF-4	4	30.0
4	22.5NF-3	3	22.5
5	37.5NF-3	3	37.5
6	22.5NF-3	3	22.5
7	30NF-2	2	30.0
8	22.5NF-3	3	22.5
9	15NF-2	2	15.0
10	7.5NF-3	3	7.5
11	22.5NF-3	3	22.5
12	22.5NF-5	5	22.5
13	15NF-4	4	15.0

3.8.4 Model validation

The regression equations obtained from the experimental data can be used to predict the water flux (J_v), and reverse salt diffusion (J_s), at any ratio of grafting time and monomer concentration within the limits tested. Thus, the validation process was the replication of the suggested optimum condition. The comparison between experimental and predicted optimum value was performed for this purpose. The model validation or error percentage was calculated based on the error percentage is shown in Eq. 3.11.

$$\text{Error percentage}= \left|\frac{V_{exp}-V_{theo}}{V_{exp}}\right| \text{x } 100\% \qquad 3.11$$

where V_{exp} is experimental value and V_{theo} is the theoretical value.

CHAPTER 4

RESULTS AND DISCUSSION

4.1 Introduction

In this chapter, the results obtained from the experimental works and discussions are presented in four major sections. The first part has to do with the applicability of surface modification on UFPES membrane for the FO application. The performances of unmodified UF membrane was tested using both RO mode and FO mode before proceeding with modified membranes. The membrane was modified following the one factor at a time (OFAT) approach. The monomer concentration and grafting time were pre-determined before the experimental works. Then, the membrane was characterized to determine the performance and intrinsic properties.

Secondly, result of the repeated experiment on the NFPES membrane is presented. Herein, the experimental procedure is similar to UFPES membrane except for the pressure used in the water flux (RO mode). NF membrane requires higher operating pressure to generate the permeate due to the smaller pore size. After this, results of the comparison of performances (membrane intrinsic properties and RSD) between both UFPES and NFPES membranes are presented.

Thirdly, the developed mathematical modelling was used to predict the water flux at different osmotic pressure and the results are reported herein. It is important to predict the generated permeate at the application of different osmotic pressure without conducting the vigorous experimental works. Moreover, the data from the modelling offers an optimal condition for the optimization process. Finally, observations from the optimization process using two factors (monomer concentration and grafting time) and two responses (water flux and reverse salt diffusion) are presented in the later part of this chapter. Notably, the surface response methodology (RSM) specifically the central composite design (CCD) was used to obtain an optimized membrane.

4.2 Filtration properties of UFPES membrane

At the lowest pressure (1 bar), the commercial flat sheet UFPES membrane has a water flux of 99.48 L.m^{-2}hr^{-1}. Each data was repeated three times to obtain the measurement. This process was repeated up to 5 bars of pressure to determine the intrinsic properties of UFPES membrane. Based on the generated water flux at different pressure, the water permeability was calculated at 99.41 L.m^{-2}hr^{-1}bar^{-1} using the gradient shown in Figure 4.1.

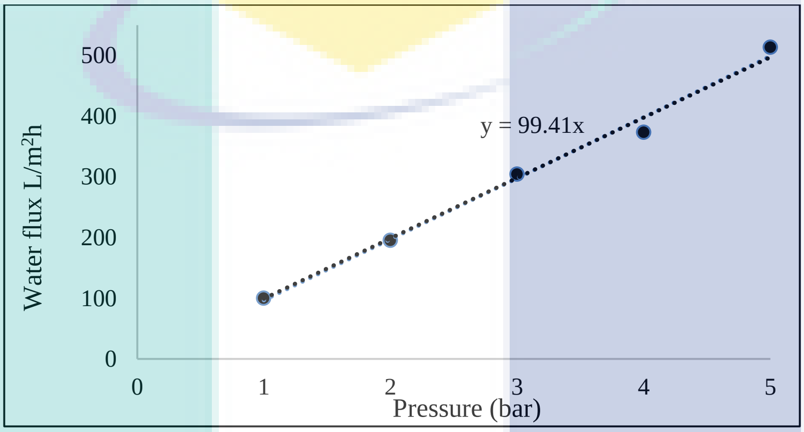

Figure 4.1 Water permeability of unmodified UFPES membrane

4.2.1 Water permeability

The result of water permeability (A) is presented in Figure 4.2. In the modification of the membrane, each of the monomer concentrations (5, 15, 30 and 50 g/L) was UV-grafted at different grafting times (1, 3 and 5 min) which applies the concept of one factor at a time (OFAT). The water permeability for UFPES membrane was conducted using the pressure of 3 bars. In this research, acrylic acid was used as the sole monomer, hence the effect of monomer size, chemical group, the degree of polymerization and surface coverage remained constant (Kato, K. et al., 2003).

The result in Figure 4.2 shows that the water permeability increases with the increase in monomer concentration until it reaches a peak when the monomer concentration used is at 30 g/L. A sudden drop in the water permeability can be observed when the monomer concentration used exceeds 30 g/L. The highest value of A is recorded for sample 30UF-5min (182.65 L.hr^{-1}.m^{-2}.bar^{-1}) while the lowest water permeability was recorded for sample 50UF-3min (93.40 L.hr^{-1}.m^{-2}.bar^{-1}). The modified membranes have higher A value compared with the unmodified membranes except for 5UF-1, 50UF-3 and 50UF-5.

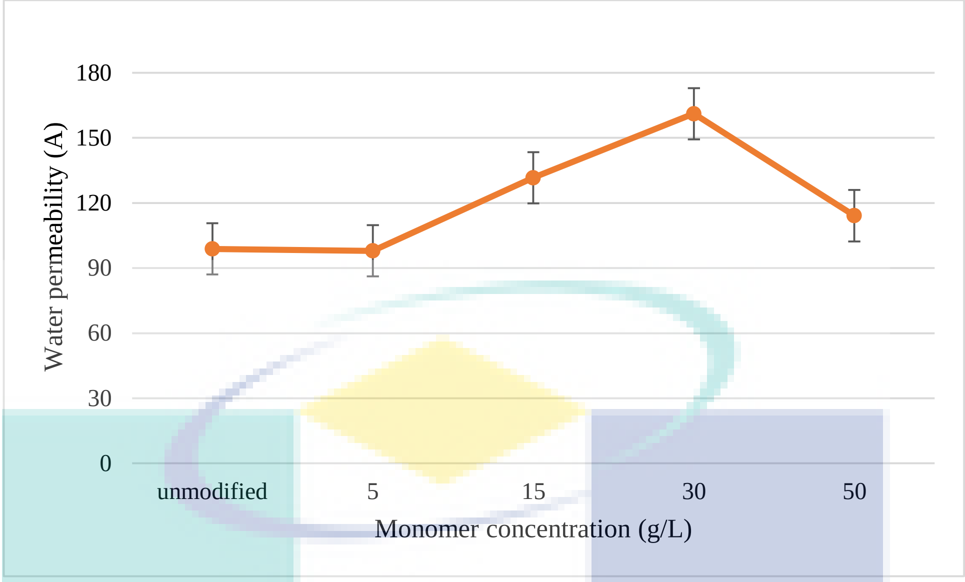

(a)

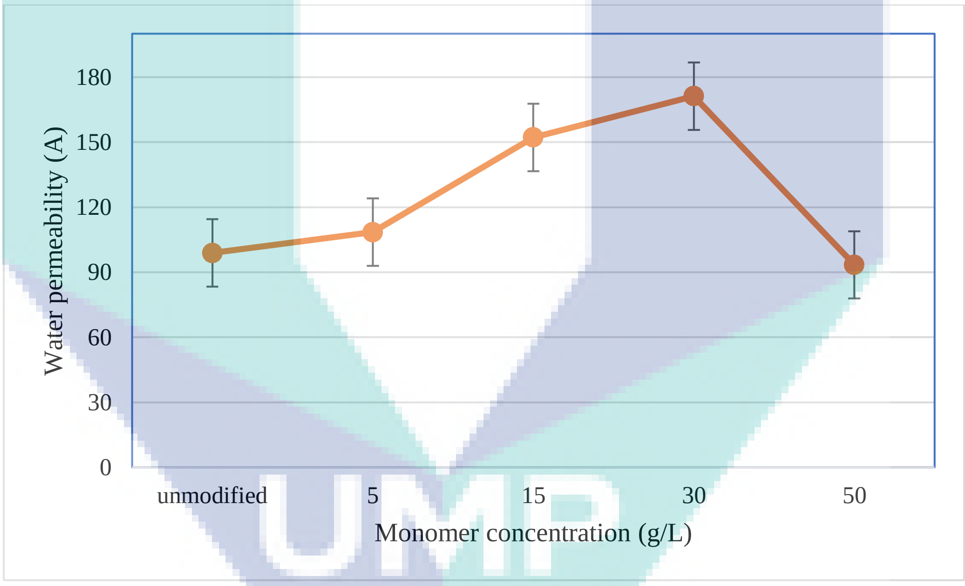

(b)

Figure 4.2 Water permeability of UFPES membrane modified at different UV grafting time of (a) 1 min, (b) 3 min, and (c) 5 min

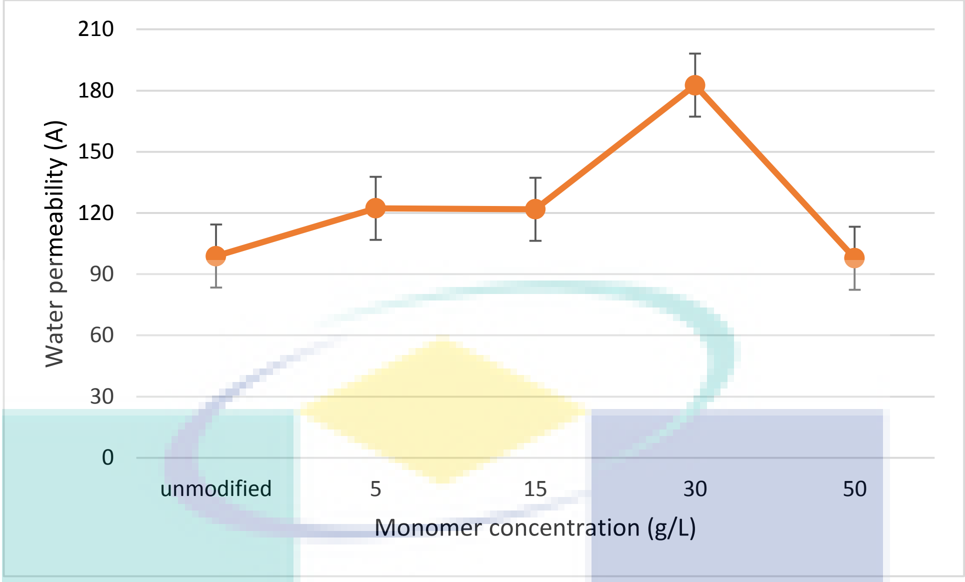

(c)

Figure 4.2 Continued

In a previous research conducted by X, W. et al. (2006), it was observed that the grafting yield increased with the increase in monomer concentration except at lower concentrations. Notably, acrylic acid is a strong acid and it provides negative charges to the modified membrane as the formation of the carboxylic group in the functional group makes it more hydrophilic. The modified membrane 5UF-1min (97.97 L/m^2.hr.bar) is believed to have insufficient effective grafting as it was conducted in low monomer concentration and short grafting time. The original functional group at the membrane surface managed to either repel the negative charges from the monomer or the number of energies received by phenoxyphenyl sulfone chromopores was below the minimal energy to form free radicals.

At 50 g/L of monomer concentration, the water permeability shows a great decline at all tested grafting times. Thus, the highest monomer concentration might lead to a competitive effective grafting at the membrane surface. A similar trend is also observed by Bilongo, T. G. et al. (2010) where the effective grafting increases with the increase of monomer concentration. The author justifies the relationships through the kinetic in photo-polymerisation where a good grafting condition must be derived from a high monomer concentration and a strong dose of UV energy. This phenomenon leads to the thickening of the grafted layer.

Further experimental works were conducted to evaluate the sudden drop in water permeability for the monomer concentration of 50 g/L as shown in Figure 4.3. In general, the value of A shows a reduction with the increase of grafting time as shown by the trendline (dotted line). The trendline was generated after the experiment was conducted under 8 different grafting times (minute). As stated, the value of water permeability shows a decreasing value as the grafting time increases up to 15min. However, as the grafting time exceeds 15 min, the water permeability shows an increasing value. The decrease in the water flux value does not correlate well with the progressive increase in the grafting time. It has been reported that the polymerisation mechanism in the membrane surface involved both effective grafting and chain scission processes instead of a steady growth of polymer chain (Kuroda, S. et al., 1989). Hence, according to Mansourpanah, Y. and Habili E. M. (2013), the longer UV radiation period could lead to the enhancement in the polymerisation degree before obtaining a denser thin layer.

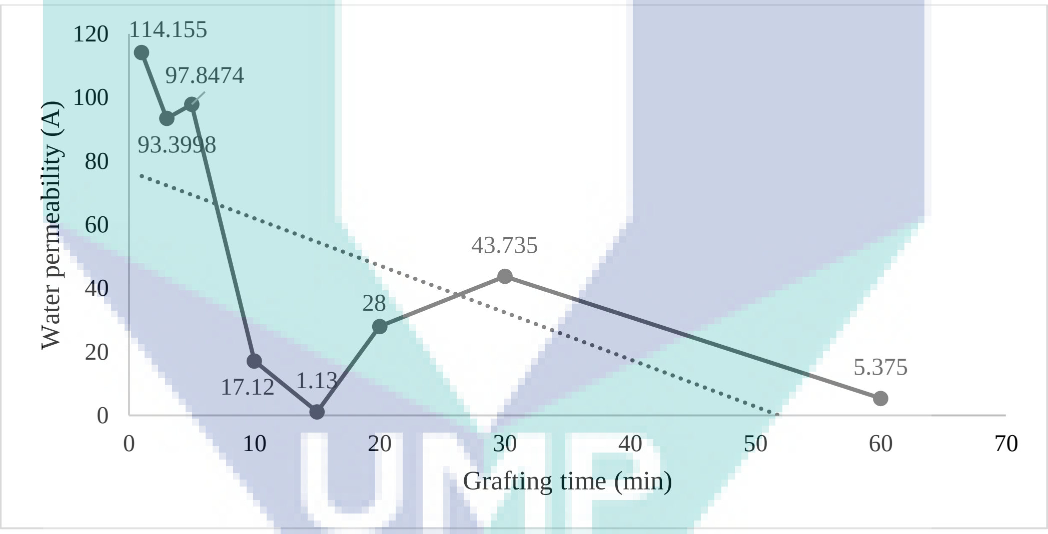

Figure 4.3 Water permeability and grafting time up to 60 minutes

Moreover, the reduction of water permeability after the modification was also observed by Yu, H. J. et al. (2009). The PES membrane was modified via UV-photografting with the use of an initiator to improve the antifouling property. The authors claimed that the reduction in water permeability was due to the formation of grafted material which had narrowed down the pore size. A similar result was also obtained by Taniguchi, M. and Belfort G. (2004) which suggests that water permeability declines with the increase of grafting time. The formation of grafted material that leads to pore plugging implies the formation of a gel layer on the modified surface. At the grafting time of 15 min, the modified membrane impeded water movement. However, when a maximum pressure of 8 bar was used the water permeability was only at 1.13 L.hr^{-1}.m^{-2}.bar^{-1}.

The trend of effective grafting increases with the increase of grafting time applied in the first 15 min. As the grafting time increase from 15 min, the water permeability starts to increase with values of 1.13 L.hr^{-1}.m^{-2}.bar^{-1}, 28 L.hr^{-1}.m^{-2}.bar^{-1}and 43.7 L.hr^{-1}.m^{-2}.bar^{-1}. It is assumed that the mechanism that occurred between the grafting time of 15 min and 30 min is chain scission. If chain scission is considered as the main reason for the increase in water permeability, the modified membrane with longer grafting time can therefore be illustrated as shown in Figure 4.4.

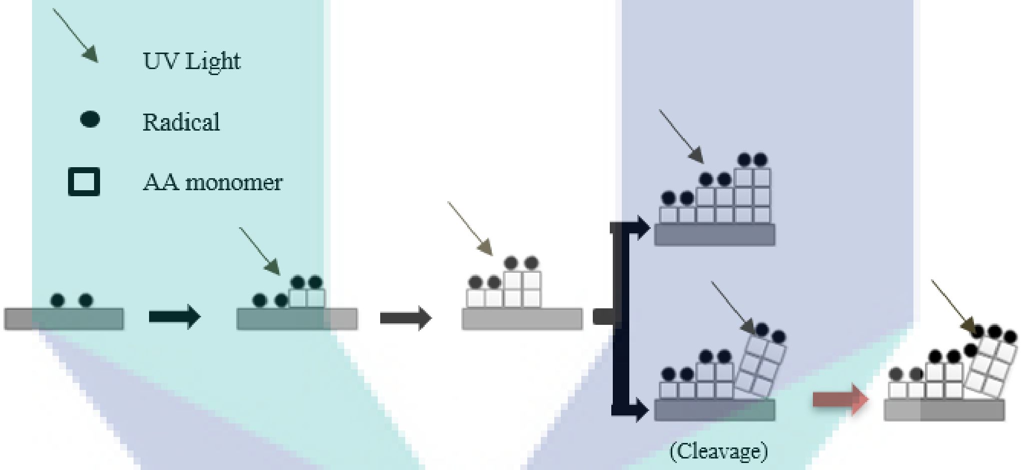

Figure 4.4 The proposed mechanism of UV-photografting on PES membrane surface. Modified from Taniguchi, M. et al. (2003).

In the area where the cleavage occurred, the membrane surface is exposed directly to the feed solution which leads to the increase in water permeability. Garcia-Ivars, J. et al. (2016) define this scenario as the deterioration of the membrane as the membrane exceeds a certain grafting parameter. As the chain scission occurs more rapidly at 30 min of grafting time, the water permeability also increases. The effect of degradation on PES due to irradiation is unavoidable. This evidence is supported by Taniguchi, M. et al. (2003) who has shown that the grafting time leads to an increase in pore size. However, at the grafting time of 60 min, the value of A reduces to 5.3 L.hr^{-1}.m^{-2}.bar^{-1}.

It is suggested that the graft polymerization occurred at the cleavage by forming a new layer of the carboxyl group. The phenomenon is relatively similar to the use of a crosslinker such as glutaraldehyde in the formation of new layers on top of the previous layer. For example, Liu, C. et al. (2015a) studied the use of crosslinker and its effect on the modified membrane that leads to a reduction in pore size, increase in hydrophilicity and lowering of surface charge.

4.2.2 Water flux in FO mode

The unmodified membrane has a water flux of 3.81 L.m^{-2}hr^{-1} while the highest water flux of the modified membrane was 5.71 L.m^{-2}.hr^{-1} (15UF-3min). As shown in Figure 4.5, the water flux slightly increased compared to the unmodified membrane. The lowest water flux (2.74 L.m^{-2}.hr^{-1}) was recorded for the sample modified at monomer concentration of 50 g/L and grafting time of 1 min. This result suggests that the formation of the carboxylic group on the membrane surface has facilitated the transportation of water molecules.

However, there is no clear trend in the water flux with the increase in monomer concentration and grafting time. For example, in the case of the membrane modified at grafting time of 1 min, the water flux fluctuates at different monomer concentrations. This suggests that the modification on this membrane support will generate an inconsistent data. Moreover, the membrane modified at lower monomer concentrations (5 g/L and 15 g/L) generates higher water fluxes compared to higher monomer concentrations (30 g/L and 50 g/L). These trends are contradicted by the result from the water permeability in Section 4.3.1. Specifically, the largest water permeability value was obtained for the membrane modified using the monomer concentration of 30 g/L.

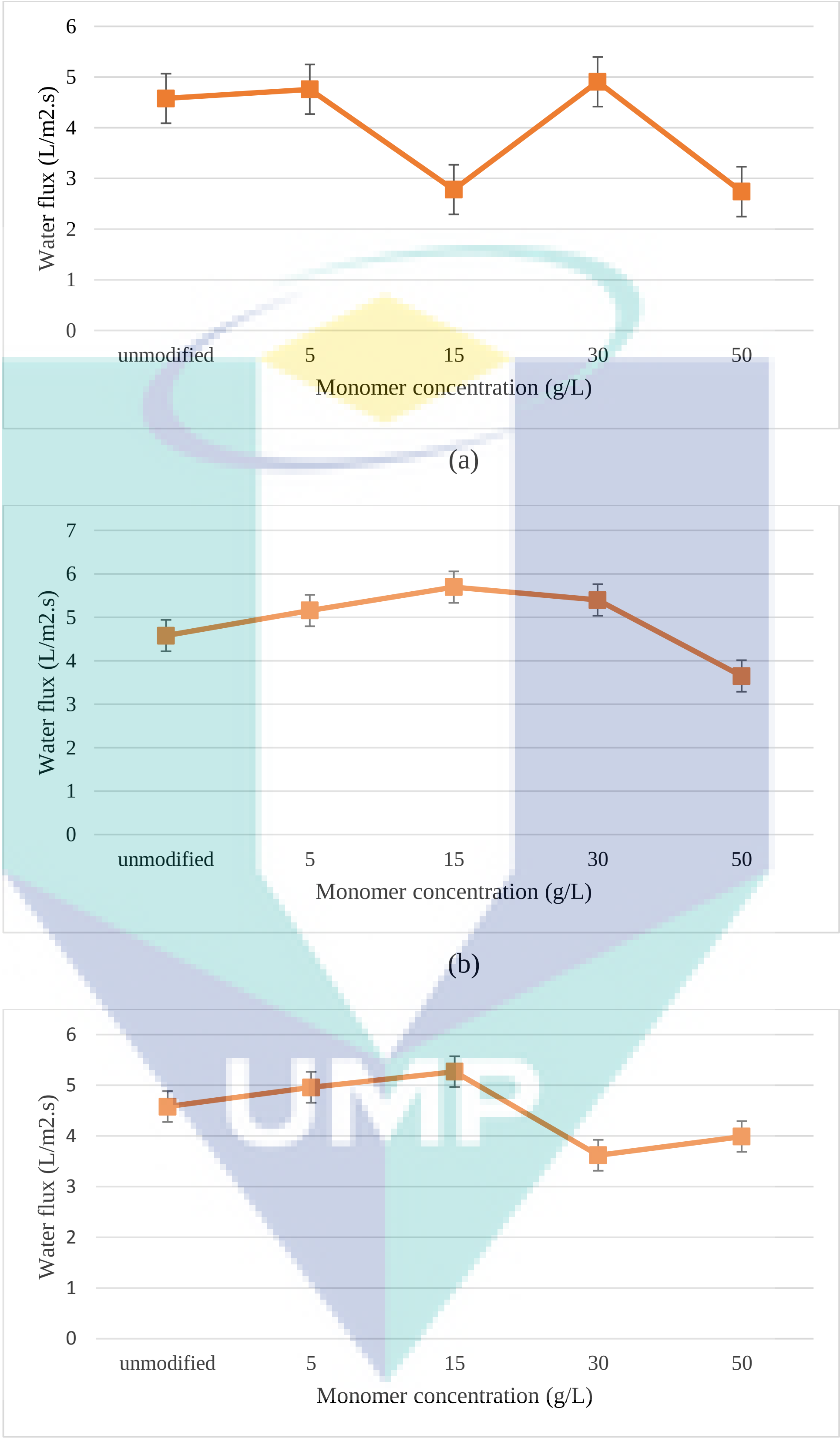

(c)

Figure 4.5 Water flux (J_v) of UFPES membrane modified at different UV grafting time of (a) 1 min, (b) 3 min, and (c) 5 min

4.2.3 Salt rejection

The salt rejection, solute permeability and the ratio of B/A are presented in Table 4.1. The UFPES membrane does not have the ability to retain the 200 ppm of sodium chloride. Even after surface modification via UV-photografting, the rejection rate is still below 1 %. The experiments were conducted using the stirred cell at a pressure of 3 bars. The value for solute permeability and the ratio of B/A are very high as the value of salt rejection is very low. This is an initial indication that the UFPES is not suitable for FO application.

Table 4.1 Salt rejection of unmodified and modified UFPES membranes

Membrane	**Salt rejection, R** (%)	**Solute permeability, B** ($x10^3$ L.$m^{-2}hr^{-1}$)	**B/A** (bar)
Unmodified	0.39	12.40	124.8
5UF-1	3.94	12.43	126.9
5UF-3	4.40	11.37	104.8
5UF-5	4.65	11.03	90.2
15UF-1	2.28	22.75	172.8
15UF-3	3.78	13.70	90.0
15UF-5	9.05	5.641	46.3
30UF-1	1.80	28.68	178.0
30UF-3	4.13	12.32	71.9
30UF-5	4.05	12.37	67.7
50UF-1	4.29	11.83	103.6
50UF-3	10.2	4.681	50.1
50UF-5	1.91	25.55	261.1

4.2.4 Solute permeability

Figure 4.6 shows the value of solute permeability using 50 g/L of acrylic acid at different grafting time up to 60 min. As can be seen, the solute permeability of the modified membrane allows a normal reaction only in the first three samples where the grafting time was 1 min, 3 min and 5 min, respectively. As the grafting time was increased from 10 min onwards, the solute permeability began to reveal negative values. The experimental data shows a higher value of what in the permeate solution compared to the feed solution. To obtain a qualitative data, the salute permeability test was conducted using the samples that were previously used in water permeability analysis.

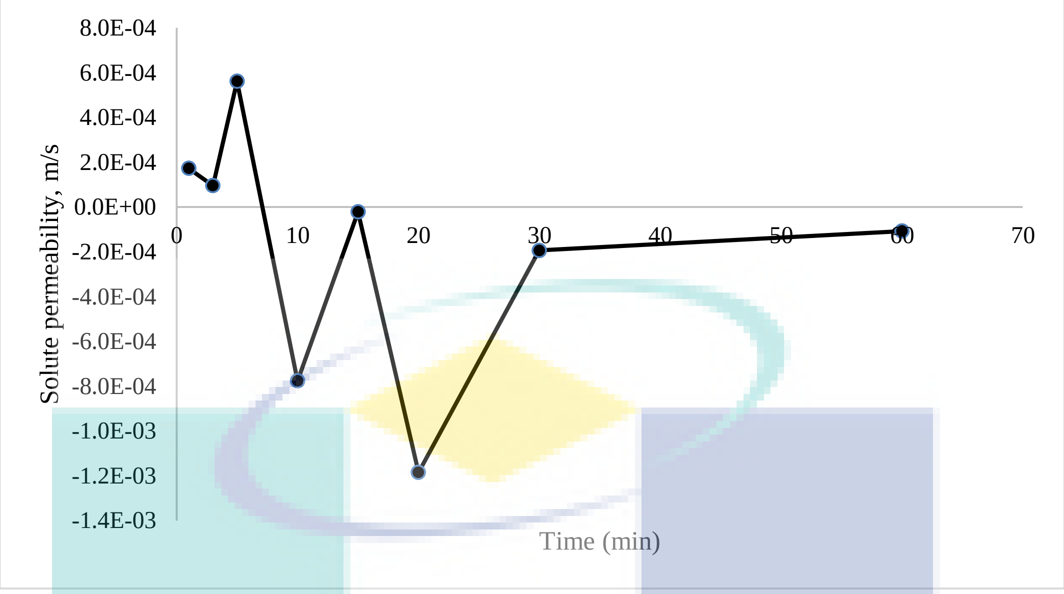

Figure 4.6 Solute permeability of the modified UFPES membrane at 50g/L of monomer concentration

As the grafting time starts to increase from 10 min onwards, the solute permeability starts to decrease from -7.7 x 10^{-4} ms^{-1} and the values remain on the negative side as the grafting time reaches 60 min. This phenomenon is identified as negative retention. Negative retention is the existence of “preferable” material that can pass through the membrane layer regardless of its size (Volkov, A. et al., 2014). In other words, the modified membranes have an interest in transporting selective material which in this research is the monovalent salt; sodium chloride (NaCl). Notably, this halophile property was detected on the modified membrane. Interestingly, this study also got the negative retention in FO application. Similar trends have also been identified by Vatanpour, V. et al. (2011) by using NaCl, sodium sulphate (Na_2SO_4) and magnesium sulphate ($MgSO_4$). Specifically, NaCl in the feed solution has been observed to have high interaction with the membrane material and consequently, becomes preferential transport.

According to Schaep, J. et al. (2001), NaCl is a single salt and this characteristic is suitable for determining the membrane charges. In the extended Nersk-Planck equation, the equation represents the transport mechanism involving diffusion, electric field gradient and convection. The existence of negative rejection in NaCl indicates that the behaviour of the modified membranes could be classified by a combination of diffusion and Donnan exclusion mechanism (Bhanushali, D. et al., 2002). Donnan exclusion in this context is defined as the reduction of ions in the feed solution due to the presence of fixed carboxylic group bearing the same sign as the mobile ions. It is however worthy of note that the rejection of a charged solute depends on the pore radius of the effective membrane and the two electrical parameters, namely the effective membrane charge density and the dielectric exclusion energy barrier (Qiu, C. Q. et al., 2006).

Furthermore, this charged solute is dependent on the ionic strength, the valence of the solutes and the concentration of the feed solution (Nilsson, M. et al., 2008; Schaep, J. et al., 2001). It is quite impossible to differentiate which ions penetrate more in the modified membrane since the flux for Na^+ and Cl^- are nearly equimolar (Phillip, W. A. et al., 2010). Nevertheless, it is well known that the interaction between the carboxylic group on the membrane surface and the NaCl feed solution are either by dissociation of functional groups or adsorption of ions from the solutions (Elimelech, M. et al., 1994). This would cause the ions in the feed solution to be attracted to the permeate solution.

4.2.5 Structural parameter and reverse salt diffusion

The membrane structural parameter, S, is an intrinsic membrane parameter used to determine the degree of ICP in the porous support of the membrane (Park, M. et al., 2011). It is useful in quantifying the mass transport length scale across the membrane support layer (Tiraferri, A. et al., 2013). Hence, the aim of having a surface modification is to lower the value of the structural parameter. In the solute permeability, it was found that the carboxylic group on the membrane surface causes a negative rejection as the grafting time increases. This indicates that the diffusion transport of salts within the membrane plays a crucial role in regressing the FO processes.

Since the negative rejection starts to develop as the grafting time increases from 10 min onwards, the measurement of the structural parameter is only applicable to samples grafted at 1 min, 3 min and 5 min. It is worthy of note that under minimal modification (5UF-1min), the value decreases to 54 x 10^{-3} m which shows that surface modification on PES membrane via UV-photografting has great potential and is comparable with the pristine UFPES membrane. However, the performance of the modified membrane in Table 4.2 contradicts the expected result. For example, for the modification using 30 g/L of monomer concentration, the values of S obtained are 38 x 10^{-3} m, 73 x 10^{-3} m and 1.1 x 10^{-3} m while at 50 g/L of monomer concentration, the values obtained are 1.1 x 10^{-3} m, 1.4 x 10^{-3} m and 33 x 10^{-3} m. The structural parameter value increases due to the decrease in water permeability and the low value of solute permeability.

On the other hand, the value of RSD for the modified UFPES membranes increased compared to the unmodified (12.46 g.m^{-2}hr^{-1}) membrane. The UFPES membrane is unable to retain the salt in the draw solution. Unfortunately, once the salt is able to easily penetrate the semipermeable membrane in the FO system, the whole system will experience a high cost in an attempt to replenish the draw solution.

Table 4.2 Structural parameter and RSD of UFPES membrane

Membrane	**Structural parameter, S** (10^{-3}m)	**Reverse salt diffusion** (g.m^{-2}hr^{-1})
Unmodified	33	12.46
5UF-1	52	33.15
5UF-3	56	26.56
5UF-5	66	54.99
15UF-1	68	29.25
15UF-3	58	29.64
15UF-5	1	30.63
30UF-1	38	26.57
30UF-3	73	14.83
30UF-5	1.1	23.11
50UF-1	1.1	40.27
50UF-3	1.4	35.29
50-UF-5	33	21.78

4.3 Characterization of UFPES membrane

4.3.1 Functional group analysis

To confirm the effectiveness of the modification via UV-photografting, the membrane was analysed using ATR-FTIR. The spectra for unmodified and modified (15AA-3min) membranes were illustrated in Figure 4.7. Obviously, new peaks are formed at a wavelength of 1721 cm^{-1} in the spectra of the modified membranes (15AA-3min) in comparison to the spectra of the unmodified membrane. This can be attributed to the new carboxyl group (Abu Seman, M. N. et al., 2010a).

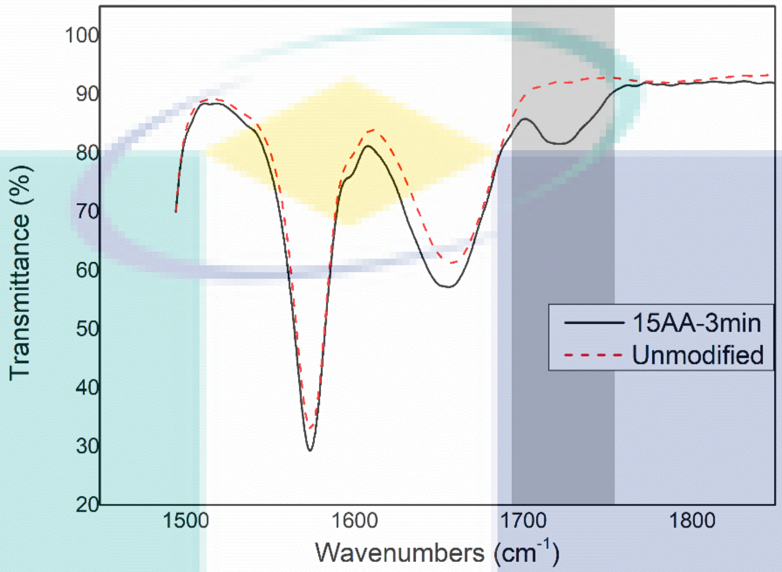

Figure 4.7 ATR-FTIR spectrum of modified and unmodified UFPES membranes

4.3.2 Surface morphology

The cross-section of the UFPES membrane was characterised by FESEM and the images are shown in Figure 4.8. One of the downsides in using the UF membrane to determine the cross-section is that the support layer must be removed before any sample can be observed. The support layer prevents the sample from getting fractured easily even after a prolonged time of immersion in liquid nitrogen. After the active layer was separated from the support layer, the sample was coated with platinum for characterization process.

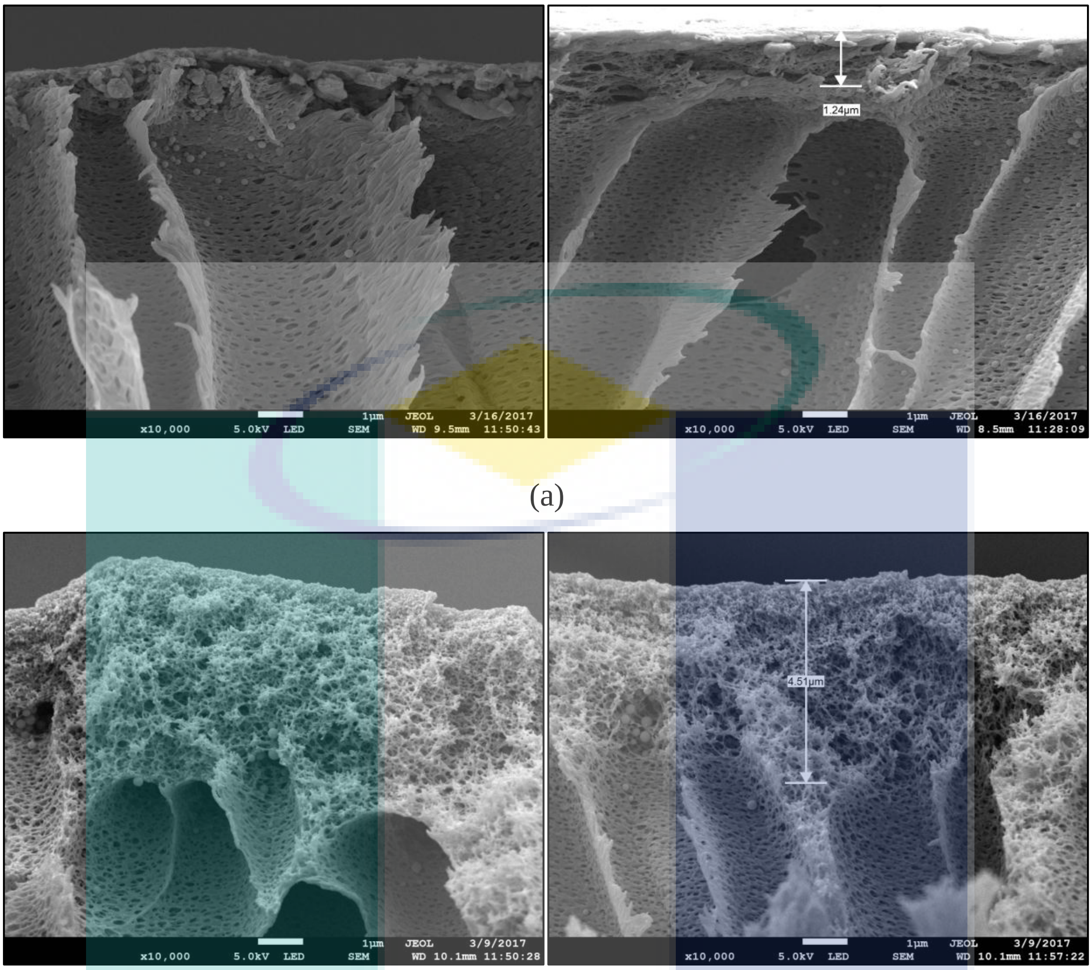

(a)

(b)

Figure 4.8 Cross section of (a) unmodified and (b) 50UF-5 membranes

As can be seen from the image, a skin layer is present on the active layer of the UF membrane which resembles a finger-like structure. The finger-like structure is believed to have formed during the phase inversion process. The active layer of the unmodified membrane is 1.24 µm as manufactured. Compared with the modified membrane (50UF-5), the active layer has increased to 4.51 µm. A uniform dense top layer was formed on the modified membrane and as can be observed, the uniform layer cosists of interconnected holes reduces the initial pore size of the UF membrane. This is believed to be the new polyacrylic layer with carboxyl functional group as reported previously (Wang, D. et al., 2011).

4.3.3 Hydrophilicity

The contact angle was commonly used to identify the hydrophilicity or hydrophobicity of the membrane. However, this measurement is subjected to debate as the value are affected by hydrophilicity, roughness, porosity, pore size, and its distribution of the data (Li, S.-S. et al., 2016). In this study, the value of hydrophilicity was obtained from unmodified and modified membrane using the monomer concentration of 50 g/L acrylic acid and at different grafting time (10-60 min). From Figure 4.9 the value of experimental data does not clearly indicate whether there is an increase or a decreasing trend in hydrophilicity.

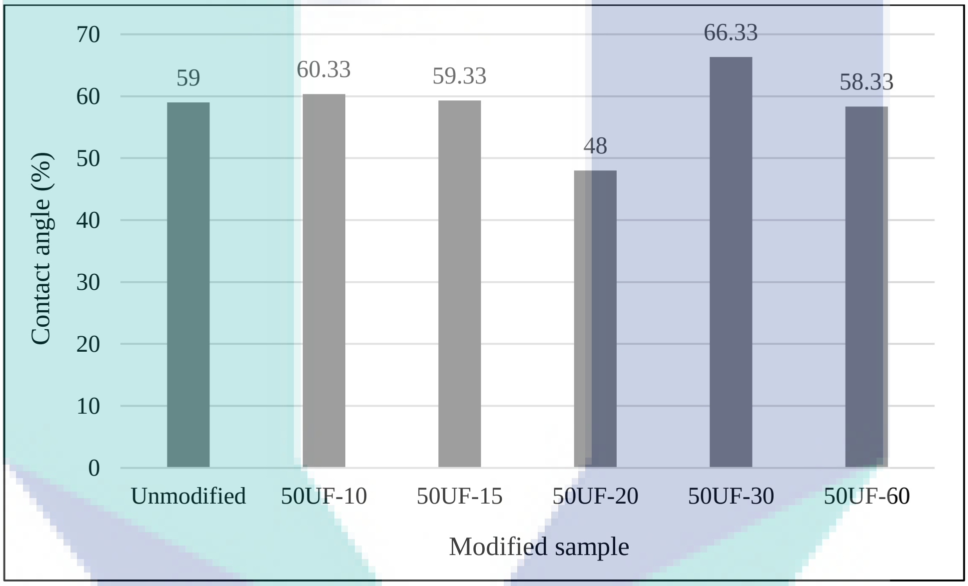

Figure 4.9 Hydrophilicity of the unmodified and modified UFPES membranes

The hydrophilicity was increased as the value of contact angle on the modified membrane was lower than the unmodified membrane. However, the experimental data does not provide a clear picture to indicate that the addition of carboxylic group on the membrane surface contributes to the increase or decrease of the membrane hydrophilicity. Unmodified membrane with the contact angle value of 59% shows an inconsistent data after modification.

This is attributed the morphological changes on the membrane surface whereby the surface of the fabricated carboxyl layer was not smooth. Similar study on the hydrophobicity of PES is well documented by Zhao, C. et al. (2013) who reported that in most cases, the membrane often tends towards increased hydrophilicity at the selected application. Hence, it may be inferred that the hydrophilicity of the modified UFPES membrane do not significantly increase after modification. Notably, this aligns with the water flux as reported in the previous section.

4.3.4 Summary of UFPES membrane

In the previous sections, the applicability of surface modification on UFPES membrane for the FO application is presented. Notably, the unmodified UF membrane has the water permeability of 99.41 L.m^{-2}hr^{-1}.bar^{-1}, solute permeability of 12.4 L.m^{-2}hr^{-1}, salt rejection of below 1 percent, water flux in FO mode at 4.58 L.m^{-2}hr^{-1}, as well as the RSD value of 12.46 g.m^{-2}hr^{-1}. The membranes were characterized with ATR-FTIR, FESEM and hydrophilicity. The results show that the unmodified membrane was unsuitable for the FO technology. The main reason for the rejection of this membrane support was the low value of the salt rejection. As such, this membrane support does not seem to have the capacity to retain the draw solution from entering the feed solution.

However, previous research has modified the surface of nano-porous PES membrane using the UV-photografting technique (Rahimpour, A., 2011). The results show that the surface mean pore size decreased from 15.8 nm to 3.9 and 5.5 nm using the acrylic acid (AA), 2-hydroxyethylmethacrylate (HEMA) and 1,3-phenylenediamine (mPDA) as the monomers.

It was initially hypothesized that the UF membrane will experience a pore size reduction after undergoing the surface modification process. Interestingly, modified membrane does not produce a significant improvement upon modifications. In fact, the salt rejection remained low which will restrict the application of this membrane support in FO system. Thus, it can be inferred that the UFPES membrane is not suitable for the FO application. However, there is the possibility for this membrane support to suit another FO application which uses a bigger molecular size as the draw solute.

4.4 Filtration properties of NFPES membrane

The second membrane support is the commercial nanofiltration polyethersulfone (NFPES) membrane. The experimental procedure for NFPES membrane is similar with the UFPES membrane except for the operating pressures. NFPES requires higher pressure to generate the permeate, thus the initial pressure was 4 bars.

This is due to the smaller pore size and porosity of the membrane itself. The water flux is 36.52 L.m^{-2}hr^{-1} at 4 bars of applied pressure and 63.93 L.m^{-2}hr^{-1} at 7 bars. Thus, the water permeability for NF membrane was 9.0 L.m^{-2}hr^{-1}bar^{-1} as shown in Figure 4.10. Notably, the value of water permeability for NFPES membrane was measured over the range of 4-8 bars.

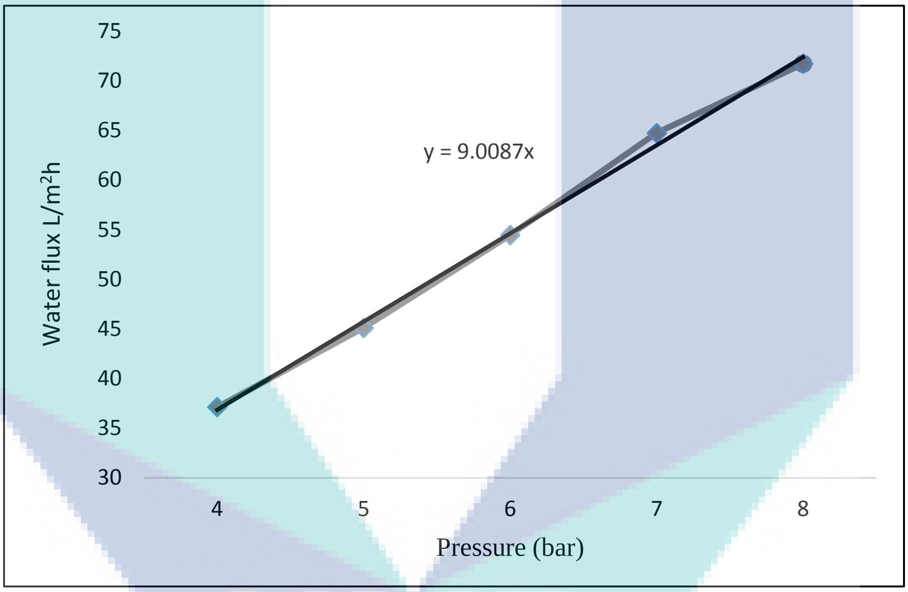

Figure 4.10 Water permeability of unmodified NFPES membrane

4.4.1 Water permeability

The result of water permeability (A), is shown in Table 4.3. In the modification of the membrane, each of the monomer concentrations (5, 15, 30 and 50 g/L) was UV-grafted at different grafting times (1, 3 and 5 min). The surface modification techniques follow the same protocol as in the UFPES membrane. However, the NF membrane support requires a higher pressure to generate the permeate. Thus, the value of A was obtained at the constant pressure of 7 bars. The experimental works were repeated three times to obtain the average measurement values.

Table 4.3 Water permeability for NFPES membrane

Membrane	**Monomer concentration (g/L)**	**Grafting time (min)**	**Water permeability ($L.hr^{-1}.m^{-2}.bar^{-1}$)**
5NF-1	5	1	7.37 ±0.26
5NF-3	5	3	8.11 ±0.05
5NF-5	5	5	6.84 ±1.08
15NF-1	15	1	10.67 ±1.81
15NF-3	15	3	7.37 ±0.26
15NF-5	15	5	8.39 ±0.26
30NF-1	30	1	6.91 ±0.95
30NF-3	30	3	7.34 ±0.29
30NF-5	30	5	7.39 ±0.24
50NF-1	50	1	7.91 ±0.03
50NF-3	50	3	8.39 ±0.47
50NF-5	50	5	7.89 ±1.12

In the graft polymerization technique, there are competitive mechanism between effective grafting and chain scission whereby only one mechanism will dominate at a time (Kaeselev, B. et al., 2002). Sample 15NF-1 exhibited an increase in water flux after being subjected to chain scission mechanism. This mechanism is attributed to pore enlargement where the membrane experienced severe pore enlargement through extensive chain scission.

A similar trend in the increase of water permeate flux for modified membrane was also observed by Abu Seman et al. (2010a). The pore size was smaller for the modified membrane compared to the unmodified one, which results in higher water flux. Similar trends were recorded by Puro et al. (Puro, L. et al., 2006) in their similar research on modification of PES membranes (NTR 7450, Nitto-Denko). Invariably, water permeation increased for the modified membrane due to pore size enlargement.

The effective grafting mechanism influences the water permeates flux on the modified membrane. Rahimpour, A. (2011) reported that PES membrane was affected as the mean pore size decreased upon surface modification. Smaller pores were formed due to the formation of monomer chains on the membrane surface. Meanwhile, at the lowest monomer concentration (5 g/L), some molecules penetrated the membrane pores during the immersion process and then underwent polymerization processes.

The penetration occurred deep within the pores and narrowed the membrane pores. It correlates with the experimental data for sample 5NF-5 as it was grafted using the lowest monomer concentration (5 g/L) and the highest grafting time (5 min). Thus, the development of compact membrane matrix has maximized the amount of effective grafting once it penetrates deep into the pores (Abu Seman, M. N. et al., 2012). Hence, the reduction in water permeability is correlated with the reduction of pore size due to effective grafting inside the membrane, which occurs due to the use of lower monomer concentration.

On the other hand, the detrimental effect was recorded for samples 30NF-3, 30NF-5, and 50NF-1. The results were poorer compared to the unmodified membrane in terms of B and salt rejection. The reduction of membrane performance is attributed to the increase of pore size as PES membrane is dependent on pH value (Deng, B. et al., 2009). The pore size increased coincidently with the decrease of pH value.

As presented in Table 4.4, it can be seen that as monomer concentration increased, pH value decreased. This indicates that salt rejection value fluctuates at higher monomer concentrations (30 and 50 g/L), where the pH value is less than 3. The increase in pore size on the membrane surface enhanced the penetration of draw solution into feed solution (Shim, J. K. et al., 1999). Thus, two factors of pore enlargement, i.e. chain scission and pH effect, contributes to the drawback of PES application.

Table 4.4 pH of different monomer concentrations

Monomer concentration, g/L	**pH**
5	3.5
15	3.2
30	2.7
50	2.2

4.4.2 Salt rejection and solute permeability

The salt rejection, solute permeability and the ratio of B/A are presented in Table 4.5. As can be seen, the unmodified NFPES membrane has the value of 59% of salt rejection using the 200 ppm of sodium chloride as the feed solution. Noteworthy, the value of salt rejection decreases in the modified membrane. Similar trend is recorded in the value of solute permeability. It is postulated that the membrane experienced pore enlargement, leading to decreased ability to retain the salt (She, Q. H. et al., 2012b). Hence, the volume of sodium chloride which was originally in the draw solution might have been facilitated across the membrane to the feed side.

Table 4.5 Separation properties of NFPES membrane

Membrane	**Salt rejection, R (%)**	**Solute permeability, B (x10L.h-1m-2)**	**B/A (bar)**
Unmodified	59	1.54	1.71
5NF-1	43	2.93	3.98
5NF-3	46	2.58	3.18
5NF-5	44	2.81	4.10
15NF-1	49	2.33	2.18
15NF-3	56	1.75	2.38
15NF-5	48	2.46	2.94
30NF-1	53	1.92	2.77
30NF-3	20	8.89	12.12
30NF-5	16	1.17	15.87
50NF-1	22	7.90	9.99
50NF-3	50	2.23	2.66
50NF-5	47	2.51	3.19

In sample 30NF-1, effective grafting exceeded chain scission, i.e. salt rejection of 53%. On the other hand, for sample 50NF-1, chain scission dominated the graft polymerization process, i.e. salt rejection of 22%, despite using low grafting time. A similar trend was observed in the graft polymerization process involving both effective grafting and chain scission. Unsurprisingly, under UV-photografting technique, polymer backbone undergoes two parallel competitive processes (Abu Seman, M. N. et al., 2012).

Interestingly, the membrane modified at the monomer concentration of 50 g/L produced a different result. The modified membranes at 3 and 5 min were comparable with the unmodified membrane in terms of salt rejection. This correlates with previous research in which higher monomer concentration is associated with higher effective grafting rate. Yu, H. Y. et al. (2010) claimed that in graft polymerization, the ratio of the active site to monomer concentration needs to be considered.

This is because as monomer concentration increases, the free radicals on the membrane surface have more chances to interact with the monomers, thereby resulting into higher grafting degree. A similar observed has been previously reported where hydrophilicity was found to initially decrease after which it increased (Zhao, G. W. et al., 2007). This observation was attributed to the degradation of substrates under UV irradiation.

The results of B/A are also presented in Table 4.5. Smaller B/A ratio shows more satisfactory performance in decreasing RSD from DS into FS in FO process (Niksefat, N. et al., 2014). Among the modified membranes, the monomer concentration of 15 g/L was found to be the best condition in the graft polymerization process.

Moreover, it gave high water permeability and low B/A ratio. Interestingly, the B/A value obtained from RO results is commonly used as an indicator of selectivity for FO membrane. However, this is not sufficient as the mass transport direction of the draw solutes (i.e. NaCl) in FO is completely opposite to that in RO (Kim, B. et al., 2014). Hence, another parameter namely specific reverse salt flux (J_s/J_v) was further evaluated through FO mode and correlated to B/A.

4.4.3 Water flux and reverse salt diffusion

Modified membranes had a water flux of four times higher compared to the unmodified membrane as shown in Figure 4.11 (a). Notably, the unmodified NFPES had a water flux of 0.75 $L.m^{-2}.h^{-1}$. Water flux increased drastically at the lowest monomer concentration of 5 g/L. This result suggests that the formation of the carboxylic group on the membrane surface has facilitated the transportation of water molecules. Sample 15NF-1 recorded the lowest water flux (1.55 $L.m^{-2}.h^{-1}$) compared to other samples modified at the same monomer concentration (15 g/L). This is believed to be due to lack of effective grafting as it was conducted at low grafting time (1 min). Normally, the original functional group at the membrane surface often tends to either repel the negative charges from the monomer or the number of energy received by phenoxyphenyl sulfone chromopores to values below the minimum energy necessary to form free radicals (Abu Seman, M. N. et al., 2012).

This indicates that the graft polymerization process must be conducted at selective grafting time as it has distinctive effective irradiation time (Shim, J. K. et al., 1999). Moreover, since graft polymerization is conducted at the lowest grafting time, there is a possibility that effective grafting does not form a uniform layer on the membrane surface. This inherent drawback has also been recorded in previous research where the grafting process diminished pore dimension and formed a non-uniform pore size distribution (Pieracci, J. et al., 2002).

However, monomer concentrations of 30 and 50 g/L showed declining values compared to lower monomer concentrations. The trend can be seen in Figure 4.11 (b) and (c). The enhanced grafted layer on the membrane surface leads to the reduction of water flux at higher monomer concentration. Effective grafting mechanism on membrane surface results in the thickening of the grafted layer, thereby increasing the flux resistance. The relationships of kinetics in photopolymerization can be explained by the use of high monomer concentration and a strong dose of UV energy (Bilongo, T. G. et al., 2010).

As discussed earlier, the graft polymerization process involves effective grafting and chain scission simultaneously. Effective grafting leads to the formation of smaller pores and increases in membrane thickness whereas chain scission is the mechanism that reduces membrane performances. During surface modification, larger amounts of carboxylic groups are formed on either the membrane surface or pore walls, which contribute to the increase in hydrophilicity. Hence, denser packing of monomers is generated on membrane layers.

Membrane surface is chemically modified and contributes significantly to water transport resistance and thus increasing water flux (Wang, Y. Q. et al., 2013; Yu, H. Y. et al., 2006). By looking at the trend of water flux, several assumptions could be made: (i) a significant increase in water flux for modified membrane, (ii) as monomer concentration increases, water flux decreases and RSD increases, and (iii) the increase in grafting parameter does not correlate with the increase in water flux. These assumptions are well corroborated by previous report on surface modification via UV-photografting technique (Shim, J. K. et al., 1999).

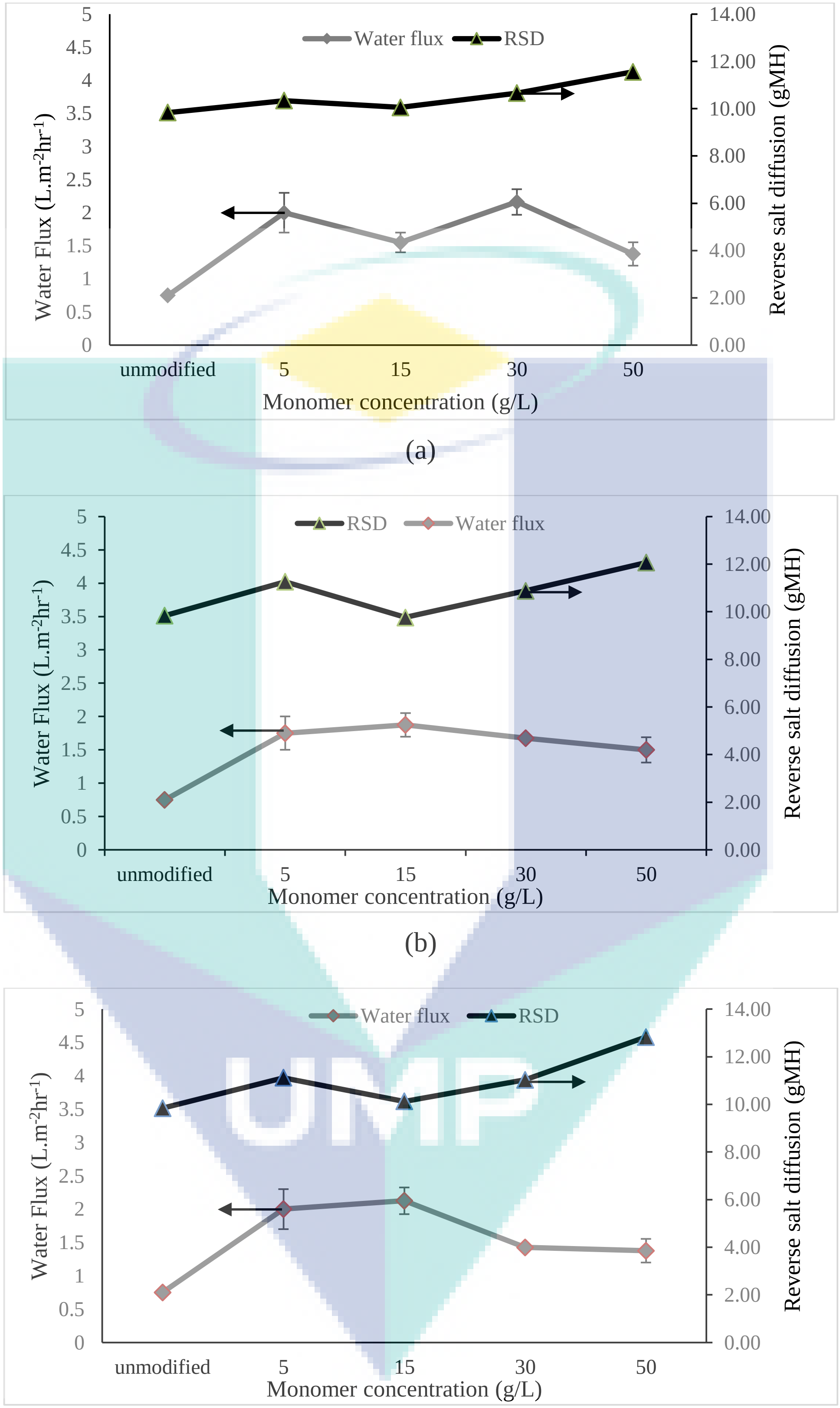

(a)

(b)

(c)

Figure 4.11 NFPES membrane modified at different UV grafting time of (a) 1 min, (b) 3 min, and (c) 5 min

The value of RSD for the unmodified membrane was 9.84 g.m^{-2}.h^{-1}. The highest value was recorded at 12.83 g.m^{-2}.h^{-1} (50NF-5) while the lowest value was 9.76 g.m^{-2}.h^{-1} (15NF-3). From the figures, similar trends in RSD could be observed. The values increased for the membranes grafted with 5 g/L of monomer concentration, decreased by 15 g/L and increased gradually for both 30 and 50 g/L.

In general, lower values in RSD were recorded for modified membranes using 15 g/L of monomer concentration whereas those modified with 50 g/L of monomer concentration showed a contrary trend. RSD is an unfavourable condition in FO system as it leads to various detrimental effects. Normally, modified membranes with the lowest RSD value are favourable in FO application.

From the Figure 4.11, the modified membranes using monomer concentration of 15 g/L showed the lowest RSD value and consistently high-water flux. It is also worthwhile to note that the values of water flux in both reverse osmosis (J_w) and FO (J_v) configuration in this study are not comparable. In fact, each of the data in each configuration provides a different set of values.

A comparison may be made for modified PES membrane using UV-the photografting technique in reverse osmosis (RO) configuration as reported earlier (Abu Seman, M. N. et al., 2010a). However, since the aim of this surface modification is in FO configuration, this makes it the first time it is being reported. As an initial conclusion, this study was aimed to obtain NF membranes with higher water fluxes achieved in FO configuration.

4.4.4 Structural parameter

Table 4.6 depicts the structural parameters of commercial, unmodified, and modified membranes. The membranes were denoted as thin-film composite (TFC) polyamide membrane, CTA, RO membrane made of TFC-PA (BW30), woven (W), non-woven (NW) and without backing layer (XW), NF, and PES. The value of S for the unmodified NFPES membrane was 28.02 mm.

Table 4.6 Structural parameters of commercial, unmodified, and modified NF membranes

Membrane	Manufacturer	Structural parameter, mm	Ref
TFC-NW	Toray Chemical Korea	0.461	(Nguyen, T. P. N. et al., 2015)
TFC-W	Toray Chemical Korea	0.266	(Nguyen, T. P. N. et al., 2015)
CTA-NW	Hydration Technology Innovation	1.38	(Wei, J. et al., 2011b)
CTA-W	Hydration Technology Innovation	1.00	(Wei, J. et al., 2011b)
BW30-NW	Dow FilmTec	37.5	(Wei, J. et al., 2011b)
BW30-XW	Dow FilmTec	14.0	(Wei, J. et al., 2011b)
SW30-W	Dow FilmTec	80.0	(Arena, J. T. et al., 2014)
NF-PES	Imfor Inc.	28.02	In this work
5NF-1		8.11	In this work
5NF-3		9.71	In this work
5NF-5		7.87	In this work
15NF-1		12.54	In this work
15NF-3		9.76	In this work
15NF-5		8.26	In this work
30NF-1		8.2	In this work
30NF-3		6.02	In this work
30NF-5		5.89	In this work
50NF-1		8.10	In this work
50NF-3		12.17	In this work
50NF-5		12.51	In this work

In surface modification via UV photografting, two components of the membrane were modified chemically and physically, namely active and support layers. The active layer was modified with carboxyl group while the support layer of PES membrane was modified either with the presence or absence of carboxyl group. Using UV light (λ = 365 nm), the photochemical modification technique not only took place at the surface but could penetrate up to 20 µm into PES membrane (Yamagishi et al., 1995). It could achieve the support layer of the membrane as the thickness of the thin top layer of the membrane was approximately 323.8 nm (as shown in Figure 4.12a).

It was postulated that UV energy was sufficient to penetrate almost 30% of the top part of the membrane support layer and thus changed the properties. Since PES is photosensitive, this polymer generates active sites via homolytic cleavage of a carbon-sulfur bond at the sulfone linkage or known as chain scission mechanism. This mechanism increases pore size, which leads to the increase of porosity on the support layer. In fact, He, D. M. et al. (2009) in a review paper mentioned that it is mainly attributed to polymer degradation by UV photografting.

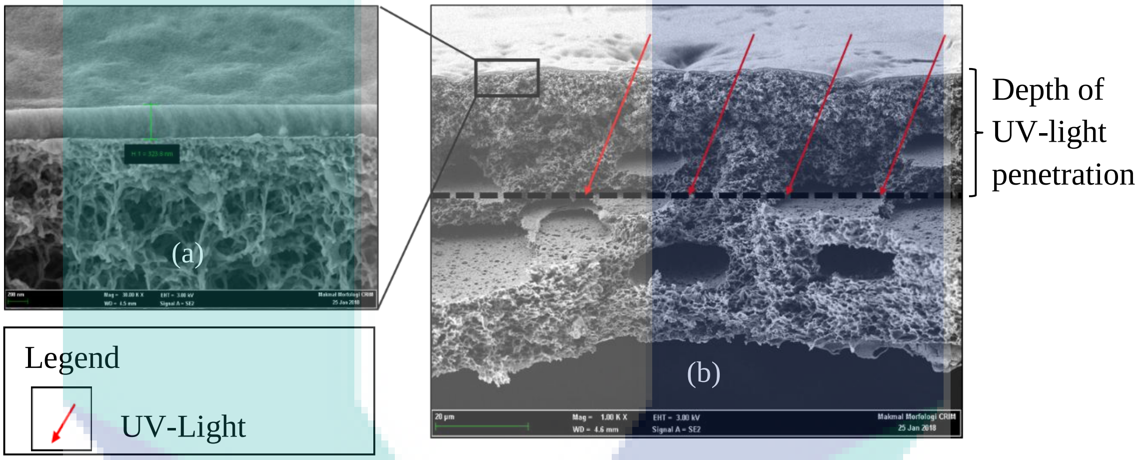

Figure 4.12 (a) Thin layer (323 nm) of the modified membrane and (b) thickness of the overall support layer (≈ 60 µm) where depth modification could achieve up to 20 µm of the support layer.

Unfortunately, this polymer degradation does not only influence the increase in porosity but also membrane tortuosity. The movement of water molecules across the membrane is facilitated as pore size increases, thus tortuosity value decreases. Therefore, physical changes on support layer are dominant using this surface modification technique. Experimentally, the value of the structural parameter on modified membrane exhibits significant reduction by a marginal percentage.

In fact, this reduction correlates with the reduction of internal concentration polarization (ICP) (Qasim, M. et al., 2015). It justifies that surface modification via UV photografting reduces the structural parameter, thus facilitates higher water molecules across the semi-permeable membrane. The ICP effect on FO membrane can be reduced by lowering structural parameter by means of high hydrophilicity, low tortuosity, and high porosity, which allow for higher water flux (McCutcheon, J. R. & Elimelech M., 2006). In comparison to the unmodified membrane, the performance of modified membranes was enhanced as the modification lowered the structural parameter value.

4.4.5 Specific reverse salt flux

The specific reverse salt flux for the experimental and predicted data is depicted in Figure 4.13. The predicted value of J_s/J_v was measured using values of B/A obtained from RO results as presented in the sub-section 4.4.2. For the unmodified membrane, the experimental result was different from the predicted one. This is because the unmodified membrane had the lowest water flux (0.75 L.m^{-2}.h^{-1}) and relatively high solute permeability (9.84 g.m^{-2}.h^{-1}).

At lower monomer concentrations (5 and 15 g/L), the values for specific reverse salt flux were low compared to the values at higher concentrations. This is a good indicator that the modified membranes are better in FO application upon modification at lower monomer concentration. Furthermore, the variation between experimental and predicted results is low as the penetration of draw solution into feed solution is minimal.

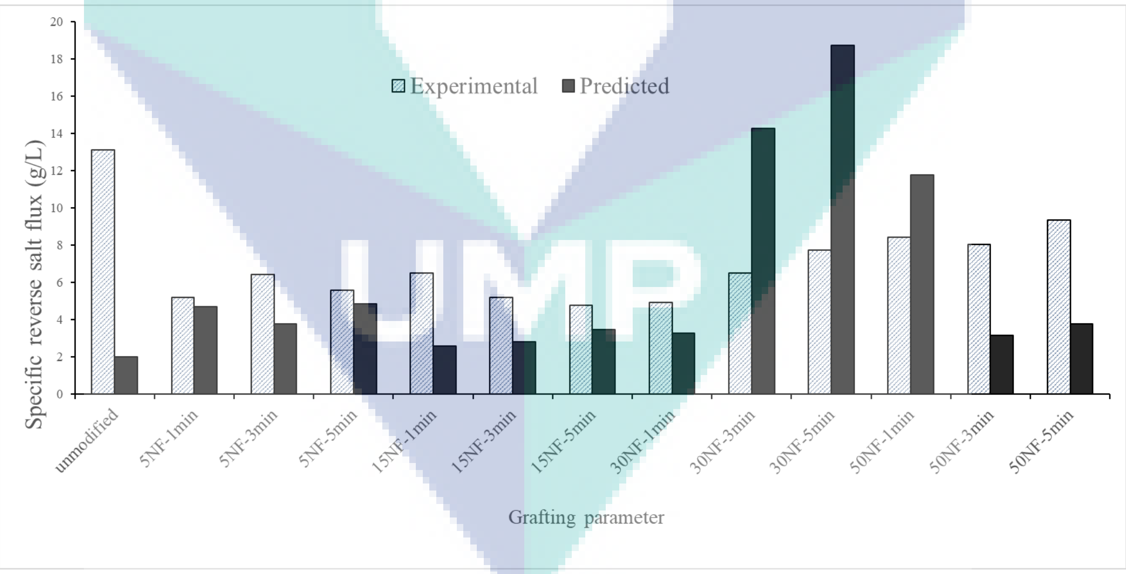

Figure 4.13 Specific reverse salt fluxes for NFPES membrane

However, the differences were obvious for the samples grafted at higher monomer concentrations, especially for samples 30NF-3, 30NF-5, and 50NF-1. These three samples suffered the highest specific reverse salt flux both experimentally and theoretically due to unexpected lower salt rejection in reverse osmosis mode. In general, lower monomer concentrations (5 and 15 g/L) are better compared to higher monomer concentrations (30 and 50 g/L). Therefore, it can be inferred that the lower monomer is a good option for surface modification via UV-photografting. Hence, it is thought that lower monomer concentration is more appropriate for the optimization of modified membrane. The details of optimization on the modification of NF using UV-photografting are presented in section 4.9.

4.5 Characterization of NFPES membrane

4.5.1 Functional group analysis

The chemical composition of both unmodified and modified membranes can be determined using ATR-FTIR as shown in Figure 4.14. The additional peaks at 1710–1721 cm^{-1} that correspond to carboxyl group bands were found on samples (b) and (c), proving that the functional group was successfully grafted on the surface of NFPES membrane (Mansourpanah, Y. & Habili E. M., 2013).

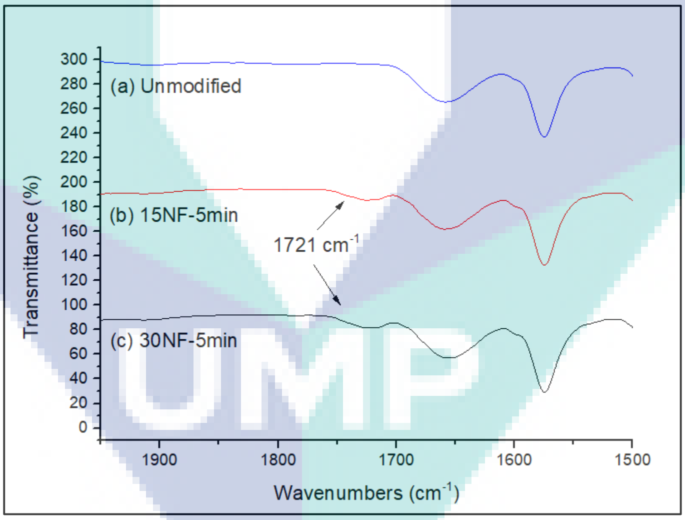

Figure 4.14 ATR-FTIR spectra for (a) unmodified and (b) 15NF-5, and (c) 30NF-5

4.5.2 Elemental analysis

XPS analysis was conducted to confirm the functional group on the membrane. Based on the chemical structure, the unmodified membrane has three different chemical bonds (C-C, C-O and C=O) as shown in Figure 4.15 (a). The modified membrane, however, has an additional chemical bond (O=C-OH) as presented in Figure 4.15 (b). This carboxyl functional group was measured at a binding energy of 287.83 eV which contribute about 3.2 per cent to the total area.

A similar trend was reported by Yeo, G. C. et al. (2017) in the development of irreversible immobilization of bioactive proteins and peptides on a PES. In addition, Wavhal, D. S. and Fisher E. R. (2002) found that the modified PES membrane with acrylic acid fabricated through low-temperature plasma-induced graft polymerization has recorded a similar trend in XPS results.

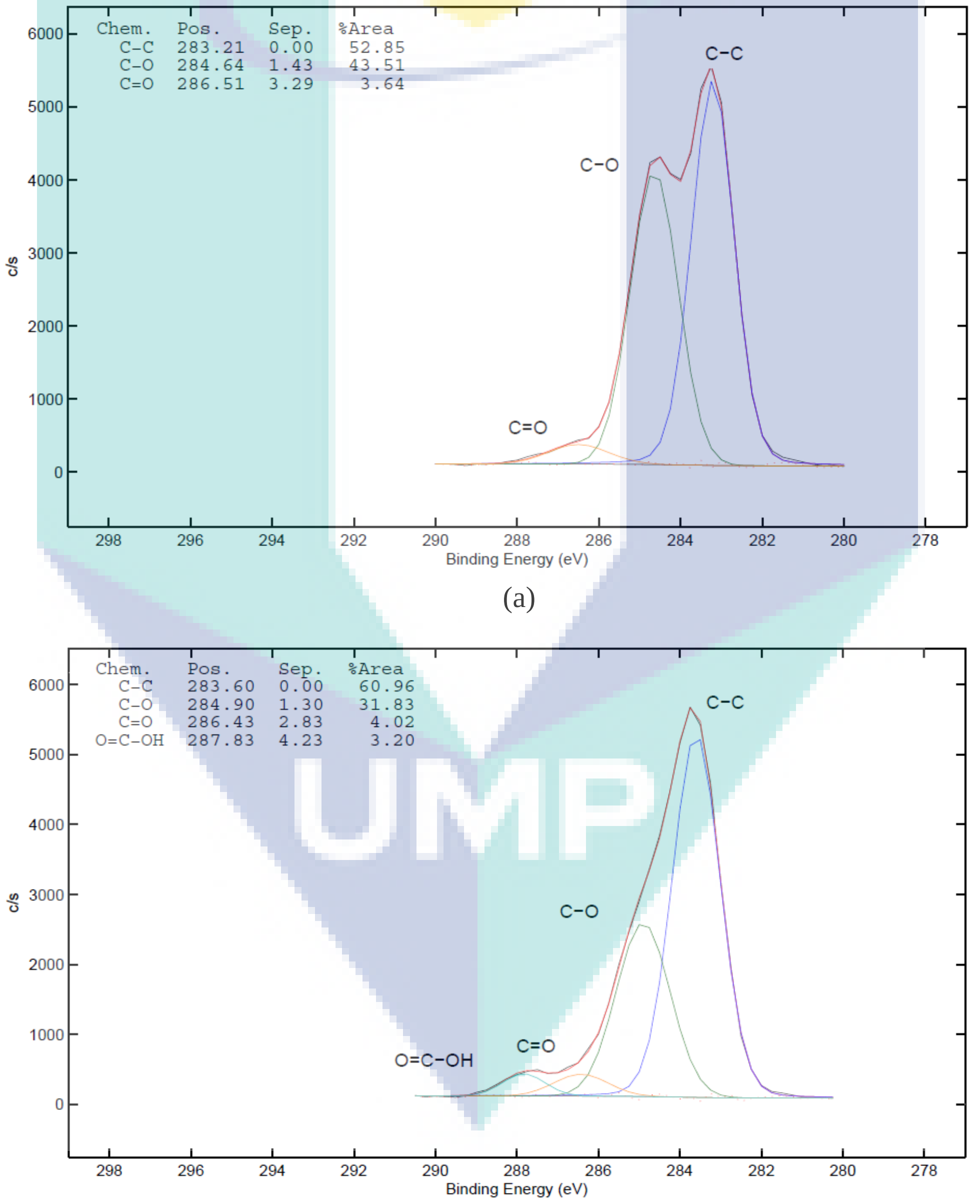

(a)

(b)

Figure 4.15 XPS spectra for (a) unmodified NFPES membrane and (b) modified membrane (30NF-5)

4.5.3 Surface roughness

The AFM results present the roughness (S_a), root-mean-square roughness (RMS, S_q), and maximum peak (S_z) for unmodified and modified membranes as shown in Table 4.7. Initially, it was expected that surface roughness would increase upon surface modification. However, only samples 30NF-1 and 50NF-3 experienced great changes. The lower roughness of modified membranes could be due to graft polymerization process, which results in the formation of a smooth surface on the membranes.

Table 4.7 Surface roughness of NFPES membrane

No.	Membrane	Roughness (S_a, nm)	Root mean square (S_q, nm)	Maximum peak (S_z, nm)
1	Unmodified	1.28	1.71	17.99
2	5NF-1	1.28	1.68	11.94
3	5NF-3	1.61	2.12	15.53
4	5NF-5	0.73	1.02	6.07
5	15NF-1	1.75	2.68	24.93
6	15NF-3	1.47	2.02	15.58
7	15NF-5	1.40	1.80	14.79
8	30NF-1	22.67	28.84	95.97
9	30NF-3	1.44	1.98	20.57
10	30NF-5	1.44	2.08	24.75
11	50NF-1	1.36	1.85	10.77
12	50NF-3	13.72	21.23	113.99
13	50NF-5	1.48	2.11	11.05

The AFM analysis in Figure 4.16 to Figure 4.19 shows the images of the tridimensional and topographic surface of NFPES membranes. The dark areas represent pores while the brighter regions correspond to developed peaks. As can be seen, at lower monomer concentrations of 5 and 15 g/L, surface roughness decreased as grafting time increased.

At smaller pores, the dimensions obtained by AFM were only reflected by the convolution between the tip and pore shapes (Bowen, W. R. et al., 1997). The differences in AFM values were due to the grafting parameters of monomer concentration and grafting time that were applied to PES membrane to form carboxyl layer.

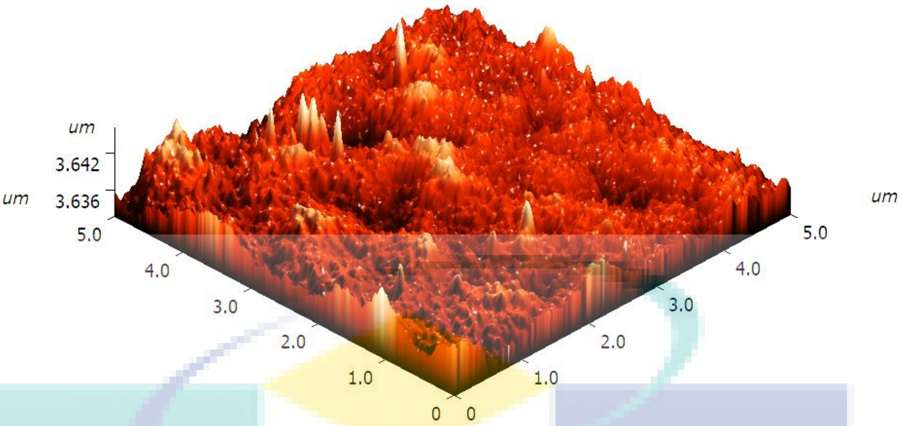

5NF-1

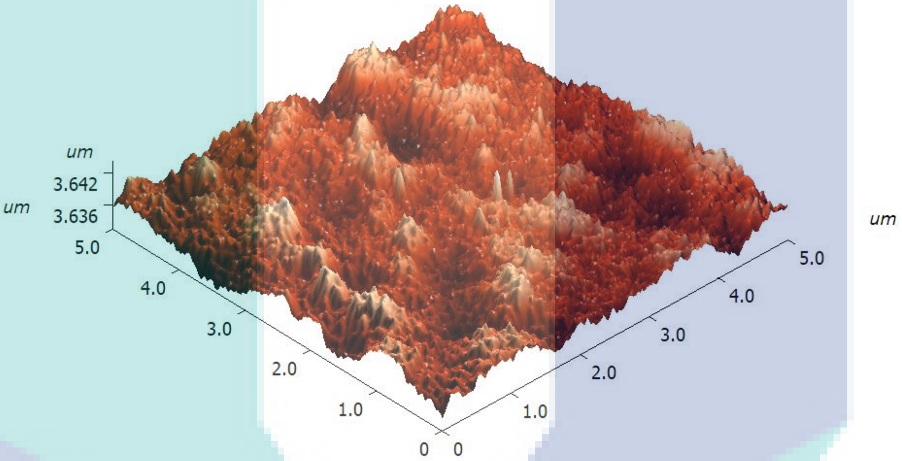

5NF-3

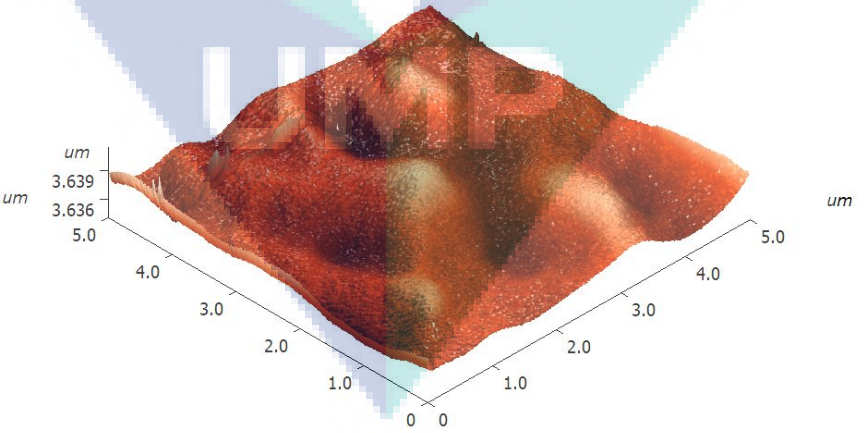

5NF-5

Figure 4.16 The effect of time at monomer concentration of 5 g/L

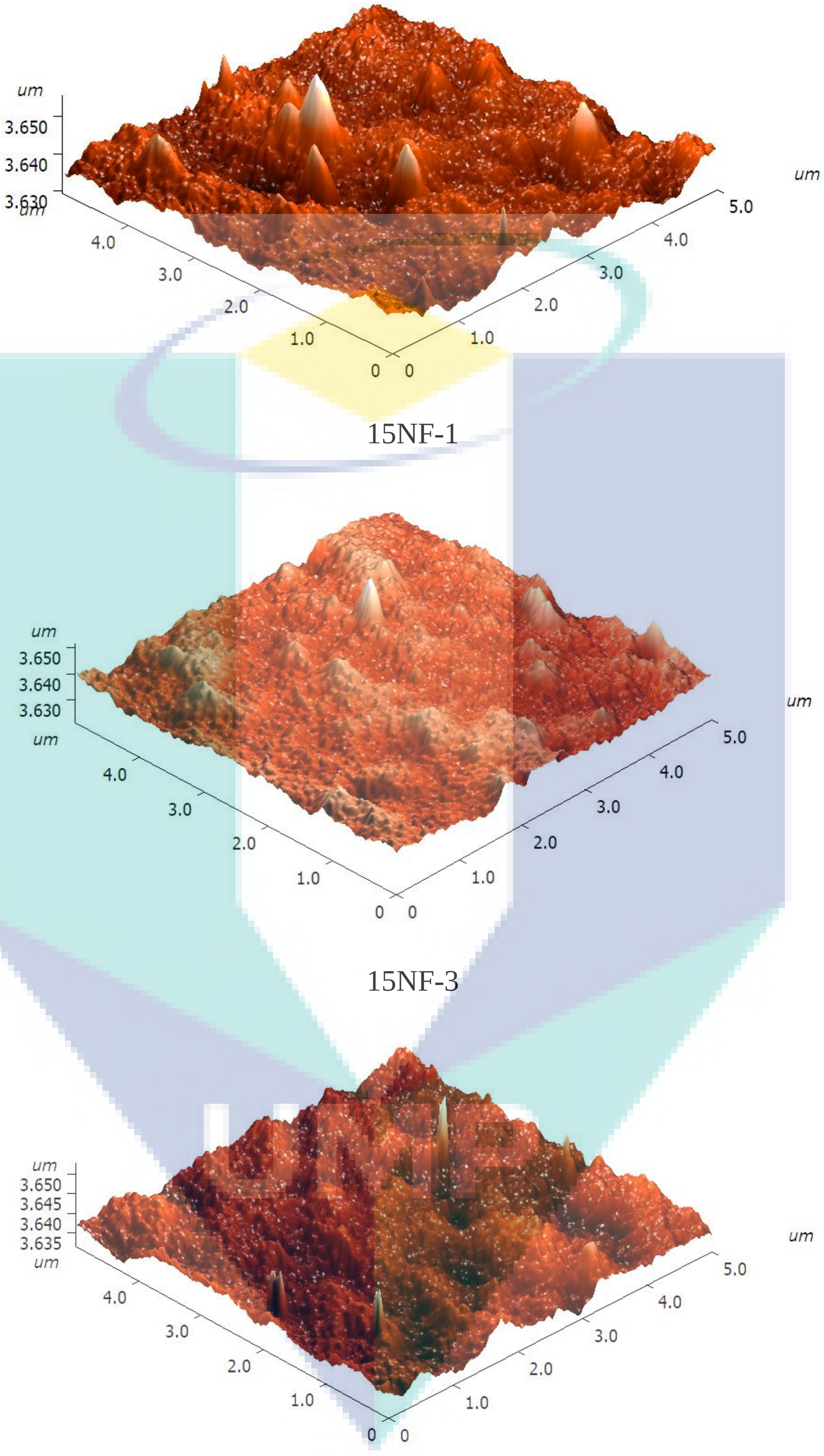

15NF-1

15NF-3

15NF-5

Figure 4.17 The effect of time at monomer concentration of 15 g/L

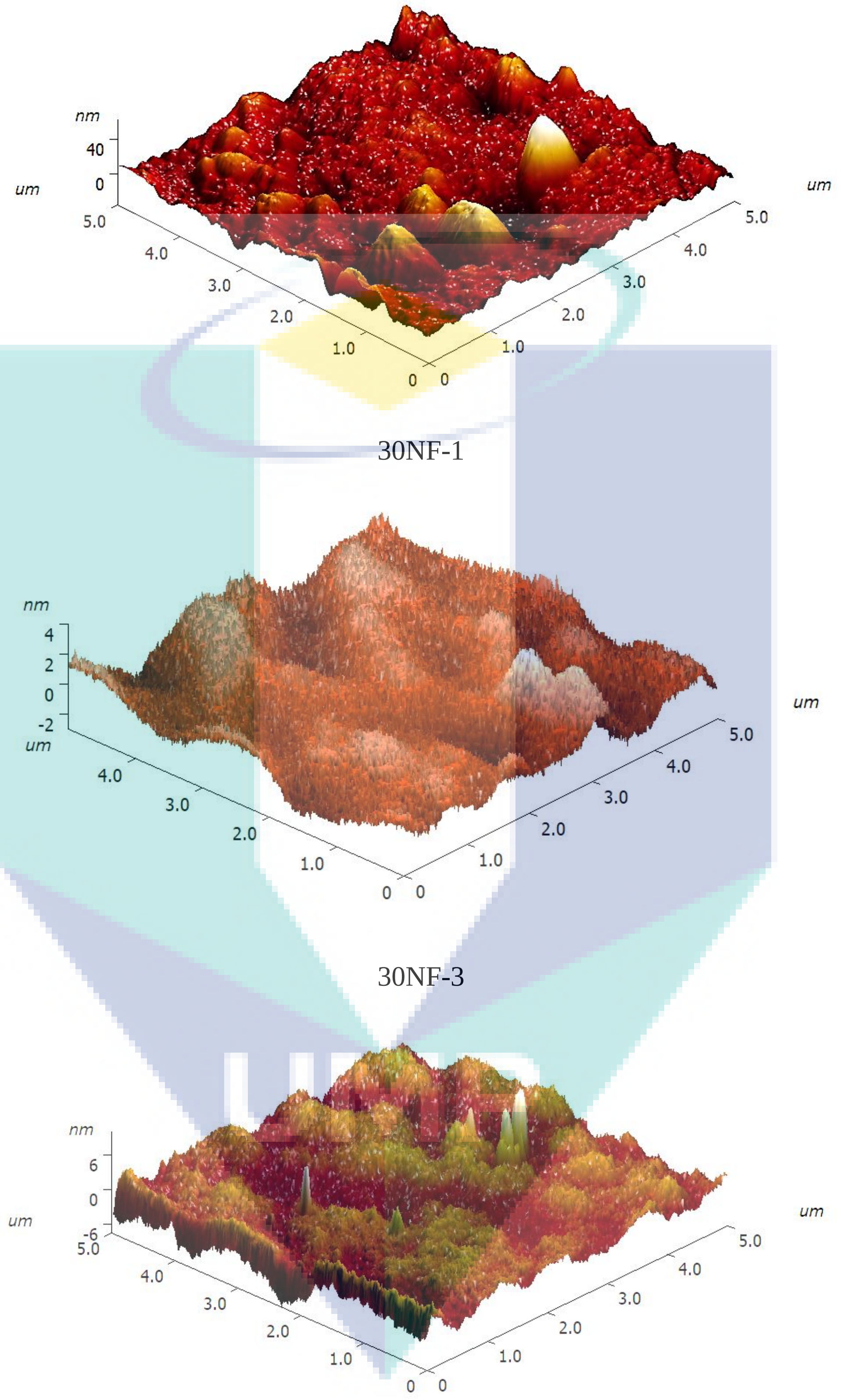

30NF-1

30NF-3

30NF-5

Figure 4.18 The effect of time at monomer concentration of 30 g/L

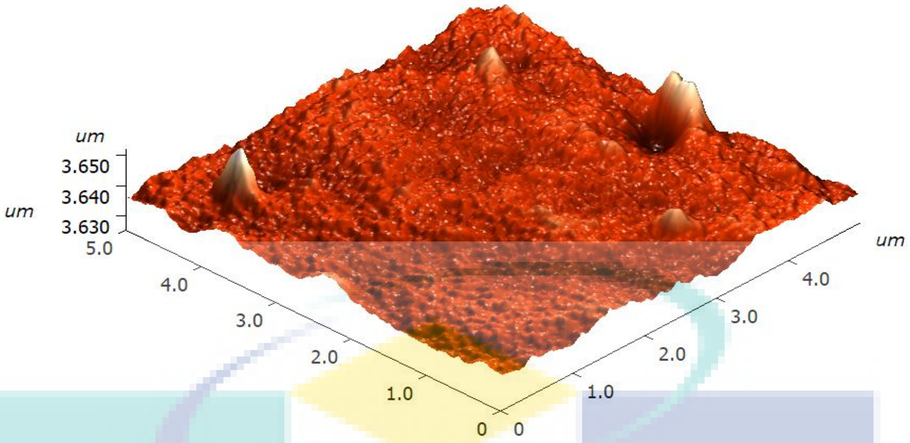

50NF-1

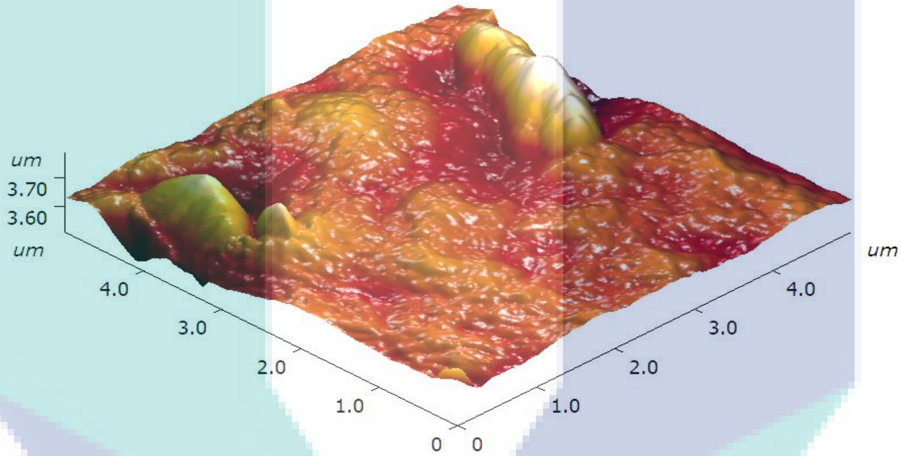

50NF-3

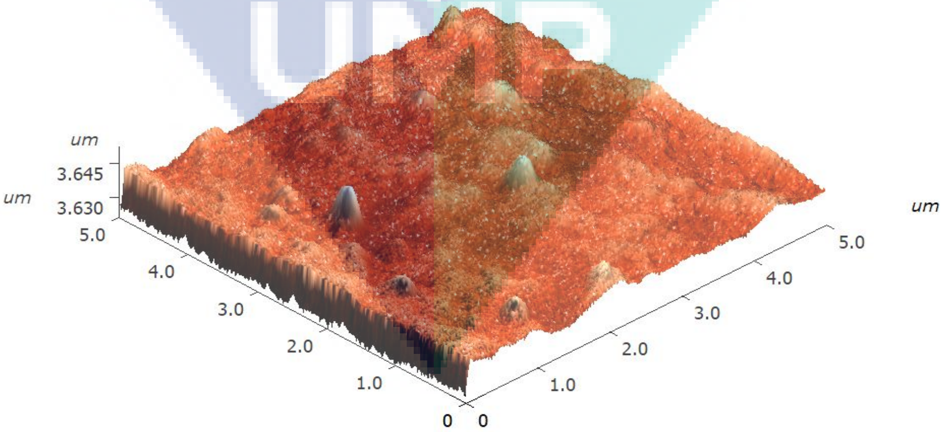

50NF-5

Figure 4.19 The effect of time at monomer concentration of 50 g/L

4.5.4 Surface morphology

The field emission scanning electron microscopy (FESEM) images in Figure 4.20 (a) and (b) illustrate the surface and cross-section of the unmodified membrane. It has a uniform interconnected cross-section of the porous layer. This commercial product is commonly prepared by phase inversion on non-woven PET and followed by immersion precipitation technique (Wei, J. et al., 2011b).

Sample 30NF-5 was selected for FESEM analysis as this sample produced the highest water flux. The cross-section and top surface of this modified membrane are shown in Figure 4.20 (c) and (d). The significant changes in the membrane surface were due to the formation of the grafted layer. There were evident pits and homogeneously-distributed large particles resulting from the rougher surface of modified membranes.

It formed a valley associated with previous research where rougher surface increased water flux as surface area increased (Rahimpour, A., 2011). Meanwhile, the lowest water flux was recorded for sample 30NF-5 and the morphology is presented in Figure 4.20. (e) and (f). The surface roughness decreased reasonably, which could be attributed to the continuous formation of uniform valleys that eventually decreased the surface area.

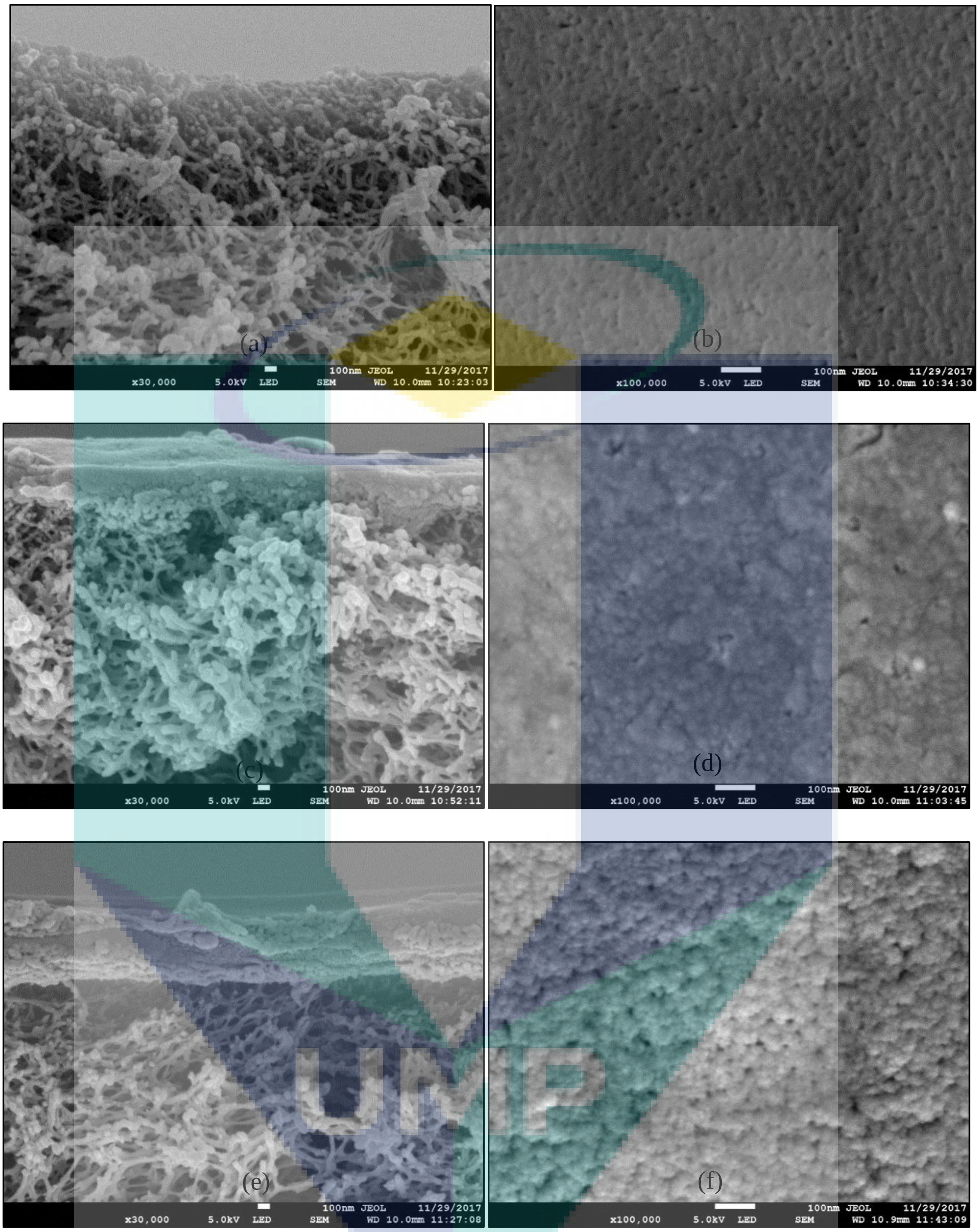

Figure 4.20 FESEM images for cross-section of (a) unmodified membrane, (c) 30NF-5, and (e) 50NF-5 and top view of (b) unmodified membrane, (d) 30NF-5, and (f) 50NF-5

4.5.5 Hydrophilicity

The hydrophilicity of the membranes was measured through contact angle analysis and the results are illustrated in Figure 4.21. Generally, the lower value of contact angle corresponds to the more hydrophilic membrane (Mehrparvar, A. & Rahimpour A., 2015). As can be seen from the figure, the unmodified PES membrane, known as a hydrophobic material, recorded a value of 67.5°. For modified membranes, the values decreased, ranging between 51.8° and 38.2°. This reduction can be attributed to the formation of carboxyl group on the membrane surface. This indicates that surface modification via UV grafting improves the hydrophilicity of the NFPES membrane.

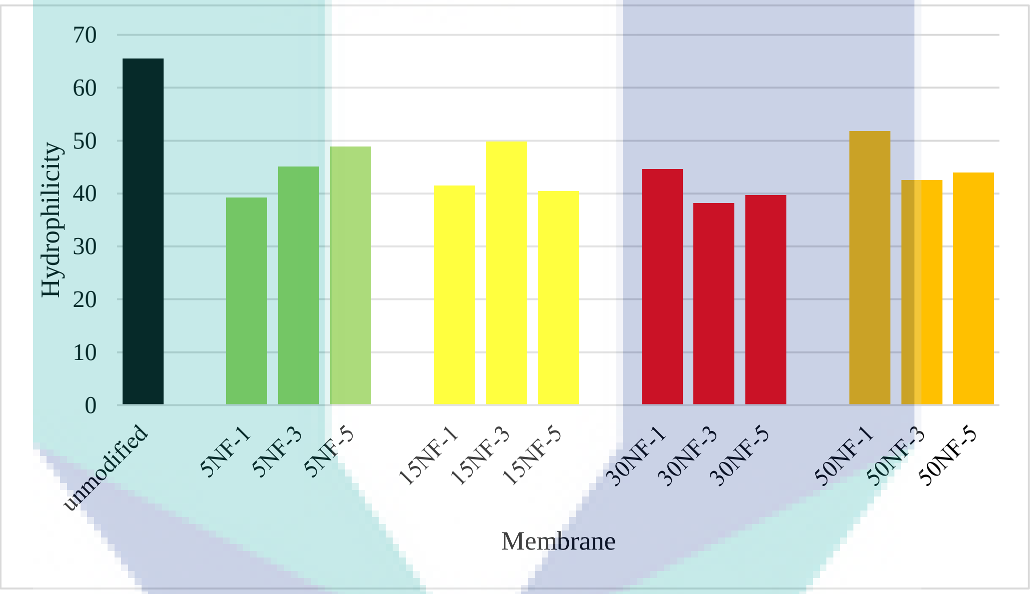

Figure 4.21 The hydrophilicity of NFPES membrane

4.5.6 Summary of NFPES membrane

Commercial NFPES membrane was modified via UV-photografting for forward osmosis (FO) application. Two grafting parameters, namely monomer concentration (acrylic acid) and grafting time were considered. Characterization was done with respect to modification using different techniques to evaluate the functional group, elemental analysis, surface roughness, surface morphology, hydrophilicity as well as the performances in terms of water flux, reverse salt diffusion and structural parameter. The result shows that the modified membrane exhibits highly desirable performance compared to the unmodified one. Interestingly, chemical and physical modification did not only reflect on the surface of the active layer but also the porous support layer of the membrane. Therefore, UV-photografting of polyethersulfone membrane can be considered as an alternative technique to improve commercial membrane performance in FO application.

4.6 Comparison of performances between UFPES and NFPES membranes

This study aimed to apply the commercial pressure-driven membrane into the FO system. As such, it is necessary that the membrane should have the ability to retain the draw solution in both RO mode and FO mode. Both UFPES and NFPES membranes were modified using the same grafting time and monomer concentration. A summarized comparison in the data obtained for UFPES and NFPES for different parameters are presented in Table 4.8.

Notably, the table shows an increase in water permeability for modified UFPES membrane while there was a significant reduction in the modified membranes using NFPES membrane as support. In the UFPES membrane, most of the modified membranes revealed increased water flux except for samples 5UF-1min, 50UF-3min and 50UF-5min. In comparison to the other modified UFPES membrane, it can be said that these 3 samples were the minimum and maximum condition in the grafting parameters.

Sample 5UF-1min reveals low water permeability which is attributed to possible insufficient effective grafting as it was conducted at low grafting time and monomer concentration. The original functional group on the membrane surface managed to either repel the negative charges from the monomer or the number of energy received by phenoxyphenyl sulfone chromopores was below the minimal energy to form free radicals (Rahman, A. F. H. B. A. & Seman M. N. B. A., 2018).

Likewise, both 50UF-3min and 50UF-5min membranes also recorded low values in the water permeabilities. It could possibly be that the membranes are covered with a thick layer of the carboxyl group. This trend was also recorded by Bilongo, T. G. et al. (2010) where the effective grafting increases with the increase of monomer concentration. The author justifies the relationships through kinetic in photo-polymerisation where a good grafting condition must be derived from a high monomer concentration and a strong dose of UV energy.

On the other hand, the value of A for NFPES membranes experienced reduction except for sample 15NF-1min. Using this support layer, it can be said that the reduction of water flux is attributed to the changes in pore size and porosity of the membrane.

Normally, the nanofiltration membrane has the molecular weight cut-offs to neutral solutes between 150 and 1500 Dalton (Baker, R. W., 2004). Hence, the addition of carboxyl group on the membrane would tend to decrease the effective pore size and porosity of the membrane. A similar result was also obtained by Taniguchi, M. and Belfort G. (2004) who suggests that water permeability declines as the formation of grafted material that leads to pore plugging implying a formation of gel layer on the modified surface.

Moreover, the graph polymerization is affected by the monomer concentration. At lower concentration, the monomer can penetrate deep into the membrane during the immersion method. Thus, it can be said that at the monomer concentration of 5 g/L, it can penetrate better compared to the higher monomer concentration. Notably, Sample 15NF-1min reveals low water permeability which could be due to the inability of monomer concentration to penetrate deep into the membrane, coupled with the low grafting time (1min).

The salt rejection (R) is an important parameter in any membrane process, especially in the desalination system. Each of the membrane namely the microfiltration (MF), ultrafiltration (NF), nanofiltration (NF) and reverse osmosis (RO) has their own rejection capabilities. In this research, we have identified that the UF membrane is not suitable for FO application. Specifically, unmodified UF membrane has the salt rejection of 0.39 percent using the 200 ppm of NaCl. In fact, the membrane was tested at a pressure of 3 bar and the permeate was highly contaminated with NaCl.

On the overall, modified UF membrane has R values which ranges below than 1 percent. Interestingly, the pristine NF membrane was able to reject 59 percent of NaCl at 200 ppm and pressure of 5 bars. On the other hands, the value of R starts to decrease on the modified membranes. The highest salt rejection for NF membranes was recorded by sample 15NF-3min (56 per cent) while the lowest value was recorded by sample 30NF-5min (16 per cent). These two samples have very similar water permeabilities (7.37 and 7.39 L.m^{-2}hr^{-1}). Thus, under these two grafting conditions, it can be inferred that the performance of modified membranes in terms of salt rejection does not correlate with the membrane water permeabilities. Based on the observations presented thus far in this study, UFPES membrane has been excluded from the theoretical modelling and optimization processes. Hence, only NFPES membrane was subjected to the theoretical modelling as well as the optimization process.

Table 4.8 Comparison between ultrafiltration and nanofiltration membranes

Acrylic acid (g/L)	**Time** (min)	**Ultrafiltration membrane** (UFPES)					**Nanofiltration membrane** (NFPES)				
		A $L.m^{-2}.hr^{-1}.bar^{-1}$	**B** $x10^{3}$ $L.m^{-2}hr^{-1}$	**R**	**Jv** $L.m^{-2}hr^{-1}$	**RSD** $g.m^{-2}hr^{-1}$	**A** $L.m^{-2}.hr^{-2}.bar^{-1}$	**B** $L.m^{-2}hr^{-1}$	**R**	**Jv** $L.m^{-2}hr^{-1}$	**RSD** $g.m^{-2}hr^{-1}$
unmodified		98.87	12.40	0.39	4.58	12.46	9.00	15.38	59	0.75	9.84
5	1	97.97	12.43	0.39	4.76	33.15	7.37	29.32	43	2	10.35
5	3	108.48	11.37	0.44	5.16	26.56	8.11	25.78	46	1.75	11.26
5	5	122.31	11.03	0.46	4.96	54.99	6.84	28.07	44	2	11.12
15	1	131.66	22.75	0.23	2.78	29.25	10.67	23.26	49	1.55	10.05
15	3	152.21	13.70	0.38	5.71	29.64	7.37	17.51	56	1.87	9.76
15	5	121.83	5.641	0.91	5.27	30.63	8.39	24.64	48	2.12	10.12
30	1	161.1	28.68	0.18	4.91	26.57	6.91	19.16	53	2.16	10.66
30	3	171.2	12.32	0.41	5.41	14.83	7.34	88.92	20	1.67	10.88
30	5	182.65	12.37	0.40	3.62	23.11	7.39	117.27	16	1.42	11.03
50	1	114.16	11.83	0.004	2.74	40.27	7.91	78.99	22	1.37	11.56
50	3	93.40	4.681	0.010	3.65	35.29	8.39	22.29	50	1.5	12.07
50	5	97.85	25.55	0.002	3.99	21.78	7.89	25.15	47	1.37	12.83

4.7 Mathematical modelling

In this section, the theoretical model shown in Eq. 2.12 was used to predict the water flux for NFPES membrane. The model was used on both unmodified and modified membranes. It should be noted that details of the abbreviation are presented in section 3.7.

$$\mathrm{J_V}=\mathrm{A}\left[\frac{\pi_{\mathrm{D,b}}\exp\left(-\frac{\mathrm{J_V}K}{\mathrm{D}}\right)-\pi_{\mathrm{F,b}}\exp\left(\frac{\mathrm{J_V}}{\mathrm{k}}\right)}{1+\frac{\mathrm{B}}{\mathrm{J_V}}\left[\exp\left(\frac{\mathrm{J_V}}{\mathrm{k}}\right)-\exp\left(-\frac{\mathrm{J_V}\mathrm{S}}{\mathrm{D}}\right)\right]}\right] \qquad 2.12$$

4.7.1 Unmodified NFPES membrane

By using deionized water in the feed solution and 1M of NaCl in the draw solution, the impacts of both dilutive ICP and concentrative ECP can be investigated concomitantly (McCutcheon, J. R. & Elimelech M., 2006). In this research, the NF membrane with the commercial name of NF2 was purchased from Amfor Inc. However, the manufacturer has limited the NF membrane application up to 10 bars. Thus, using equation modelling, the model can predict the water flux up to 60 bars of osmotic pressure.

Results of the predicted water flux for the unmodified NFPES membrane using the model shown in Eq 2.12 and experimental data shown in Table 4.8 are plotted in Figure 4.22. The non-linear flux behaviour with increasing osmotic pressure is attributed to the dilutive ICP. It is named dilutive ICP because the draw solution is normally diluted by the permeate water within the porous layer. The prediction of flux was performed exactly according to what has been described in previous FO modelling study (McCutcheon, J. R. et al., 2006).

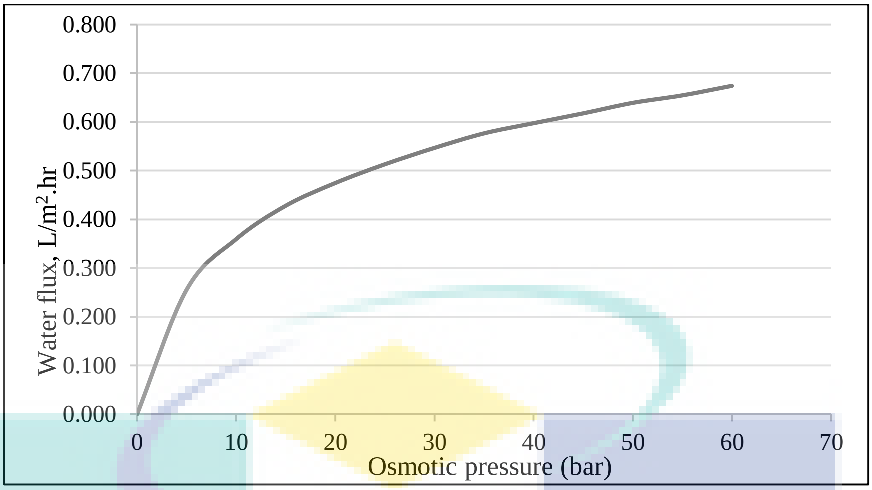

Figure 4.22 Prediction of water flux for unmodified NFPES membrane at different osmotic pressure.

In developing of a model for any FO membrane system, it is essential to determine the value of water permeability (A), the mass transfer coefficient (k), and the solute diffusivity (D). The water permeability is determined experimentally using the RO mode.

The mass transfer coefficient is determined using the forward osmosis-pressure retard osmosis (FO-PRO) mode while the solute diffusivity is determined from the literature (Kim, B. et al., 2017). However, it has been reported that at a higher concentration of more than 1.0M NaCl for the draw solution and at higher water flux, the ECP and ICP models over-predicted the water flux across the membrane at the corresponding osmotic pressure (Tan & Ng, 2013).

4.7.2 Modified NFPES membrane

In general, modified membrane exhibit enhanced water flux property. The predicted water flux at different osmotic pressure generates more than two-fold compared to the unmodified membrane. **Error! Reference source not found.** (a)-(d) shows the effect of osmotic pressure on the permeation flux of water for membrane modified at different monomer concentration.

The water flux increases with increasing osmotic pressure were recorded in the modified membrane. It can be explained that higher osmotic pressure facilitates the rapid penetration of water molecules across the FO membrane (Kim, B. et al., 2017). Moreover, the increases of water flux was attributed to the addition of carboxyl (-COOH) group on the membrane surface, resulting in higher hydrophilicity (Mansourpanah, Y. & Habili E. M., 2013).

In Figure 4.23a, the membrane was modified using the monomer concentration of 5 g/L. Maximum water flux recorded at 1.8 L.m^{-2}.hr^{-1} (1min) while the lowest is at 1.6 L.m^{-2}.hr^{-1} (3min). At this monomer concentration, the gap range of maximum water flux at different grafting time was small. Research conducted by Abu Seman, M. N. et al. (2012) reported that at lower monomer concentration, the monomer can penetrate deep into the pores. Thus, the effective grafting on the membrane occurs at the various site due to the mobility of the monomer within the membrane area.

However, for membrane modified at a monomer concentration of 15g/L (Figure 4.23b) and 30g/L (Figure 4.23c), the grafting time of 1min and 3min shows higher values of water flux compared to 5min. From the trends, the increases of the grafted layer on the membrane surface lead to the reduction of water flux at higher grafting time.

Effective grafting mechanism on membrane surface results in the thickening of the grafted layer thus increases flux resistance (Rahimpour, A., 2011). Interestingly, the gap range of water flux was big on both monomer concentrations. This is correlated with the effect of thickness from the graph polymerization reduces the water flux.

On the other hand, using the highest monomer concentration (50g/L), the model has predicted the lowest water flux compared to the lower monomer concentrations. The maximum water flux was only at 1.33 L.m^{-2}.hr^{-1} (3min) even though the gap range between the water flux is small.

This result is contradicting with the lowest monomer concentration (5g/L). It can be said that due to the high concentration of the monomer, it cannot penetrate the membrane surface. Hence, the graph polymerization was limited to the active layer of the membrane only.

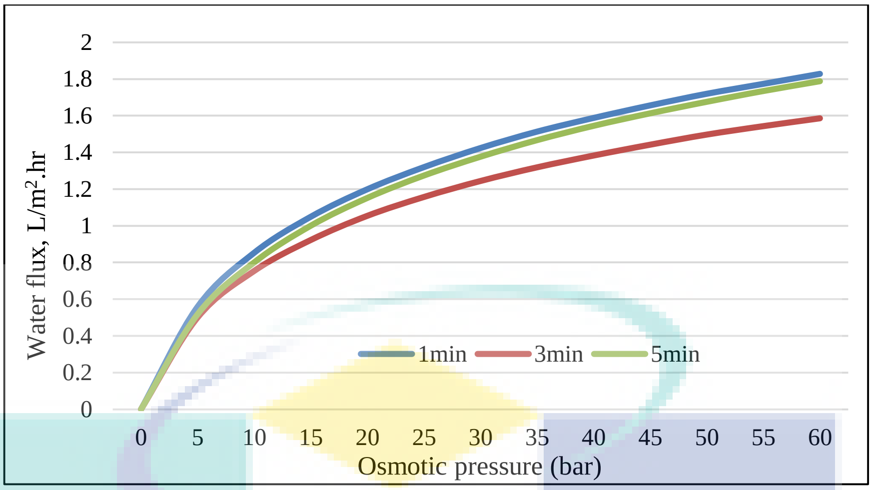

(a) 5 g/L

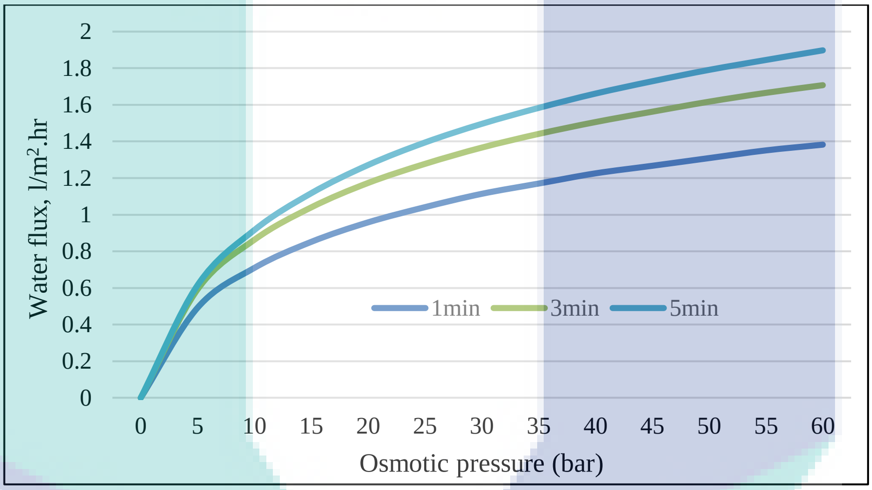

(b) 15 g/L

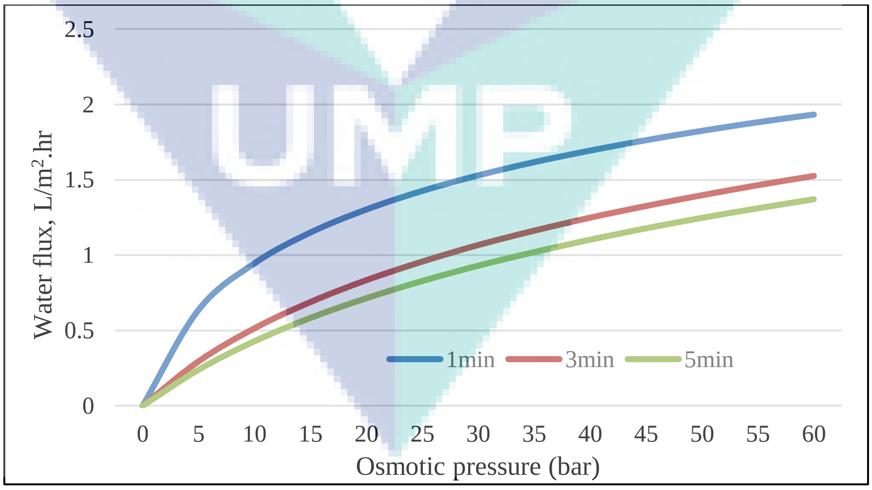

(c) 30 g/L

Figure 4.23 Prediction of water fluxes at monomer concentrations of (a) 5g/L, (b) 15g/L, (c) 30g/L and (d) 50g/L

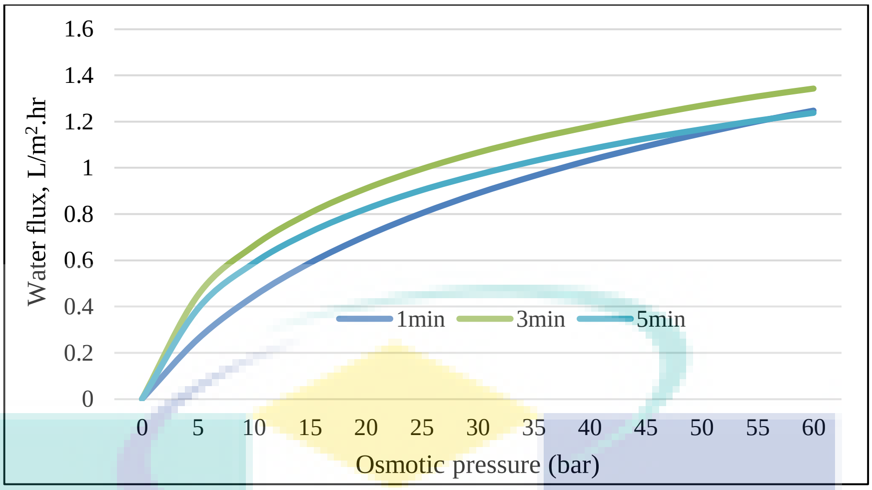

(d) 50 g/L

Figure 4.23 Continued

Figure 4.24 (a-c) shows the predicted water flux for modified NF membrane using the osmotic pressure up to 60bar. At different grafting time, the model predicts the highest water flux using the monomer concentrations of 15g/L and 30g/L. It shows that these two monomer concentrations will have a higher impact on the water flux at different osmotic pressure.

Interestingly, the lowest (5g/L) and highest (50g/L) monomer concentration have recorded the lowest water flux. It can be said that in the surface modification of the NF membrane via UV-photografting technique, there is a specific range of monomer concentration to increase the water flux. Similar trend was recorded by Taniguchi, M. and Belfort G. (2004) in their research paper. They have identified that although all the grafted and polymerized monomers increased the membrane properties, there is a specific condition to obtain optimal performance.

On a different angle, there was big gap range for water flux in Figure 4.24a (1min) and Figure 4.24c (5min). At grafting time of 1min and 5min, both monomer concentrations of 15g/L and 30g/L recorded a high value compared to the monomer concentration of 5g/L and 50g/L. This finding concludes that the grafting time of 3min will produce a small range gap in the water flux.

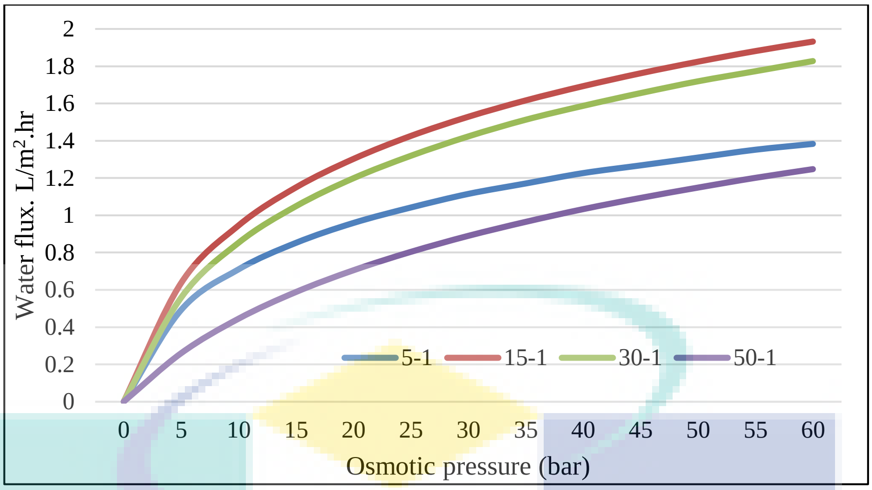

(a) 1 min

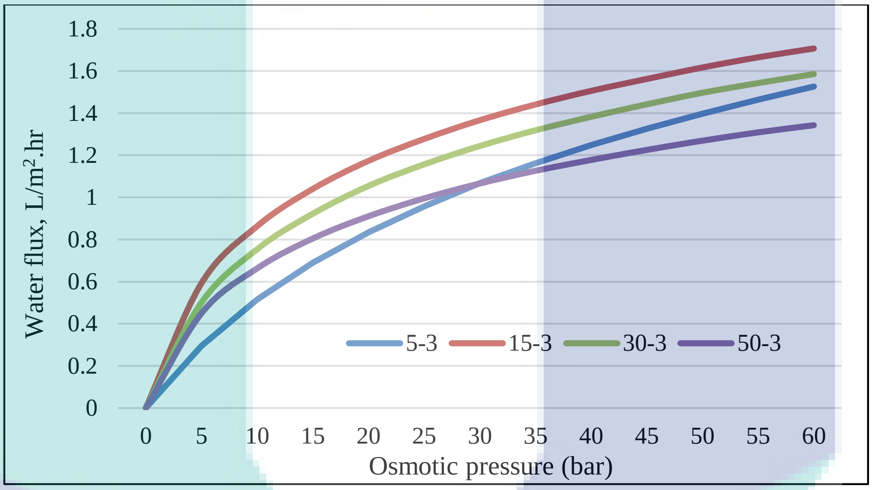

(b) 3 min

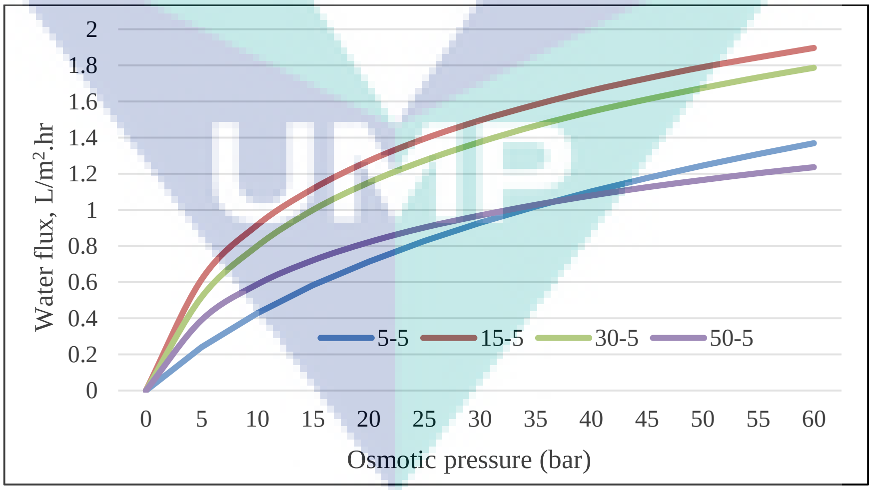

(c) 5 min

Figure 4.23 Prediction of water fluxes at grafting times of (a) 1min, (b) 3min and (c) 5min

4.7.3 Solute resistivity for diffusion

The solute resistivity for diffusion (K) shown in Eq. 2.11 is defined as the structural parameter (S) of the support layer over the solute diffusion (D) in the support layer. The solute resistivity for diffusion is discussed on the unmodified membrane and modified membrane at grafting time of 1 min. From Figure 4.23, unmodified membrane ($K=1.61x10^7$) generates the lowest water flux while sample 15AA-1min generates the highest water flux ($K=7.21x10^6$).

A similar trend was reported by McCutcheon, J. R. and Elimelech M. (2007) in the flux modelled in the FO mode (dilutive ICP in the absence of concentrative ECP) for membrane with variable solute resistivity. Thus, as the osmotic pressure (π) increases, the lower the value of K, the higher water flux will be generated.

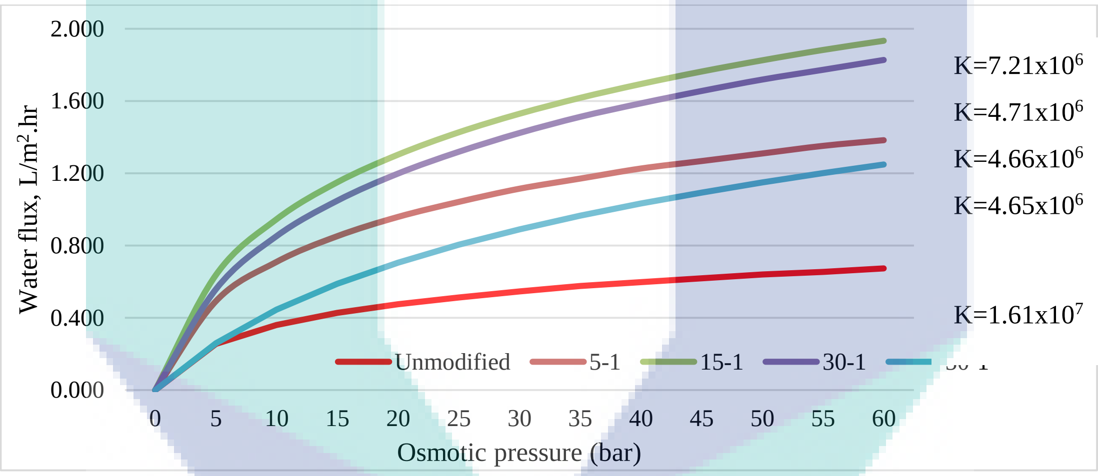

Figure 4.23 Solute resistivity of modified membrane at grafting time 1 minute

4.8 Response surface methodology performances

Details of the screening process shows in Figure 4.24. The data shows two responses namely the water flux and RSD. However, the model of F-value of 1.48 implies that the model is not significant relative to the noise (25.7%). In this screening processes, there are no significant model terms. Nevertheless, the ANOVA suggested that there are many insignificant model terms (not counting those required to support hierarchy), model reduction may improve your model.

This was supported by the poor value of R-squared (0.2175), adjusted R-squared (0.0708), predicted R-squared (-0.4327) and adequate precision (3.820). Thus, we eliminate the factor the UV-intensity due to the poor result in screening and this factor was not utilised in the earlier study.

Figure 4.24 Performance of modified membranes in screening process

Run		**Responses**	
		Water flux	**RSD**
N	Membrane	L.hr^{-1}.m^{-2}	g.hr^{-1}.m^{-2}
1	16.25NF-2-15UV	0.67	0.267
2	38.75NF-2-25UV	3.67	0.237
3	27.5NF-3-10UV	1.67	0.258
4	27.5NF-5-20UV	1.67	0.217
5	27.5NF-3-30UV	0.97	0.237
6	27.5NF-1-20UV	1.42	0.197
7	27.5NF-3-20UV	2.07	0.233
8	27.5NF-3-20UV	2.05	0.223
9	27.5NF-3-20UV	2.24	0.238
10	16.25NF-4-15UV	1.33	0.271
11	27.5NF-3-20UV	2.05	0.235
12	27.5NF-3-20UV	1.98	0.241
13	27.5NF-3-20UV	1.98	0.235
14	38.75NF-4-25UV	2.2	0.241
15	38.75NF-4-15UV	2	0.23
16	5NF-3-20UV	1.8	0.255
17	16.25NF-2-25UV	1.8	0.217
18	16.25NF-4-25UV	3.11	0.208
19	38.75NF-2-15UV	1.66	0.264
20	50NF-3-20UV	2.27	0.282

We proceed the optimization process focusing on two factors (monomer concentration and grafting time) and two responses (water flux and RSD. Initially, the water flux and the reverse salt diffusion of the unmodified membrane were 0.75 L.m^{-2}.h^{-1} and 9.84 g.m^{-2}h^{-1}, respectively. Upon modification, the membranes exhibited significantly improved water permeate flux (see Table 4.9). The highest water permeates flux was recorded in run 3, where the water flux and RSD were 1.42 L.m^{-2}.h^{-1} and 8.90 g.m^{-2}h^{-1}, respectively. In the preliminary study of optimization, we have the option of having three factors with two responses.

Table 4.9 Performance of modified membranes

Run		Responses	
		Water flux	**RSD**
N	Membrane	L.hr^{-1}.m^{-2}	g.hr^{-1}.m^{-2}
1	22.5NF-3	1.23	12.38
2	22.5NF-1	1.12	9.86
3	30NF-4	1.42	8.90
4	22.5NF-3	1.01	5.61
5	37.5NF-3	1.40	9.41
6	22.5NF-3	1.29	10.64
7	30NF-2	1.50	9.85
8	22.5NF-3	1.27	11.39
9	15NF-2	1.07	9.77
10	7.5NF-3	1.39	8.95
11	22.5NF-3	1.23	9.97
12	22.5NF-5	1.11	10.00
13	15NF-4	1.36	8.63

At a lower monomer concentration, some molecules penetrated the membrane pores during immersion and then underwent graft polymerization (Abu Seman, M. N. et al., 2010a). However, membrane pores indirectly narrowed down upon modification. This was experimentally evident in the sample at run 10 (7.5NF-3) where the water flux decreased at a lower monomer concentration as the graft polymerization occurred deep in the porous layer.

However, it is worthy of note that the water flux also decreased at a higher monomer concentration. This may be explained by the fact that higher monomer concentrations are associated with higher effective grafting rates which are supported experimentally by the sample at run 5 (37.5NF-3). Yu, H. Y. et al. (2010) suggested that in graft polymerization, the ratio of active sites to monomer concentration needs to be considered. Indeed, as the monomer concentration increases, the free radicals on the membrane surface have more chances to get into contact with the monomer, thereby resulting in a higher grafting degree.

4.8.1 Central composite design

Based on the design of the experiment, the quadratic models were established for both responses. The multiple linear regression model was developed from six coefficients, two main effects, two quadratic effects, one interaction and one constant. The general form of the final empirical models from coded parameters for each response is presented in Eq. 4.1.

$$\text{Coded Factors}=b_0+b_1x_1+b_2x_2+b_{11}x_1^2+b_{22}x_2^2+b_{12}x_1x_2 \qquad 4.1$$

while the actual factors are presented in Eq. 4.2.

$$\text{Actual Factors}=\gamma_0+\gamma_1C+\gamma_2t+\gamma_{11}C^2+\gamma_{22}t^2+\gamma_{12}Ct \qquad 4.2$$

The values of the regression coefficients calculated in the coded factors are presented in Table 4.10, whereas the developed regression coefficient of the actual variables is presented in Table 4.11.

Table 4.10 Regression coefficients of the coded variables

Response	**Coefficients**					
	b_0	b_1	b_2	b_{11}	b_{22}	b_{12}
Water flux	1.39	-0.06	-0.02	-0.07	-0.08	-0.04
RSD	9.25	-0.61	-0.95	0.54	-0.33	0.08

Table 4.11 Developed regression coefficients of the actual variables

Response	**Coefficients**					
	γ_0	γ_1	γ_2	γ_{11}	γ_{22}	γ_{12}
Water flux	-0.23	0.51	0.08	-0.07	-1.55×10^{-3}	-6.5×10^{-3}
RSD	16.52	-4.08	0.1	0.53	-5.88×10^{-3}	0.01

The normal plot of residuals and residuals *versus* predicted values for both factors are shown in Figure 4.25 and Figure 4.26. In the first response (water flux), the normal plot of residuals and residuals versus predicted in Figure 4.25 (a) and (b) falls on a straight line, suggesting that the errors are scattered normally, which support the suitability of the least-square fit. Similar trends were obtained in the second response (reverse salt diffusion) in Figure 4.26. It is proven that there is no obvious pattern and unusual behaviour not to support the model accuracy. The results are also scattered equally on both *x*-axes. It shows that the proposed models are acceptable and there is no reason to suspect any violation of the independence or constant variance assumption.

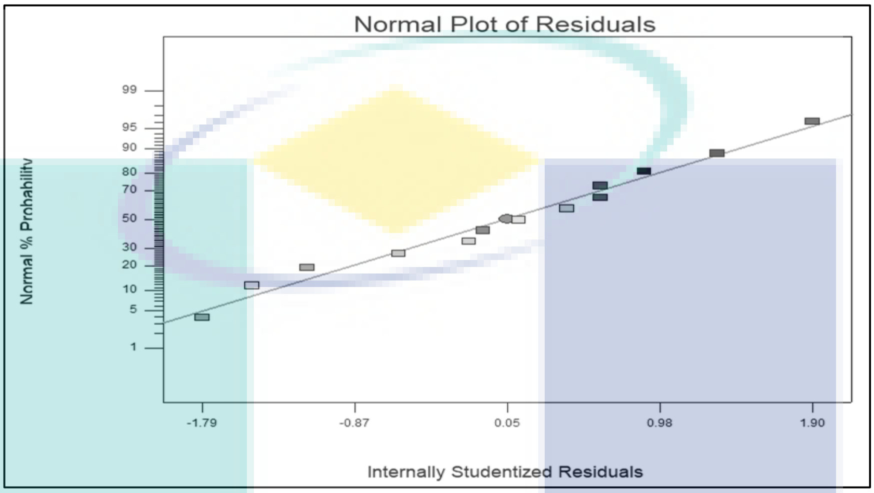

(a) Normal plot of residuals

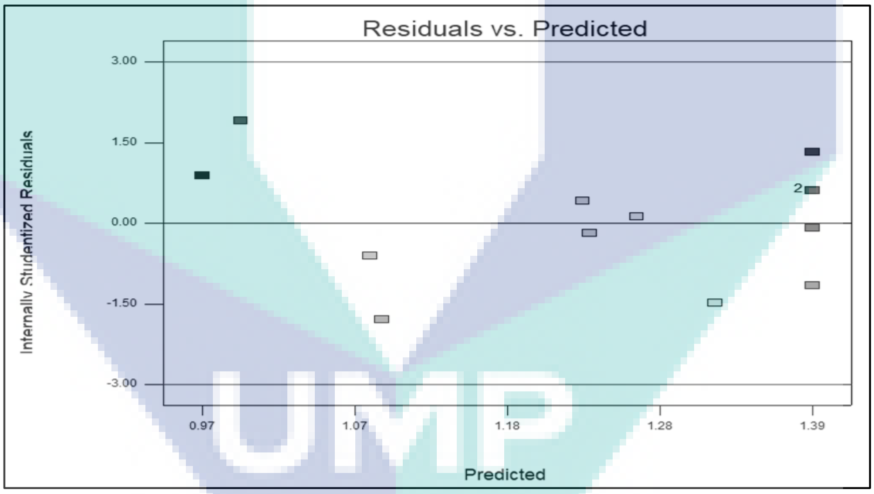

(b) Plot of residuals vs. predicted

Figure 4.25 (a) Normal plot of residuals and (b) plot of residuals *vs.* predicted for water flux

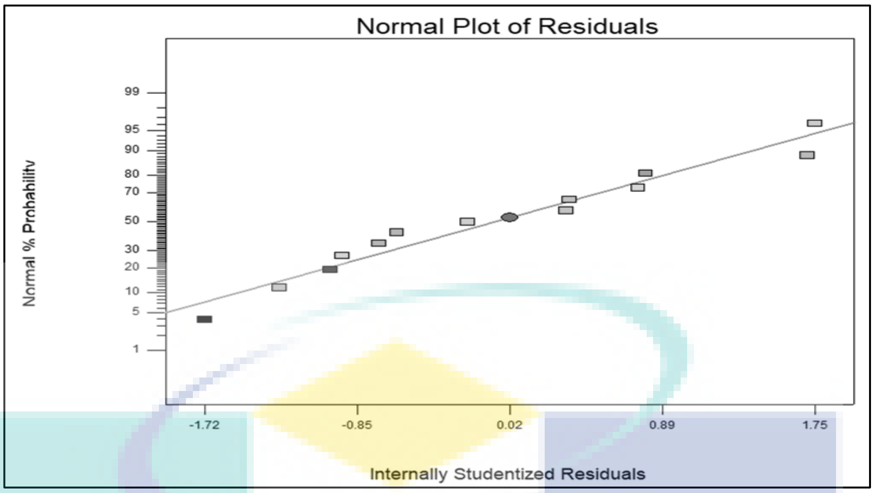

(a) Normal plot of residuals

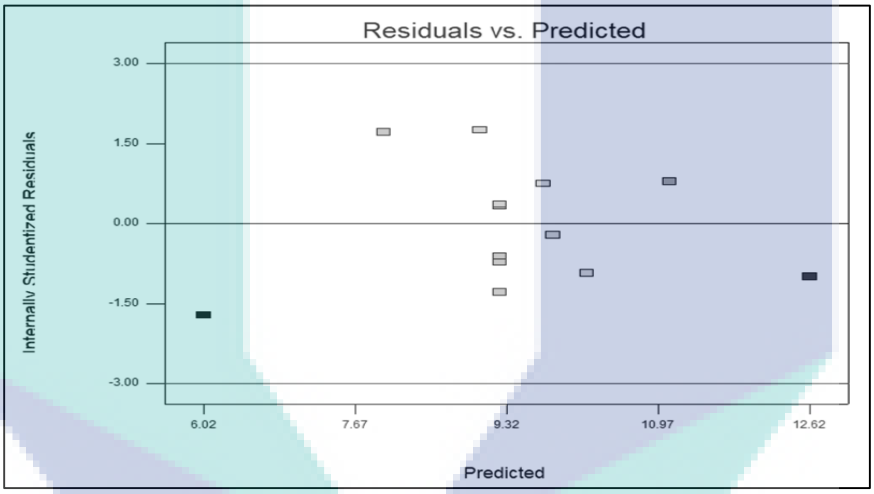

(b) Plot of residuals vs. predicted

Figure 4.26 (a) Normal plot of residuals and (b) plot of residuals vs. predicted for reverse salt diffusion

4.8.2 Analysis of variance

Analysis of variance (ANOVA) was employed to verify the determined regression model which identify the main factors and combinations that are statistically significant. It provides a summary of the sum of squares of residuals and regression, degrees of freedom, *F* value, *p* value, and ANOVA coefficients. *F* value is the variance measurement of the data about the mean value (Khayet, M. et al., 2011). It may also be calculated manually by dividing the mean of the sum of squares between groups divided by the mean sum of squares within groups. The surface response models are confirmed using ANOVA analysis below 0.05 level of significance, where the *p*-level is treated as a “borderline acceptable” error level (Xiangli, F. et al., 2008).

The summary of ANOVA analysis of the water flux is presented in Table 4.12. The obtained *F* value (110.86) implies that the model is significant. The *p* value of 0.2757 implies that the lack of fit is insignificant. The *R* squared value of 0.9875 is close to the adjusted *R* squared value (0.9786) while the predicted *R* squared is at 0.9306. In general, the values from ANOVA indicates a good agreement between the predicted and experimental values of the modified membranes. The model obtained is applied to predict the optimum grafting parameters that will maximize the water flux.

The same procedure was applied to the reverse salt diffusion flux and the obtained values are shown in Table 4.13. The *F* value of 20.07 for the model implies that the model is significant. Meanwhile, the “lack of fit” of this model was insignificant with the *p* value being 0.1027. The variability in the response by the model can be explained by the adjusted *R* squared of 0.8882, which is lower than the *R* squared value (0.9348). However, the predicted *R* squared recorded a low value (0.6189) due to the selection of five terms into the model. In general, it can be concluded that the predicted and experimental values of modified membranes in the second response are also in good agreement.

Table 4.12 ANOVA analysis of the water flux

Source	**Sum of Squares**	**DF**	**Mean Square**	***F* Value**	**Prob > *F***	
Model	0.30	5	0.06	110.86	<0.0001	Significant
A – Grafting Time	0.052	1	0.052	95.64	<0.0001	
B – Monomer Concentration	5.963×10^{-3}	1	5.963×10^{-3}	11.03	0.0127	
AB	9.752×10^{-3}	1	9.752×10^{-3}	18.05	0.0038	
A^2	0.12	1	0.12	223.08	<0.0001	
B^2	0.18	1	0.18	324.89	<0.001	
Residual	3.783×10^{-3}	7	5.404×10^{-4}			
Lack of Fit	2.208×10^{-3}	3	7.359×10^{-4}	1.87	0.2757	Not significant
R-squared	0.9875					
Adjusted *R*-squared	0.9786					
Predicted R-squared	0.9306					
Adequate Precision	26.682					
Std. Deviation	0.023					
Mean	1.24					

Table 4.13 ANOVA analysis of the reverse salt diffusion

Source	**Sum of Squares**	**DF**	**Mean Square**	***F* Value**	**Prob > *F***	
Model	27.8	5	5.56	20.07	0.0005	Significant
A – Grafting Time	4.41	1	4.41	15.93	0.0052	
B – Monomer Concentration	10.83	1	10.83	39.08	0.0004	
AB	0.026	1	0.026	0.094	0.7686	
A^2	6.68	1	6.68	24.11	0.0017	
B^2	2.52	1	2.52	9.08	0.0196	
Residual	1.94	7	0.28			
Lack of Fit	1.46	3	0.49	4.11	0.1027	Not significant
R-squared	0.9348					
Adjusted *R*-squared	0.8882					
Predicted R-squared	0.6189					
Adequate Precision	18.451					
Std. Deviation	0.53					
Mean	9.44					

The response surface plots are shown in Figure 4.27 (a) and (b) which depicts the influence of the grafting time and monomer concentration on the water flux. The result shows that optimum condition was identified. As it can be observed from the figures, optimum condition led to the water flux up to 1.349 $L.m^{-2}h^{-1}$. However, as it drifts away from the centre point, it decreases thereafter. The grafting time of 3 min and a monomer concentration of 22.5 g/L yielded better coefficient in producing a high-water flux. This is attributed to the hydrophilicity, surface area and pore enlargement. According to Abu Seman, M. N. et al. (2012), the formation of a functional group, namely the carboxyl group onto the membrane greatly affects the water permeability. The hydrophilicity of the membrane surface increases and facilitates the transportation of water molecules across the membrane.

The changes in surface area can be seen in the morphology results in the previous section. It may be inferred that the graft polymerization produced coarser surface and thus increased the membrane active area compared to the unmodified membrane. Furthermore, the enhancement of membrane water flux on polyethersulfone by UV-irradiation was attributed to the chain scission mechanism on the polymer backbone. It induced pores enlargement and increase the water flux (Puro, L. et al., 2006). Hence, it is believed that the increases in water flux were due to the increases of hydrophilicity, membrane active area and pore enlargement.

In Figure 4.27 (c), the interaction of grafting time and monomer concentration on the water flux is presented. As shown, at a monomer concentration of 15 g/L, there is a reduction in water flux as the grafting time increased. This could be explained by the development of the grafted layer on the membrane layer. According to Mansourpanah, Y. and Habili E. M. (2013), longer UV radiation period would enhance the degree of polymerization degree such that a denser thin layer can be obtained. Thus, as the grafting time increases, the water flux is expected to experience gradual reduction.

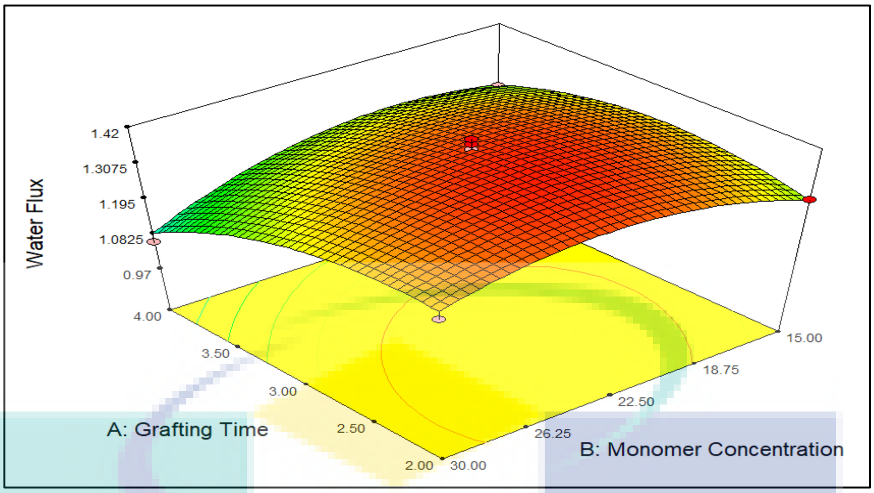

(a) Response surface plot

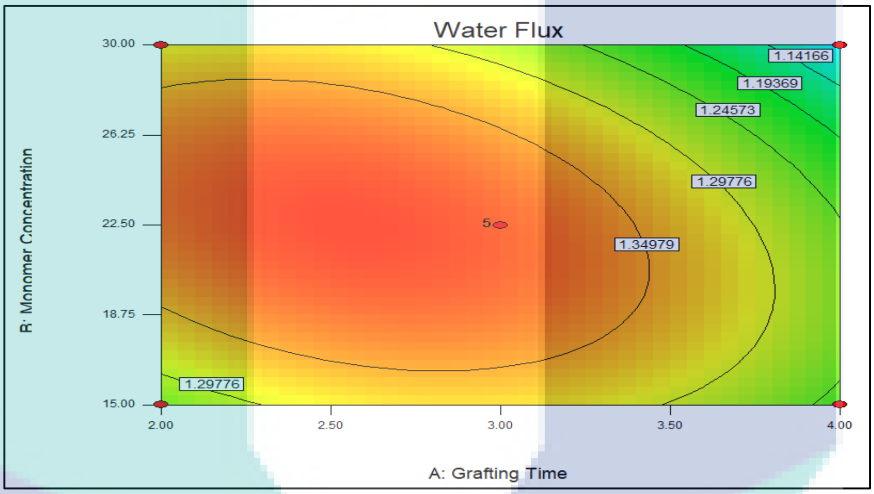

(b) Contour plot

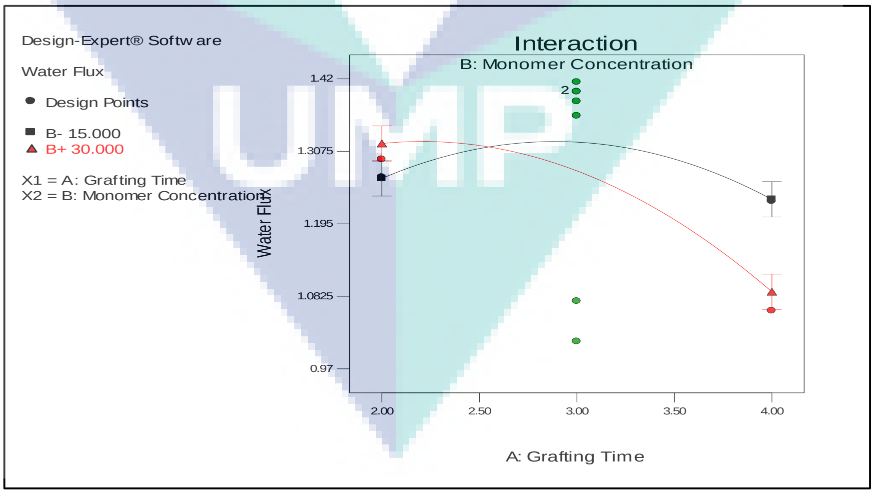

(c) Interaction of the predicted water flux

Figure 4.27 The interaction of grafting time and monomer concentration on water flux

The response surface plots in Figure 4.28 (a) reveals the influence of the grafting time and monomer concentration on RSD. At the lowest grafting time (2 min) and monomer concentration (15 g/L), the value of RSD was high (10.55 g.m^{-2}h^{-1}). However, RSD decreases as the grafting time and monomer concentration increases (8.38 g.m^{-2}h^{-1}).

The non-elliptical nature of contour plots in Figure 4.28 (b) suggests that there is no interaction between the factors whereas strong interaction is characterized by a circular contour map (Singhania, R. R. et al., 2007). The result shows that increases in both grafting time and monomer concentration had no significant effect on the reverse salt diffusion. It is postulated that the membrane experienced pore enlargement, leading to decreased ability to retain the salt.

Thus, the volume of sodium chloride which was originally in the draw solution was facilitated across the membrane to the feed side. In addition, the osmotic pressure in the draw solution is reduced concurrently with the losses of sodium chloride in the draw solution (She, Q. H. et al., 2012a). Unsurprisingly, according to Qasim et al. (Qasim, M. et al., 2015), to improve the water flux, one need to compromise either the reverse salt diffusion or mechanical stability.

On the other hand, Figure 4.28 (c) shows the interaction between grafting time and monomer concentration on RSD. The result shows that at both monomer concentrations (15 and 30 g/L), the value of reverse salt diffusion decreases. However, there is no interaction in the range studied. This is in agreement with the response surface plot which shows that there are no optimum points in the second response. Moreover, this observation is expected as the ANOVA has indicated that AB was an insignificant model term.

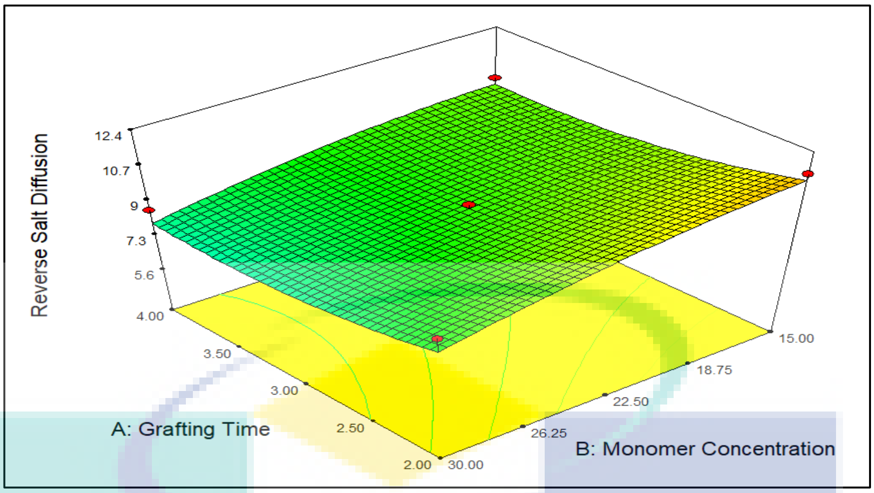

(a) Response surface plot

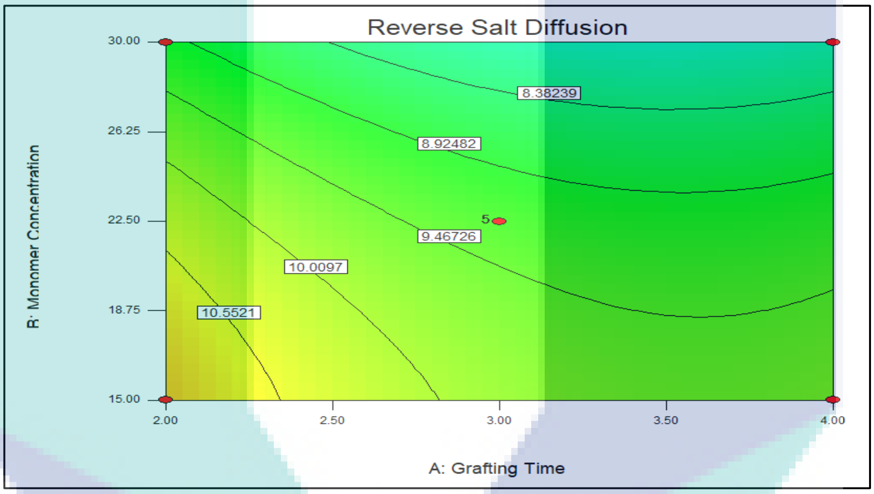

(b) Contour plot

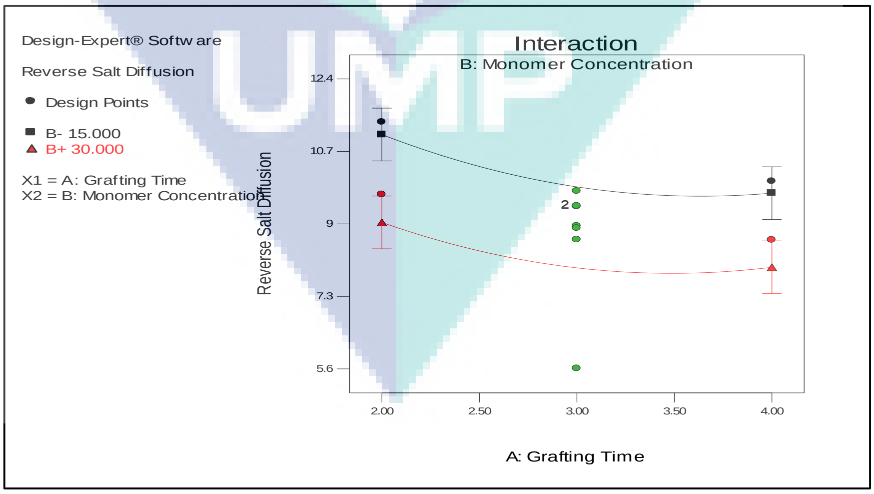

(c) Interaction of the reverse salt diffusion flux

Figure 4.28 The interaction of grafting time and monomer concentration on RSD

4.8.3 Data validation

The developed regression equations from the experimental data are suitable to predict both water flux and the RSD at any ratio of grafting time and monomer concentration, as long as it works within the limit of the experimental area. The criteria for the optimum condition are maximized water flux and minimized reverse salt diffusion. Thus, three confirmation runs were conducted based on the suggested optimum condition as presented in Table 4.14. These were used to determine the error percentage between the theoretical and experimental values.

Table 4.14 Validation of the predicted modification condition and the responses.

No.	**Grafting time** (min)	**Monomer concentration** (g/L)	**Predicted J_v** ($L.m^{-2}.h^{-1}$)	**Experiment J_v** ($L.m^{-2}.h^{-1}$)	**Predicted RSD** ($g.m^{-2}h^{-1}$)	**Experiment RSD** ($g.m^{-2}h^{-1}$)
1	2.81	27.85	1.4	1.55	9.41	10.21
2	2.81	27.85	1.4	1.54	9.41	9.77
3	2.81	27.85	1.4	1.48	9.41	10.28
			Average	1.52 ± 0.04	Average	10.09 ± 0.36
			Error percentage	8.10 %	Error percentage	6.76 %

From the Design Expert software results, the suggested optimum condition to modify membrane with maximum water flux and low RSD could be achieved at grafting time of 2.81 min and 27.85 g/L of acrylic acid concentration with predicted J_v at 1.4 $L.m^{-2}.h^{-1}$ and RSD at 9.41 $g.m^{-2}h^{-1}$. The water flux and RSD obtained from the experimental procedure (three confirmations run) was recorded as 1.52 ± 0.04 $L.m^{-2}.h^{-1}$ and 10.09 ± 0.36 $g.m^{-2}h^{-1}$ where both responses comply with the standard error percentage of less than 10%.

Thus, both regression models can be used to reasonably predict and optimize the performance of the modified membrane. The optimized membrane exhibited better water flux (two-fold of unmodified NFPES membrane) without compromising the RSD flux compared to the unmodified membrane which recorded water flux of 0.75 $L.m^{-2}.h^{-1}$ and RSD of 9.84 $g.m^{-2}h^{-1}$. As conclusion, it can be inferred that this optimization of grafting parameter namely the monomer concentration and grafting time was successful in developing high performance FO membrane.

4.9 Characterization of optimized membrane

4.9.1 Surface morphology

Figure 4.29 shows the cross-section and top surface images of unmodified and optimized (22.5NF-3min) membranes as obtained from FESEM. As can be seen, the unmodified membrane revealed a uniform dispersion of pores and a smooth top surface as shown in Figure 4.29(a). On the other hand, the surface of the modified membrane exhibits an additional layer formed as shown in Figure 4.29 (b). This may be associated with the formation of the carboxyl group from the graft polymerization process.

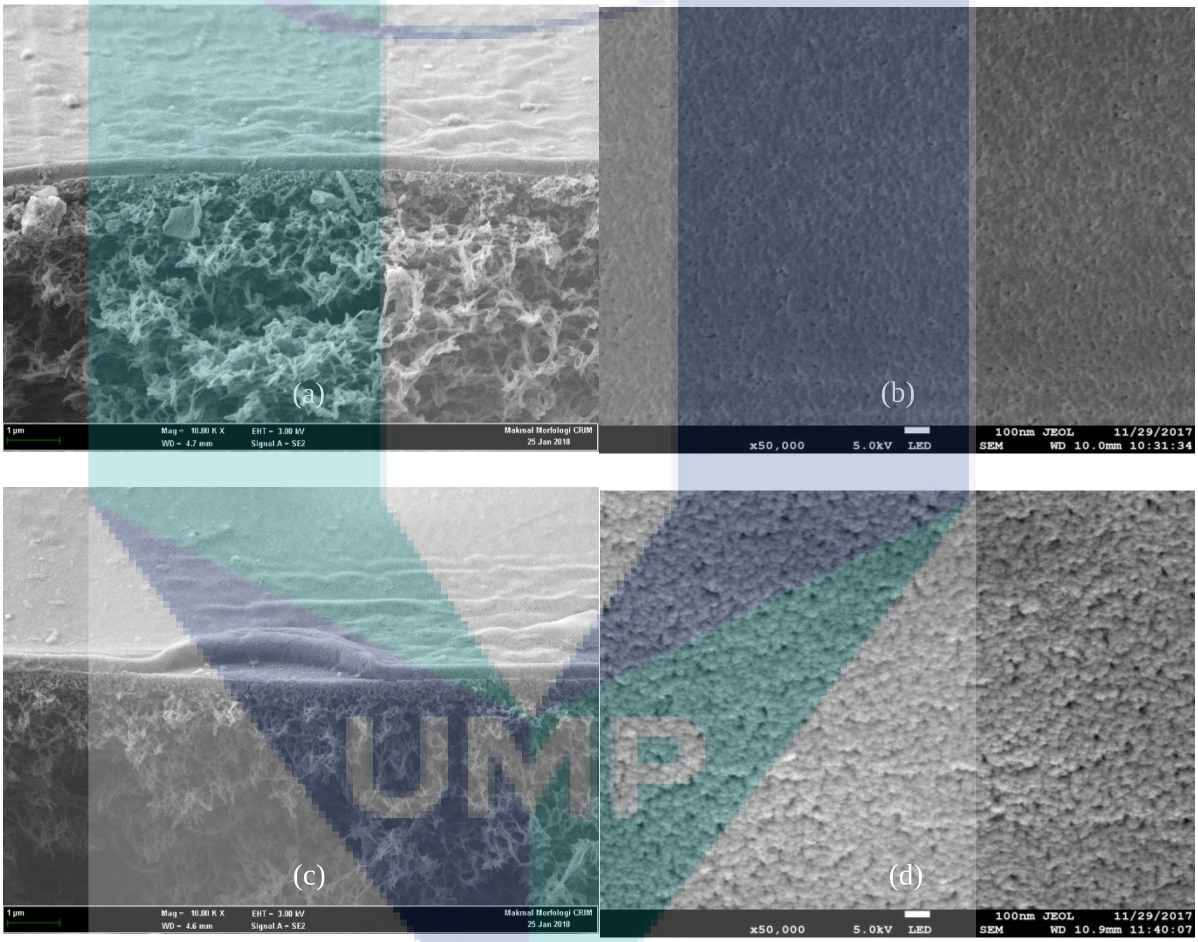

Figure 4.29 FESEM images for a cross-section of (a) unmodified, (c) optimized membrane and top view of (b) unmodified, (d) optimized membrane

4.9.2 Surface roughness

Both unmodified and optimized membranes were identified with their pores and regions that correspond to the actual membrane surface. Details of the surface characteristics are summarized in Table 4.15. The roughness of the modified membrane increased, and it can be postulated that the active area of the membrane increased. The tridimensional and topographic surfaces of the membranes are shown in Figure 4.30.

Table 4.15 AFM analysis of the unmodified and optimized membranes.

No.	**Membrane**	**Roughness (S_a, nm)**	**Root mean square (S_q, nm)**	**Maximum peak (S_z, nm)**
1	Unmodified	1.109	1.466	9.004
2	Optimized	1.28	1.68	11.94

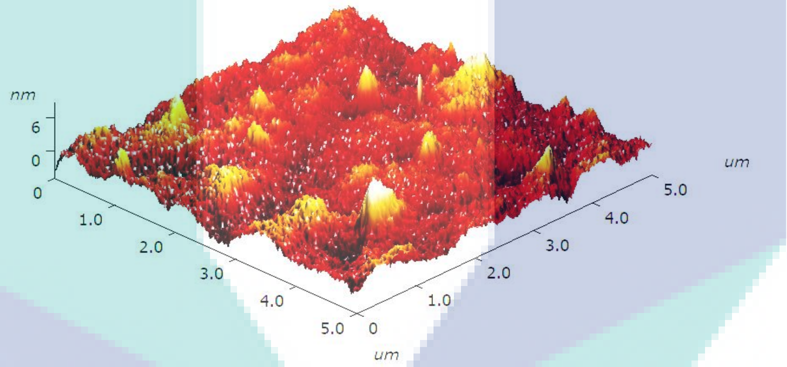

(a) Unmodified membrane

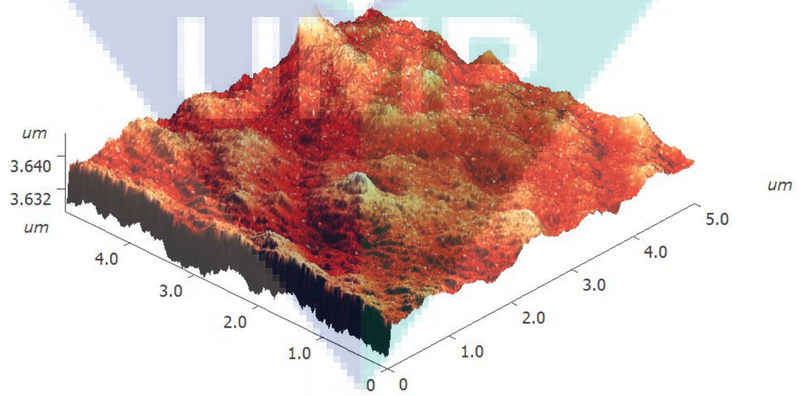

(b) Optimized membrane

Figure 4.30 AFM images for (a) unmodified and (b) optimized NFPES membranes

4.9.3 Summary of optimized membrane

NFPES membrane was modified via UV-photografting to prepare a high-performance FO membrane. The optimized condition of grafting parameters was obtained using central composite design (CCD) of response surface methodology (RSM). Herein, grafting time and monomer concentration were the considered variables with the two responses, water flux and RSD. Quadratic models were established between the responses and the independent parameters using ANOVA. The membranes were characterized with FESEM, and AFM. The obtained optimum conditions were 2.81 min grafting time and 27.85 g/L acrylic acid monomer concentration. Under these conditions, a maximum water flux of 1.52 ± 0.04 was achieved with RSD value of 10.09 ± 0.36. The optimized membrane exhibited higher water flux compared to unmodified NFPES membrane however the RSD value did not reveal significant changes

CHAPTER 5

CONCLUSION

5.1 Conclusion

Surface modification via UV-photografting technique was successfully conducted on both commercial UFPES membrane and NFPES membrane. This surface modification technique enhanced the membrane properties by the addition of the hydrophilic properties namely the carboxyl group on the polyethersulfone backbone. This affects not only the water permeability and solute permeability but also the structural parameter. By lowering the structural parameter, it will eventually lower the ICP which is one of the main problems faced by FO technology.

However, UFPES membrane is unsuitable for the FO application due to the inability of the membrane to retain the salt in both RO and FO mode. Comparison was made in both unmodified and modified membranes. On a different angle, NFPES membrane was successfully modified via UV-photografting technique for FO application. Modified membranes were able to produce enhanced water flux as well as comparative reverse salt diffusion value. The primary objective was to obtain a membrane with high water flux and low RSD. In the presence of different grafting parameters of grafting time and monomer concentration, the performances of modified membranes were discussed theoretically and compared with commercial FO membranes. Thus, the first objective namely to modify, characterize and compare UFPES and NFPES membranes in FO application was accomplished.

The second objective of this research focuses on the mathematical modelling to predict the water flux at different osmotic pressure and types of draw solution. The model successfully predicts the water flux at different grafting conditions namely the monomer concentration and grafting time. Furthermore, the effect of solute resistivity for diffusion on the generated water flux at different osmotic pressure was elucidated.

The third objective was based on subjection of NFPES membrane to optimization process using the response surface methodology. The design of experiment utilized both grafting time and monomer concentration as the factors whereas water flux and reverse salt diffusion were selected as the responses. The developed models were validated using three confirmation runs. In conclusion, modified membrane exhibited better performance compared to the unmodified membrane. However, surface modification via UV-photografting exhibit good result on the water flux but the RSD value reveals a room of improvement. Generally, this study revealed that surface modification via UV photografting provides an alternative route to modify membrane for FO application.

5.2 Recommendation for the future research

In general, the outlined research objectives for this study have been achieved. However, in producing high-performance membrane in terms of water flux and rejection, the obtained RSD seem to be quite low. Currently, most of the research involves both sides of the coins whereby obtaining an enhanced property could trigger different detrimental effect. Thus, the recommendations for the future research are as follows;

i. Application of surface modification technique via UV-photografting using different support polymer such as the Polybenzimidizole (PBI), Polyarylsulfone (PAS) and Polyacrylonitrile (PAN) in the development of FO membrane.

ii. The effect of grafting parameters namely the grafting time and monomer concentration on the removal of artificial wastewater such as the humic acid.

iii. To determine the level of electrical charges of the carboxyl group on the modified surface under different grafting parameter.

iv. The selection of different draw solution ranging from monovalent and divalent ions to reduce the effect of reverse salt diffusion.

v. FO performance must be evaluated based on specific reverse solute flux (Js/Jw) rather than water flux alone due to a strong trade-off between water flux and salt rejection.

vi. In the optimization process involving the response surface methodology, initial work must be oriented to the screening process from the experimental work. The literature could offer a certain range, but the practical approach is far greater concern rather than theoretical.

REFERENCES

Abu Seman, M. N., Khayet, M., Ali, Z. I., & Hilal, N. (2010a). Reduction of nanofiltration membrane fouling by UV-initiated graft polymerization technique. Journal of Membrane Science, 355(1-2), 133-141.

Abu Seman, M. N., Khayet, M., & Hilal, N. (2010b). Nanofiltration thin-film composite polyester polyethersulfone-based membranes prepared by interfacial polymerization. Journal of Membrane Science, 348(1-2), 109-116.

Abu Seman, M. N., Khayet, M., & Hilal, N. (2012). Comparison of two different UV-grafted nanofiltration membranes prepared for reduction of humic acid fouling using acrylic acid and N-vinylpyrrolidone. Desalination, 287, 19-29.

Abuhabib, A. A., Mohammad, A. W., Hilal, N., Rahman, R. A., & Shafie, A. H. (2012). Nanofiltration membrane modification by UV grafting for salt rejection and fouling resistance improvement for brackish water desalination. Desalination, 295, 16-25.

Achilli, A., Cath, T. Y., & Childress, A. E. (2010). Selection of inorganic-based draw solutions for forward osmosis applications. Journal of Membrane Science, 364(1-2), 233-241.

Ahmad, A., Sarif, M., & Ismail, S. (2005). Development of an integrally skinned ultrafiltration membrane for wastewater treatment: effect of different formulations of PSf/NMP/PVP on flux and rejection. Desalination, 179(1), 257-263.

Akther, N., Sodiq, A., Giwa, A., Daer, S., Arafat, H. A., & Hasan, S. W. (2015). Recent advancements in forward osmosis desalination: A review. Chemical Engineering Journal, 281, 502-522.

Amini, M., Jahanshahi, M., & Rahimpour, A. (2013). Synthesis of novel thin film nanocomposite (TFN) forward osmosis membranes using functionalized multi-walled carbon nanotubes. Journal of Membrane Science, 435, 233-241.

Ang, W. L., Mohammad, A. W., Hilal, N., & Leo, C. P. (2015). A review on the applicability of integrated/hybrid membrane processes in water treatment and desalination plants. Desalination, 363, 2-18.

Arena, J. T., Manickam, S. S., Reimund, K. K., Freeman, B. D., & McCutcheon, J. R. (2014). Solute and water transport in forward osmosis using polydopamine modified thin film composite membranes. Desalination, 343, 8-16.

Arena, J. T., McCloskey, B., Freeman, B. D., & McCutcheon, J. R. (2011). Surface modification of thin film composite membrane support layers with polydopamine:

enabling use of reverse osmosis membranes in pressure retarded osmosis. Journal of Membrane Science, 375(1-2), 55-62.

Aziz, S. N. S. A., Rahman, A. F. H. A., Abu Seman, M. N., & Hilal, N. (2018). Comparison of the intrinsic parameters (A, B, and S) of a forward osmosis membrane using pressurized and non-pressurized methods. Desalination and Water Treatment, 129, 14-23.

Baker, R. W. (2004). Membrane technology and applications. Membrane Technology.

Baker, R. W. (2012). Membrane technology and applications: Wiley Online Library.

Banerjee, A., & Ray, S. K. (2018). PVA modified filled copolymer membranes for pervaporative dehydration of acetic acid-systematic optimization of synthesis and process parameters with response surface methodology. Journal of membrane science, 549, 84-100.

Barzin, J., Feng, C., Khulbe, K., Matsuura, T., Madaeni, S., & Mirzadeh, H. (2004). Characterization of polyethersulfone hemodialysis membrane by ultrafiltration and atomic force microscopy. Journal of membrane science, 237(1-2), 77-85.

Bequet, S., Remigy, J. C., Rouch, J. C., Espenan, J. M., Clifton, M., & Aptel, P. (2002). From ultrafiltration to nanofiltration hollow fiber membranes: a continuous UV-photografting process. Desalination, 144(1-3), 9-14.

Bhanushali, D., Kloos, S., & Bhattacharyya, D. (2002). Solute transport in solvent-resistant nanofiltration membranes for non-aqueous systems: experimental results and the role of solute–solvent coupling. Journal of Membrane Science, 208(1), 343-359.

Bilongo, T. G., Remigy, J. C., & Clifton, M. J. (2010). Modification of hollow fibers by UV surface grafting. Journal of Membrane Science, 364(1-2), 304-308.

Blandin, G., Verliefde, A. R., Tang, C. Y., & Le-Clech, P. (2015). Opportunities to reach economic sustainability in forward osmosis–reverse osmosis hybrids for seawater desalination. Desalination, 363, 26-36.

Boo, C., Elimelech, M., & Hong, S. (2013). Fouling control in a forward osmosis process integrating seawater desalination and wastewater reclamation. Journal of Membrane Science, 444, 148-156.

Boo, C., Lee, S., Elimelech, M., Meng, Z. Y., & Hong, S. (2012). Colloidal fouling in forward osmosis: Role of reverse salt diffusion. Journal of Membrane Science, 390, 277-284.

Bowen, W. R., Mohammad, A. W., & Hilal, N. (1997). Characterisation of nanofiltration membranes for predictive purposes—use of salts, uncharged solutes and atomic force microscopy. Journal of Membrane Science, 126(1), 91-105.

Cai, T., Li, X., Wan, C. F., & Chung, T. S. (2016). Zwitterionic polymers grafted poly(ether sulfone) hollow fiber membranes and their antifouling behaviors for osmotic power generation. Journal of Membrane Science, 497, 142-152.

Cai, Y. F., & Hu, X. (2016). A critical review on draw solutes development for forward osmosis. Desalination, 391, 16-29.

Castrillon, S. R. V., Lu, X. L., Shaffer, D. L., & Elimelech, M. (2014). Amine enrichment and poly(ethylene glycol) (PEG) surface modification of thin-film composite forward osmosis membranes for organic fouling control. Journal of Membrane Science, 450, 331-339.

Cath, T. Y., Childress, A. E., & Elimelech, M. (2006). Forward osmosis: Principles, applications, and recent developments. Journal of Membrane Science, 281(1-2), 70-87.

Cath, T. Y., Elimelech, M., McCutcheon, J. R., McGinnis, R. L., Achilli, A., Anastasio, D., . . . Yip, N. Y. (2013). Standard Methodology for Evaluating Membrane Performance in Osmotically Driven Membrane Processes. Desalination, 312, 31-38.

Chanukya, B. S., Patil, S., & Rastogi, N. K. (2013). Influence of concentration polarization on flux behavior in forward osmosis during desalination using ammonium bicarbonate. Desalination, 312, 39-44.

Chekli, L., Phuntsho, S., Kim, J. E., Kim, J., Choi, J. Y., Choi, J. S., . . . Shon, H. K. (2016). A comprehensive review of hybrid forward osmosis systems: Performance, applications and future prospects. Journal of Membrane Science, 497, 430-449.

Chen, Q., Yu, P. P., Huang, W. Q., Yu, S. C., Liu, M. H., & Gao, C. J. (2015). High-flux composite hollow fiber nanofiltration membranes fabricated through layer-by-layer deposition of oppositely charged crosslinked polyelectrolytes for dye removal. Journal of Membrane Science, 492, 312-321.

Chen, R. C., Sun, H., Li, A., & Xu, G. Z. (2012). UV-induced Self-initiated Graft Polymerization of Acrylamide onto Poly(ether ether ketone). Chemical Research in Chinese Universities, 28(1), 162-165.

Chou, S. R., Shi, L., Wang, R., Tang, C. Y. Y., Qiu, C. Q., & Fane, A. G. (2010). Characteristics and potential applications of a novel forward osmosis hollow fiber membrane. Desalination, 261(3), 365-372.

Chung, T.-S., Li, X., Ong, R. C., Ge, Q., Wang, H., & Han, G. (2012). Emerging forward osmosis (FO) technologies and challenges ahead for clean water and clean energy applications. Current Opinion in Chemical Engineering, 1(3), 246-257.

Chung, Y. T., Ng, L. Y., & Mohammad, A. W. (2014). Sulfonated-polysulfone membrane surface modification by employing methacrylic acid through UV-grafting: Optimization through response surface methodology approach. Journal of Industrial and Engineering Chemistry, 20(4), 1549-1557.

Cojocaru, C., & Trznadel, G. Z. (2007). Response surface modeling and optimization of copper removal from aqua solutions using polymer assisted ultrafiltration. Journal of Membrane Science, 298(1-2), 56-70.

Deng, B., Yang, X. X., Xie, L. D., Li, J. Y., Hou, Z. C., Yao, S., . . . Huang, Q. (2009). Microfiltration membranes with pH dependent property prepared from poly(methacrylic acid) grafted polyethersulfone powder. Journal of Membrane Science, 330(1-2), 363-368.

Deng, H. Y., Xu, Y. Y., Chen, Q. C., Wei, X. Z., & Zhu, B. K. (2011). High flux positively charged nanofiltration membranes prepared by UV-initiated graft polymerization of methacrylatoethyl trimethyl ammonium chloride (DMC) onto polysulfone membranes. Journal of Membrane Science, 366(1-2), 363-372.

Deshmukh, A., Yip, N. Y., Lin, S. H., & Elimelech, M. (2015). Desalination by forward osmosis: Identifying performance limiting parameters through module-scale modeling. Journal of Membrane Science, 491, 159-167.

Doo Hyun, L., Hyun-Il, K., & Sung Soo, K. (2004). Surface Modification of Polymeric Membranes by UV Grafting. In Advanced Materials for Membrane Separations (Vol. 876, pp. 281-299): American Chemical Society.

Duong, P. H. H., Zuo, J., & Chung, T. S. (2013). Highly crosslinked layer-by-layer polyelectrolyte FO membranes: Understanding effects of salt concentration and deposition time on FO performance. Journal of Membrane Science, 427, 411-421.

Elimelech, M., Chen, W. H., & Waypa, J. J. (1994). Measuring the Zeta (Electrokinetic) Potential of Reverse-Osmosis Membranes by a Streaming Potential Analyzer. Desalination, 95(3), 269-286.

Elliott, J. E., Macdonald, M., Nie, J., & Bowman, C. N. (2004). Structure and swelling of poly (acrylic acid) hydrogels: effect of pH, ionic strength, and dilution on the crosslinked polymer structure. Polymer, 45(5), 1503-1510.

Garcia-Ivars, J., Clar, M. I. I., Miranda, M. I. A., Roca, J. A. M., & Alcaniz, L. P. (2014). Development of fouling-resistant polyethersulfone ultrafiltration membranes via surface UV photografting with polyethylene glycol/aluminum oxide nanoparticles. Separation and Purification Technology, 135, 88-99.

Garcia-Ivars, J., Iborra-Clar, M. I., Alcaina-Miranda, M. I., Mendoza-Roca, J. A., & Pastor-Alcaniz, L. (2016). Surface photomodification of flat-sheet PES membranes with improved antifouling properties by varying UV irradiation time and additive solution pH. Chemical Engineering Journal, 283, 231-242.

Ge, Q., Ling, M., & Chung, T.-S. (2013). Draw solutions for forward osmosis processes: Developments, challenges, and prospects for the future. Journal of Membrane Science, 442, 225-237.

Ge, Q., Su, J., Amy, G. L., & Chung, T.-S. (2012). Exploration of polyelectrolytes as draw solutes in forward osmosis processes. Water research, 46(4), 1318-1326.

Ge, Q., Su, J., Chung, T.-S., & Amy, G. (2010). Hydrophilic superparamagnetic nanoparticles: synthesis, characterization, and performance in forward osmosis processes. Industrial & Engineering Chemistry Research, 50(1), 382-388.

Ghanbari, M., Emadzadeh, D., Lau, W. J., Matsuura, T., Davoody, M., & Ismail, A. F. (2015). Super hydrophilic TiO2/HNT nanocomposites as a new approach for fabrication of high performance thin film nanocomposite membranes for FO application. Desalination, 371, 104-114.

Ghanbari, M., Emadzadeh, D., Lau, W. J., Riazi, H., Almasi, D., & Ismail, A. F. (2016). Minimizing structural parameter of thin film composite forward osmosis membranes using polysulfone/halloysite nanotubes as membrane substrates. Desalination, 377, 152-162.

Gu, Y., Wang, Y. N., Wei, J., & Tang, C. Y. (2013). Organic fouling of thin-film composite polyamide and cellulose triacetate forward osmosis membranes by oppositely charged macromolecules. Water Res, 47(5), 1867-1874.

Han, G., Zhang, S., Li, X., Widjojo, N., & Chung, T. S. (2012). Thin film composite forward osmosis membranes based on polydopamine modified polysulfone substrates with enhancements in both water flux and salt rejection. Chemical Engineering Science, 80, 219-231.

He, D. M., Susanto, H., & Ulbricht, M. (2009). Photo-irradiation for preparation, modification and stimulation of polymeric membranes. Progress in Polymer Science, 34(1), 62-98.

Hilal, N., Ismail, A. F., & Wright, C. (2015). Membrane Fabrication: CRC Press.

Hilal, N., Khayet, M., & Wright, C. J. (2012). Membrane modification: Technology and applications: CRC Press.

Holloway, R. W., Childress, A. E., Dennett, K. E., & Cath, T. Y. (2007). Forward osmosis for concentration of anaerobic digester centrate. Water research, 41(17), 4005-4014.

Huang, L. W., Arena, J. T., & McCutcheon, J. R. (2016). Surface modified PVDF nanofiber supported thin film composite membranes for forward osmosis. Journal of Membrane Science, 499, 352-360.

Jamalludin, M. R., Harun, Z., Hubadillah, S. K., Basri, H., Ismail, A. F., Othman, M. H. D., . . . Yunos, M. Z. (2016). Antifouling polysulfone membranes blended with green SiO2 from rice husk ash (RHA) for humic acid separation. Chemical Engineering Research and Design, 114, 268-279.

Jia, Q., Han, H., Wang, L., Liu, B., Yang, H., & Shen, J. (2014). Effects of CTAC micelles on the molecular structures and separation performance of thin-film composite (TFC) membranes in forward osmosis processes. Desalination, 340, 30-41.

Jia, Q. B., Xu, Y. Y., Shen, J. Q., Yang, H. J., & Zhou, L. (2015). Effects of hydrophilic solvent and oxidation resistance post surface treatment on molecular structure and forward osmosis performance of polyamide thin-film composite (TFC) membranes. Applied Surface Science, 356, 1105-1116.

Jiao, Y., Kang, Y., & Yang, C. (2015). Osmosis and Its Applications. Encyclopedia of Microfluidics and Nanofluidics, 2622-2633.

Kaeselev, B., Kingshott, P., & Jonsson, G. (2002). Influence of the surface structure on the filtration performance of UV-modified PES membranes. Desalination, 146(1-3), 265-271.

Kato, K., Uchida, E., Kang, E. T., Uyama, Y., & Ikada, Y. (2003). Polymer surface with graft chains. Progress in Polymer Science, 28(2), 209-259.

Khayet, M., Abu Seman, M. N., & Hilal, N. (2010). Response surface modeling and optimization of composite nanofiltration modified membranes. Journal of Membrane Science, 349(1-2), 113-122.

Khayet, M., Cojocaru, C., & Essalhi, M. (2011). Artificial neural network modeling and response surface methodology of desalination by reverse osmosis. Journal of membrane science, 368(1-2), 202-214.

Kim, B., Gwak, G., & Hong, S. (2017). Review on methodology for determining forward osmosis (FO) membrane characteristics: Water permeability (A), solute permeability (B), and structural parameter (S). Desalination, 422, 5-16.

Kim, B., Lee, S., & Hong, S. (2014). A novel analysis of reverse draw and feed solute fluxes in forward osmosis membrane process. Desalination, 352, 128-135.

Kim, S. M. (2013). Surface Nanostructuring of Polysulfone Membranes by Atmospheric Pressure Plasma-Induced Graft Polymerization (APPIGP).

Kiriukhin, M. Y., & Collins, K. D. (2002). Dynamic hydration numbers for biologically important ions. Biophysical chemistry, 99(2), 155-168.

Klaysom, C., Hermans, S., Gahlaut, A., Van Craenenbroeck, S., & Vankelecom, I. F. J. (2013). Polyamide/Polyacrylonitrile (PA/PAN) thin film composite osmosis membranes: Film optimization, characterization and performance evaluation. Journal of Membrane Science, 445, 25-33.

Korbutowicz, M. K., & Nowak, K. M. (2011). Membrane separation processes in environmental protection. Wrocław University of Technology, Wrocław.

Kuroda, S., Nagura, A., Horie, K., & Mita, I. (1989). Degradation of aromatic polymers—III. Crosslinking and chain scission during photodegradation of polysulphones. European polymer journal, 25(6), 621-627.

Kwon, S. B., Lee, J. S., Kwon, S. J., Yun, S. T., Lee, S., & Lee, J. H. (2015). Molecular layer-by-layer assembled forward osmosis membranes. Journal of Membrane Science, 488, 111-120.

Lau, W. J., & Ismail, A. F. (2009). Theoretical studies on the morphological and electrical properties of blended PES/SPEEK nanofiltration membranes using different sulfonation degree of SPEEK. Journal of Membrane Science, 334(1-2), 30-42.

Lau, W. J., & Ismail, A. F. (2011). Progress in interfacial polymerization technique on composite membrane preparation. Paper presented at the 2nd International Conference on Environmental Engineering and Application.

Lee, J., Kim, B., & Hong, S. (2014). Fouling distribution in forward osmosis membrane process. J Environ Sci (China), 26(6), 1348-1354.

Lee, K. P., Zheng, J. M., Bargeman, G., Kemperman, A. J. B., & Benes, N. E. (2015). pH stable thin film composite polyamine nanofiltration membranes by interfacial polymerisation. Journal of Membrane Science, 478, 75-84.

Lee, S., Boo, C., Elimelech, M., & Hong, S. (2010). Comparison of fouling behavior in forward osmosis (FO) and reverse osmosis (RO). Journal of Membrane Science, 365(1-2), 34-39.

Li, S.-S., Xie, Y., Xiang, T., Ma, L., He, C., Sun, S.-d., & Zhao, C.-S. (2016). Heparin-mimicking polyethersulfone membranes – hemocompatibility, cytocompatibility, antifouling and antibacterial properties. Journal of Membrane Science, 498, 135-146.

Li, X. F., Goyens, W., Ahmadiannamini, P., Vanderlinden, W., De Feyter, S., & Vankelecom, I. (2010). Morphology and performance of solvent-resistant nanofiltration membranes based on multilayered polyelectrolytes: Study of preparation conditions. Journal of Membrane Science, 358(1-2), 150-157.

Liu, C., Fang, W. X., Chou, S. R., Shi, L., Fane, A. G., & Wang, R. (2013). Fabrication of layer-by-layer assembled FO hollow fiber membranes and their performances using low concentration draw solutions. Desalination, 308, 147-153.

Liu, C., Shi, L., & Wang, R. (2015a). Crosslinked layer-by-layer polyelectrolyte nanofiltration hollow fiber membrane for low-pressure water softening with the presence of SO 4 2− in feed water. Journal of Membrane Science, 486, 169-176.

Liu, C., Shi, L., & Wang, R. (2015b). Enhanced hollow fiber membrane performance via semi-dynamic layer-by-layer polyelectrolyte inner surface deposition for nanofiltration and forward osmosis applications. Reactive & Functional Polymers, 86, 154-160.

Liu, F., Hashim, N. A., Liu, Y., Abed, M. M., & Li, K. (2011). Progress in the production and modification of PVDF membranes. Journal of Membrane Science, 375(1), 1-27.

Liu, L. X., Shen, F., Chen, X. R., Luo, J. Q., Su, Y., Wu, H. H., & Wan, Y. H. (2016). A novel plasma-induced surface hydrophobization strategy for membrane distillation: Etching, dipping and grafting. Journal of Membrane Science, 499, 544-554.

Liu, Y. A., Su, Y. L., Zhao, X. T., Zhang, R. N., Ma, T. Y., He, M. R., & Jiang, Z. Y. (2016). Enhanced membrane antifouling and separation performance by manipulating phase separation and surface segregation behaviors through incorporating versatile modifier. Journal of Membrane Science, 499, 406-417.

Lu, X., Castrillon, S. R. V., Shaffer, D. L., Ma, J., & Elimelech, M. (2013). In situ surface chemical modification of thin-film composite forward osmosis membranes for enhanced organic fouling resistance. Environ Sci Technol, 47(21), 12219-12228.

Mansourpanah, Y., & Habili, E. M. (2013). Preparation and modification of thin film PA membranes with improved antifouling property using acrylic acid and UV irradiation. Journal of Membrane Science, 430, 158-166.

McCutcheon, J. R., & Elimelech, M. (2006). Influence of concentrative and dilutive internal concentration polarization on flux behavior in forward osmosis. Journal of Membrane Science, 284(1-2), 237-247.

McCutcheon, J. R., & Elimelech, M. (2007). Modeling water flux in forward osmosis: implications for improved membrane design. AIChE Journal, 53(7), 1736-1744.

McCutcheon, J. R., & Elimelech, M. (2008). Influence of membrane support layer hydrophobicity on water flux in osmotically driven membrane processes. Journal of Membrane Science, 318(1-2), 458-466.

McCutcheon, J. R., McGinnis, R. L., & Elimelech, M. (2005). A novel ammonia—carbon dioxide forward (direct) osmosis desalination process. Desalination, 174(1), 1-11.

McCutcheon, J. R., McGinnis, R. L., & Elimelech, M. (2006). Desalination by ammonia–carbon dioxide forward osmosis: Influence of draw and feed solution concentrations on process performance. Journal of Membrane Science, 278(1-2), 114-123.

Mehrparvar, A., & Rahimpour, A. (2015). Surface modification of novel polyether sulfone amide (PESA) ultrafiltration membranes by grafting hydrophilic monomers. Journal of Industrial and Engineering Chemistry, 28, 359-368.

Membrana GmbH. (2015). SIPS Processes for Hollow-Fiber Membranes. (Membrana GmbH Solutions for Healthcare and Industrial Filtration), http://www.membrana.com/technology/manufacturing/sips.

Meng, J. Q., Li, J. H., Zhang, Y. F., & Ma, S. N. (2014). A novel controlled grafting chemistry fully regulated by light for membrane surface hydrophilization and functionalization. Journal of Membrane Science, 455, 405-414.

Moghimifar, V., Raisi, A., & Aroujalian, A. (2014). Surface modification of polyethersulfone ultrafiltration membranes by corona plasma-assisted coating TiO2 nanoparticles. Journal of Membrane Science, 461, 69-80.

Mulder, J. (2012). Basic principles of membrane technology: Springer Science & Business Media.

Ng, L. T., Garnett, J. L., Zilic, E., & Nguyen, D. (2001). Effect of monomer structure on radiation grafting of charge transfer complexes to synthetic and naturally occurring polymers. Radiation Physics and Chemistry, 62(1), 89-98.

Ng, L. Y., Ahmad, A., & Mohammad, A. W. (2013a). Alteration of polyethersulphone membranes through UV-induced modification using various materials: A brief review. Arabian Journal of Chemistry.

Ng, L. Y., Ahmad, A., & Mohammad, A. W. (2017). Alteration of polyethersulphone membranes through UV-induced modification using various materials: A brief review. Arabian Journal of Chemistry, 10, S1821-S1834.

Ng, L. Y., Mohammad, A. W., Leo, C. P., & Hilal, N. (2013b). Polymeric membranes incorporated with metal/metal oxide nanoparticles: A comprehensive review. Desalination, 308, 15-33.

Ng, L. Y., Mohammad, A. W., & Ng, C. Y. (2013c). A review on nanofiltration membrane fabrication and modification using polyelectrolytes: effective ways to develop membrane selective barriers and rejection capability. Adv Colloid Interface Sci, 197-198, 85-107.

Ng, L. Y., Mohammad, A. W., Ng, C. Y., Leo, C. P., & Rohani, R. (2014). Development of nanofiltration membrane with high salt selectivity and performance stability using polyelectrolyte multilayers. Desalination, 351, 19-26.

Nguyen, A., Azari, S., & Zou, L. D. (2013). Coating zwitterionic amino acid L-DOPA to increase fouling resistance of forward osmosis membrane. Desalination, 312, 82-87.

Nguyen, T. P. N., Jun, B. M., Lee, J. H., & Kwon, Y. N. (2015). Comparison of integrally asymmetric and thin film composite structures for a desirable fashion of forward osmosis membranes. Journal of Membrane Science, 495, 457-470.

Niksefat, N., Jahanshahi, M., & Rahimpour, A. (2014). The effect of SiO 2 nanoparticles on morphology and performance of thin film composite membranes for forward osmosis application. Desalination, 343, 140-146.

Nilsson, M., Tragardh, G., & Ostergren, K. (2008). The influence of pH, salt and temperature on nanofiltration performance. Journal of Membrane Science, 312(1-2), 97-106.

Park, M., Lee, J. J., Lee, S., & Kim, J. H. (2011). Determination of a constant membrane structure parameter in forward osmosis processes. Journal of Membrane Science, 375(1-2), 241-248.

Peeva, P. D., Pieper, T., & Ulbricht, M. (2010). Tuning the ultrafiltration properties of anti-fouling thin-layer hydrogel polyethersulfone composite membranes by suited crosslinker monomers and photo-grafting conditions. Journal of Membrane Science, 362(1-2), 560-568.

Phillip, W. A., Yong, J. S., & Elimelech, M. (2010). Reverse draw solute permeation in forward osmosis: modeling and experiments. Environ Sci Technol, 44(13), 5170-5176.

Phuntsho, S., Shon, H. K., Hong, S., Lee, S., & Vigneswaran, S. (2011). A novel low energy fertilizer driven forward osmosis desalination for direct fertigation: evaluating the performance of fertilizer draw solutions. Journal of Membrane Science, 375(1-2), 172-181.

Physicsopenlab. (2018, 22 January 2018). Sodium chloride (NaCl) crystal. 22 January 2018.

Pieracci, J., Crivello, J. V., & Belfort, G. (2002). UV-assisted graft polymerization of N-vinyl-2-pyrrolidinone onto poly(ether sulfone) ultrafiltration membranes using selective UV wavelengths. Chemistry of Materials, 14(1), 256-265.

Pieracci, J., Wood, D. W., Crivello, J. V., & Belfort, G. (2000). UV-assisted graft polymerization of N-vinyl-2-pyrrolidinone onto poly(ether sulfone) ultrafiltration membranes: Comparison of dip versus immersion modification techniques. Chemistry of Materials, 12(8), 2123-2133.

Puro, L., Manttari, M., Pihlajamaki, A., & Nystrom, M. (2006). Characterization of modified nanofiltration membranes by octanoic acid permeation and FTIR analysis. Chemical Engineering Research & Design, 84(A2), 87-96.

Qasim, M., Darwish, N. A., Sarp, S., & Hilal, N. (2015). Water desalination by forward (direct) osmosis phenomenon: A comprehensive review. Desalination, 374, 47-69.

Qi, S., Qiu, C. Q., Zhao, Y., & Tang, C. Y. (2012). Double-skinned forward osmosis membranes based on layer-by-layer assembly—FO performance and fouling behavior. Journal of Membrane Science, 405-406, 20-29.

Qiu, C. Q., Qi, S. R., & Tang, C. Y. Y. (2011). Synthesis of high flux forward osmosis membranes by chemically crosslinked layer-by-layer polyelectrolytes. Journal of Membrane Science, 381(1-2), 74-80.

Qiu, C. Q., Zhang, Q. T. N. L., & Ping, Z. H. (2006). Nanofiltration membrane preparation by photomodification of cardo polyetherketone ultrafiltration membrane. Separation and Purification Technology, 51(3), 325-331.

Rahimpour, A. (2011). UV photo-grafting of hydrophilic monomers onto the surface of nano-porous PES membranes for improving surface properties. Desalination, 265(1-3), 93-101.

Rahimpour, A., Madaeni, S. S., Zereshki, S., & Mansourpanah, Y. (2009). Preparation and characterization of modified nano-porous PVDF membrane with high antifouling property using UV photo-grafting. Applied Surface Science, 255(16), 7455-7461.

Rahman, A. F. H. B. A., & Seman, M. N. B. A. (2018). Surface modification of polyethersulfone membrane via UV-grafting for forward osmosis technology. Malaysian Journal of Analytical Sciences, 22(3), 542-552.

Rana, D., & Matsuura, T. (2010). Surface modifications for antifouling membranes. Chem Rev, 110(4), 2448-2471.

Ren, P. F., Fang, Y., Wan, L. S., Ye, X. Y., & Xu, Z. K. (2015). Surface modification of polypropylene microfiltration membrane by grafting poly(sulfobetaine methacrylate) and poly(ethylene glycol): Oxidative stability and antifouling capability. Journal of Membrane Science, 492, 249-256.

Richard, W. B. (2004). Membrane technology and applications. John Wiley & Sons Ltd.

Sairam, M., Sereewatthanawut, E., Li, K., Bismarck, A., & Livingston, A. (2011). Method for the preparation of cellulose acetate flat sheet composite membranes for forward osmosis—desalination using MgSO 4 draw solution. Desalination, 273(2), 299-307.

Sanyal, O., Liu, Z. G., Meharg, B. M., Liao, W., & Lee, I. (2015). Development of polyelectrolyte multilayer membranes to reduce the COD level of electrocoagulation treated high-strength wastewater. Journal of Membrane Science, 496, 259-266.

Sato, N., Sato, Y., & Yanase, S. (2014). Forward osmosis using dimethyl ether as a draw solute. Desalination, 349, 102-105.

Schaep, J., Vandecasteele, C., Mohammad, A. W., & Bowen, W. R. (2001). Modelling the retention of ionic components for different nanofiltration membranes. Separation and Purification Technology, 22-3(1-3), 169-179.

Scott, K., & Hughes, R. (2012). Industrial membrane separation technology: Springer Science & Business Media.

Setiawan, L., Wang, R., Shi, L., Li, K., & Fane, A. G. (2012). Novel dual-layer hollow fiber membranes applied for forward osmosis process. Journal of Membrane Science, 421, 238-246.

Setiawan, L., Wang, R., Tan, S. H., Shi, L., & Fane, A. G. (2013). Fabrication of poly(amide-imide)-polyethersulfone dual layer hollow fiber membranes applied in forward osmosis by combined polyelectrolyte cross-linking and depositions. Desalination, 312, 99-106.

Shaari, N. Z. K., Rahman, N. A., Sulaiman, N. A., & Tajuddin, R. M. (2017). Thin Film Composite Membranes: Mechanical and Antifouling Properties. Paper presented at the MATEC Web of Conferences.

Shaffer, D. L., Werber, J. R., Jaramillo, H., Lin, S., & Elimelech, M. (2015). Forward osmosis: Where are we now? Desalination, 356, 271-284.

She, Q. H., Jin, X., Li, Q., & Tang, C. Y. (2012a). Relating reverse and forward solute diffusion to membrane fouling in osmotically driven membrane processes. Water Res, 46(7), 2478-2486.

She, Q. H., Jin, X., & Tang, C. Y. Y. (2012b). Osmotic power production from salinity gradient resource by pressure retarded osmosis: Effects of operating conditions and reverse solute diffusion. Journal of Membrane Science, 401, 262-273.

She, Q. H., Wang, R., Fane, A. G., & Tang, C. Y. Y. (2016). Membrane fouling in osmotically driven membrane processes: A review. Journal of Membrane Science, 499, 201-233.

Shi, H. Y., Xue, L. X., Gao, A. L., Fu, Y. Y., Zhou, Q. B., & Zhu, L. J. (2016). Fouling-resistant and adhesion-resistant surface modification of dual layer PVDF hollow fiber membrane by dopamine and quaternary polyethyleneimine. Journal of Membrane Science, 498, 39-47.

Shibuya, M., Yasukawa, M., Takahashi, T., Miyoshi, T., Higa, M., & Matsuyama, H. (2015). Effect of operating conditions on osmotic-driven membrane performances of cellulose triacetate forward osmosis hollow fiber membrane. Desalination, 362, 34-42.

Shim, J. K., Lee, Y. B., & Lee, Y. M. (1999). pH-dependent permeation through polysulfone ultrafiltration membranes prepared by ultraviolet polymerization technique. Journal of applied polymer science, 74(1), 75-82.

Singhania, R. R., Sukumaran, R. K., & Pandey, A. (2007). Improved cellulase production by Trichoderma reesei RUT C30 under SSF through process optimization. Applied Biochemistry and Biotechnology, 142(1), 60-70.

So, M., Eirich, F., Strathmann, H., & Baker, R. (1973). Preparation of asymmetric loeb-sourirajan membranes. Journal of Polymer Science: Polymer Letters Edition, 11(3), 201-205.

Solouk, A., Hashjin, M. S., Najarian, S., Mirzadeh, H., & Seifalian, A. M. (2011). Optimization of Acrylic Acid Grafting onto POSS-PCU Nanocomposite Using Response Surface Methodology. Iranian Polymer Journal, 20(2), 91-107.

Song, B., Meng, L. H., & Huang, Y. D. (2012). Surface modification of PBO fiber through oxygen plasma induced vapor phase grafting of acrylic acid. Materials Letters, 83, 118-120.

Song, X., Liu, Z., & Sun, D. D. (2011). Nano gives the answer: breaking the bottleneck of internal concentration polarization with a nanofiber composite forward osmosis membrane for a high water production rate. Advanced materials, 23(29), 3256-3260.

Stephenson, T., Brindle, K., Judd, S., & Jefferson, B. (2000). Membrane bioreactors for wastewater treatment: IWA publishing.

Stone, M. L., Rae, C., Stewart, F. F., & Wilson, A. D. (2013). Switchable polarity solvents as draw solutes for forward osmosis. Desalination, 312, 124-129.

Su, B. W., Wang, T. T., Wang, Z. W., Gao, X. L., & Gao, C. J. (2012). Preparation and performance of dynamic layer-by-layer PDADMAC/PSS nanofiltration membrane. Journal of Membrane Science, 423, 324-331.

Su, J. C., Chung, T. S., Helmer, B. J., & de Wit, J. S. (2012). Enhanced double-skinned FO membranes with inner dense layer for wastewater treatment and macromolecule recycle using Sucrose as draw solute. Journal of Membrane Science, 396, 92-100.

Suh, C., & Lee, S. (2013). Modeling reverse draw solute flux in forward osmosis with external concentration polarization in both sides of the draw and feed solution. Journal of Membrane Science, 427, 365-374.

Sun, Y. N., Xue, L. X., Zhang, Y. J., Zhao, X. L., Huang, Y., & Du, X. D. (2014). High flux polyamide thin film composite forward osmosis membranes prepared from porous substrates made of polysulfone and polyethersulfone blends. Desalination, 336, 72-79.

Tan, C. H., & Ng, H. Y. (2013). Revised external and internal concentration polarization models to improve flux prediction in forward osmosis process. Desalination, 309, 125-140.

Taniguchi, M., & Belfort, G. (2004). Low protein fouling synthetic membranes by UV-assisted surface grafting modification: varying monomer type. Journal of Membrane Science, 231(1-2), 147-157.

Taniguchi, M., Pieracci, J., Samsonoff, W. A., & Belfort, G. (2003). UV-Assisted graft polymerization of synthetic membranes: Mechanistic studies. Chemistry of Materials, 15(20), 3805-3812.

Thelin, W. R., Sivertsen, E., Holt, T., & Brekke, G. (2013). Natural organic matter fouling in pressure retarded osmosis. Journal of Membrane Science, 438, 46-56.

Tian, E., Hu, C., Qin, Y., Ren, Y., Wang, X., Wang, X., . . . Yang, X. (2015). A study of poly (sodium 4-styrenesulfonate) as draw solute in forward osmosis. Desalination, 360, 130-137.

Tiraferri, A., Yip, N. Y., Phillip, W. A., Schiffman, J. D., & Elimelech, M. (2011). Relating performance of thin-film composite forward osmosis membranes to support layer formation and structure. Journal of Membrane Science, 367(1-2), 340-352.

Tiraferri, A., Yip, N. Y., Straub, A. P., Castrillon, S. R. V., & Elimelech, M. (2013). A method for the simultaneous determination of transport and structural parameters of forward osmosis membranes. Journal of Membrane Science, 444, 523-538.

Torres, J. G., Sylla, D., Molina, L., Crespo, E., Mota, J., & Bautista, L. (2014). Surface modification of cellulosic substrates via atmospheric pressure plasma polymerization of acrylic acid: Structure and properties. Applied Surface Science, 305, 292-300.

Tracton, A. A. (2006). Coatings technology: fundamentals, testing, and processing techniques: CRC Press.

UNICEF. (2017). Progress on drinking water, sanitation and hygiene: 2017 update and SDG baselines.

United Nations. (2018). The Sustainable Development Goals Report.

Van Der Bruggen, B. (2009a). Chemical modification of polyethersulfone nanofiltration membranes: a review. Journal of applied polymer science, 114(1), 630-642.

Van der Bruggen, B. (2009b). Comparison of redox initiated graft polymerisation and sulfonation for hydrophilisation of polyethersulfone nanofiltration membranes. European Polymer Journal, 45(7), 1873-1882.

Vatanpour, V., Madaeni, S. S., Moradian, R., Zinadini, S., & Astinchap, B. (2011). Fabrication and characterization of novel antifouling nanofiltration membrane prepared from oxidized multiwalled carbon nanotube/polyethersulfone nanocomposite. Journal of Membrane Science, 375(1-2), 284-294.

Volkov, A., Yushkin, A., Kachula, Y., Khotimsky, V., & Volkov, V. (2014). Application of negative retention in organic solvent nanofiltration for solutes fractionation. Separation and Purification Technology, 124, 43-48.

Wang, C. X., Du, M., Lv, J. C., Zhou, Q. Q., Ren, Y., Liu, G. L., . . . Jin, L. M. (2015). Surface modification of aramid fiber by plasma induced vapor phase graft polymerization of acrylic acid. I. Influence of plasma conditions. Applied Surface Science, 349, 333-342.

Wang, D., Zou, W., Li, L., Wei, Q., Sun, S., & Zhao, C. (2011). Preparation and characterization of functional carboxylic polyethersulfone membrane. Journal of Membrane Science, 374(1-2), 93-101.

Wang, L. K., Chen, J. P., Hung, Y. T., & Shammas, N. K. (2008). Membrane and desalination technologies (Vol. 13): Springer.

Wang, R., Shi, L., Tang, C. Y. Y., Chou, S. R., Qiu, C., & Fane, A. G. (2010). Characterization of novel forward osmosis hollow fiber membranes. Journal of Membrane Science, 355(1-2), 158-167.

Wang, Y. Q., Li, X. Y., Cheng, C. L., He, Y. B., Pan, J. F., & Xu, T. W. (2016). Second interfacial polymerization on polyamide surface using aliphatic diamine with improved performance of TFC FO membranes. Journal of Membrane Science, 498, 30-38.

Wang, Y. Q., Ou, R. W., Ge, Q. Q., Wang, H. T., & Xu, T. W. (2013). Preparation of polyethersulfone/carbon nanotube substrate for high-performance forward osmosis membrane. Desalination, 330, 70-78.

Wavhal, D. S., & Fisher, E. R. (2002). Hydrophilic modification of polyethersulfone membranes by low temperature plasma-induced graft polymerization. Journal of membrane science, 209(1), 255-269.

Wei, J., Liu, X., Qiu, C., Wang, R., & Tang, C. Y. (2011a). Influence of monomer concentrations on the performance of polyamide-based thin film composite forward osmosis membranes. Journal of Membrane Science, 381(1-2), 110-117.

Wei, J., Qiu, C., Tang, C. Y., Wang, R., & Fane, A. G. (2011b). Synthesis and characterization of flat-sheet thin film composite forward osmosis membranes. Journal of Membrane Science, 372(1-2), 292-302.

Wei, Q., Li, J., Qian, B. S., Fang, B. H., & Zhao, C. S. (2009). Preparation, characterization and application of functional polyethersulfone membranes blended with poly (acrylic acid) gels. Journal of Membrane Science, 337(1-2), 266-273.

Wei, X., Wang, R., Li, Z., & Fane, A. G. (2006). Development of a novel electrophoresis-UV grafting technique to modify PES UF membranes used for NOM removal. Journal of membrane science, 273(1), 47-57.

Welty, J. R., Wicks, C. E., Rorrer, G., & Wilson, R. E. (2009). Fundamentals of momentum, heat, and mass transfer: John Wiley & Sons.

Widjojo, N., Chung, T. S., Weber, M., Maletzko, C., & Warzelhan, V. (2011). The role of sulphonated polymer and macrovoid-free structure in the support layer for thin-film composite (TFC) forward osmosis (FO) membranes. Journal of Membrane Science, 383(1-2), 214-223.

Wilson, A. D., & Stewart, F. F. (2013). Deriving osmotic pressures of draw solutes used in osmotically driven membrane processes. Journal of Membrane Science, 431, 205-211.

Witek-Krowiak, A., Chojnacka, K., Podstawczyk, D., Dawiec, A., & Pokomeda, K. (2014). Application of response surface methodology and artificial neural network methods in modelling and optimization of biosorption process. Bioresour Technol, 160, 150-160.

X, W., Wang, R., Li, Z. S., & Fane, A. G. (2006). Development of a novel electrophoresis-UV grafting technique to modify PES UF membranes used for NOM removal. Journal of Membrane Science, 273(1-2), 47-57.

Xiangli, F., Wei, W., Chen, Y., Jin, W., & Xu, N. (2008). Optimization of preparation conditions for polydimethylsiloxane (PDMS)/ceramic composite pervaporation membranes using response surface methodology. Journal of Membrane Science, 311(1), 23-33.

Xiao, D., Tang, C. Y., Zhang, J., Lay, W. C., Wang, R., & Fane, A. G. (2011). Modeling salt accumulation in osmotic membrane bioreactors: implications for FO membrane selection and system operation. Journal of membrane science, 366(1-2), 314-324.

Xiarchos, I., Jaworska, A., & Trznadel, G. Z. (2008). Response surface methodology for the modelling of copper removal from aqueous solutions using micellar-enhanced ultrafiltration. Journal of Membrane Science, 321(2), 222-231.

Xu, G. R., Wang, S. H., Zhao, H. L., Wu, S. B., Xu, J. M., Li, L., & Liu, X. Y. (2015). Layer-by-layer (LBL) assembly technology as promising strategy for tailoring pressure-driven desalination membranes. Journal of Membrane Science, 493, 428-443.

Xu, W.-T., Zhao, Z.-P., Liu, M., & Chen, K.-C. (2015). Morphological and hydrophobic modifications of PVDF flat membrane with silane coupling agent grafting via plasma flow for VMD of ethanol–water mixture. Journal of Membrane Science, 491, 110-120.

Yamagishi, James V. Crivello, & Georges Belfort. (1995). Development of a novel photochemical technique for modifying poly(arylsulfone) ultrafiltration membranes.

Yang, Q., Wang, K. Y., & Chung, T. S. (2009). A novel dual-layer forward osmosis membrane for protein enrichment and concentration. Separation and Purification Technology, 69(3), 269-274.

Yang, Y. F., Li, Y., Li, Q. L., Wan, L. S., & Xu, Z. K. (2010). Surface hydrophilization of microporous polypropylene membrane by grafting zwitterionic polymer for anti-biofouling. Journal of Membrane Science, 362(1-2), 255-264.

Yen, S. K., Su, M., Wang, K. Y., & Chung, T.-S. (2010). Study of draw solutes using 2-methylimidazole-based compounds in forward osmosis. Journal of Membrane Science, 364(1-2), 242-252.

Yeo, G. C., Kondyurin, A., Kosobrodova, E., Weiss, A. S., & Bilek, M. M. (2017). A sterilizable, biocompatible, tropoelastin surface coating immobilized by energetic ion activation. Journal of The Royal Society Interface, 14(127), 20160837.

Yin, J., & Deng, B. L. (2015). Polymer-matrix nanocomposite membranes for water treatment. Journal of Membrane Science, 479, 256-275.

Yong, J. S., Phillip, W. A., & Elimelech, M. (2012). Coupled reverse draw solute permeation and water flux in forward osmosis with neutral draw solutes. Journal of Membrane Science, 392, 9-17.

Yu, H. J., Cao, Y. M., Kang, G. D., Liu, J. H., Li, M., & Yuan, Q. (2009). Enhancing antifouling property of polysulfone ultrafiltration membrane by grafting zwitterionic copolymer via UV-initiated polymerization. Journal of Membrane Science, 342(1-2), 6-13.

Yu, H. Y., Xu, Z. K., Yang, Q., Hu, M. X., & Wang, S. Y. (2006). Improvement of the antifouling characteristics for polypropylene microporous membranes by the sequential photoinduced graft polymerization of acrylic acid. Journal of Membrane Science, 281(1-2), 658-665.

Yu, H. Y., Zhou, J., Gu, J. S., & Yang, S. (2010). Manipulating membrane permeability and protein rejection of UV-modified polypropylene macroporous membrane. Journal of Membrane Science, 364(1-2), 203-210.

Yu, Y., Seo, S., Kim, I.-C., & Lee, S. (2011). Nanoporous polyethersulfone (PES) membrane with enhanced flux applied in forward osmosis process. Journal of membrane science, 375(1-2), 63-68.

Zhang, S., Wang, K. Y., Chung, T. S., Chen, H. M., Jean, Y. C., & Amy, G. (2010). Well-constructed cellulose acetate membranes for forward osmosis: Minimized internal concentration polarization with an ultra-thin selective layer. Journal of Membrane Science, 360(1-2), 522-535.

Zhao, B., & Brittain, W. J. (2000). Polymer brushes: surface-immobilized macromolecules. Progress in Polymer Science, 25(5), 677-710.

Zhao, C., Xue, J., Ran, F., & Sun, S. P. (2013). Modification of polyethersulfone membranes – A review of methods. Progress in Materials Science, 58(1), 76-150.

Zhao, G. W., Chen, Y. S., & Wang, X. L. (2007). Surface modification of polyethylene film by acrylamide graft and alcoholysis for improvement of antithrombogenicity. Applied Surface Science, 253(10), 4709-4714.

Zhao, S., Zou, L., & Mulcahy, D. (2012). Brackish water desalination by a hybrid forward osmosis–nanofiltration system using divalent draw solute. Desalination, 284, 175-181.

Zhong, P. S., Widjojo, N., Chung, T. S., Weber, M., & Maletzko, C. (2012). Positively charged nanofiltration (NF) membranes via UV grafting on sulfonated polyphenylenesulfone (sPPSU) for effective removal of textile dyes from wastewater. Journal of Membrane Science, 417, 52-60.

Zhou, Z. Z., Lee, J. Y., & Chung, T. S. (2014). Thin film composite forward-osmosis membranes with enhanced internal osmotic pressure for internal concentration polarization reduction. Chemical Engineering Journal, 249, 236-245.

Zhu, L. P., Zhu, B. K., Xu, L., Feng, Y. X., Liu, F., & Xu, Y. Y. (2007). Corona-induced graft polymerization for surface modification of porous polyethersulfone membranes. Applied Surface Science, 253(14), 6052-6059.

Zhu, W. P., Gao, J., Sun, S. P., Zhang, S., & Chung, T. S. (2015). Poly(amidoamine) dendrimer (PAMAM) grafted on thin film composite (TFC) nanofiltration (NF) hollow fiber membranes for heavy metal removal. Journal of Membrane Science, 487, 117-126.

Zirehpour, A., Rahimpour, A., Seyedpour, F., & Jahanshahi, M. (2015). Developing new CTA/CA-based membrane containing hydrophilic nanoparticles to enhance the forward osmosis desalination. *Desalination, 371*, 46-57.

APPENDIX A

A. Standard Curve

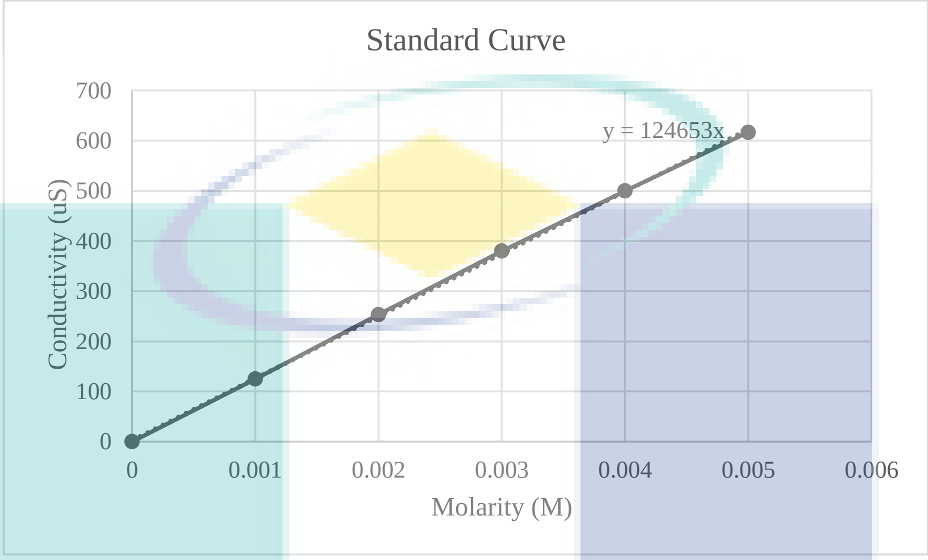

Figure A.1 Curve used to measure molarity for conductivity range between 900µS to 1 µS of NaCl solution.

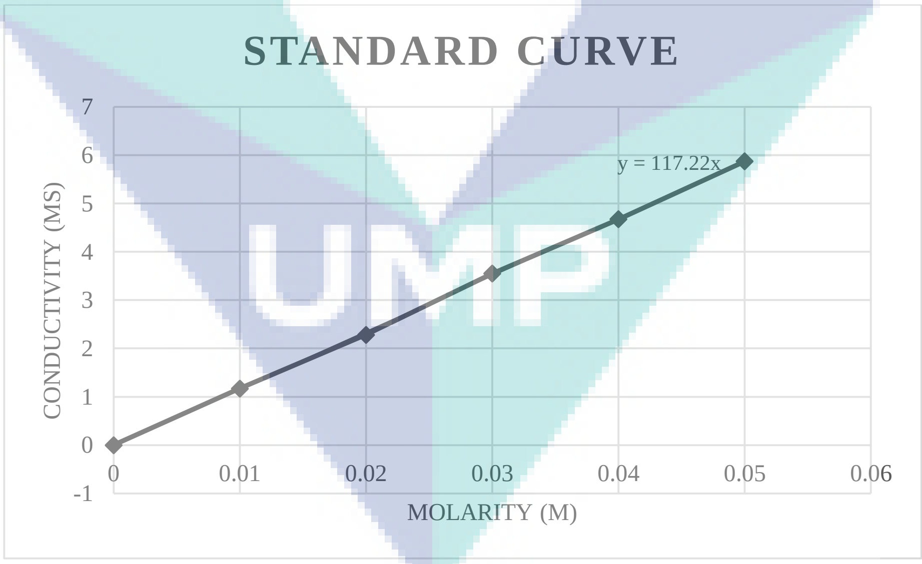

Figure A.2 Curve used to measure molarity for conductivity range between 6mS to 1 mS of NaCl solution.

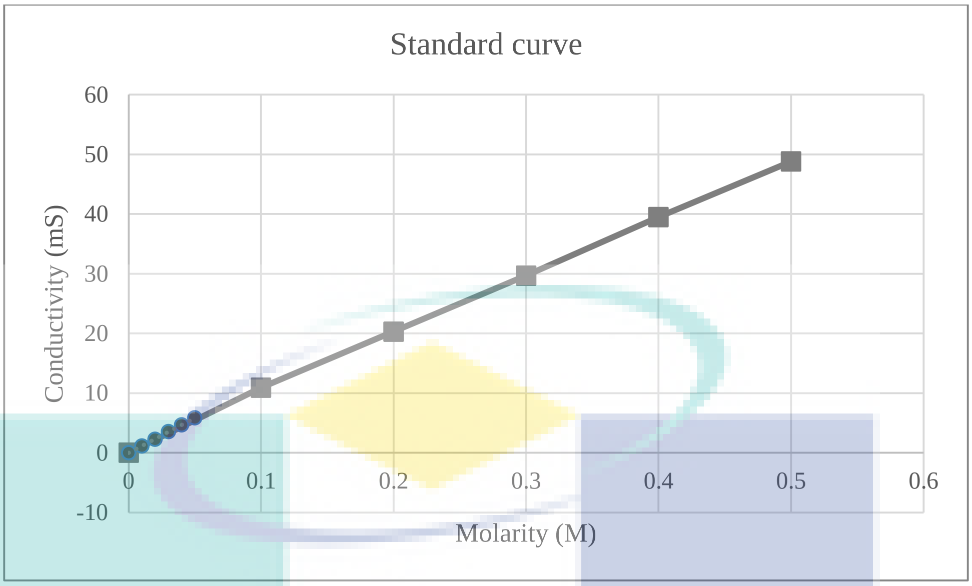

Figure A.3 Curve used to measure molarity for conductivity range between 50mS to 10 mS of NaCl solution.

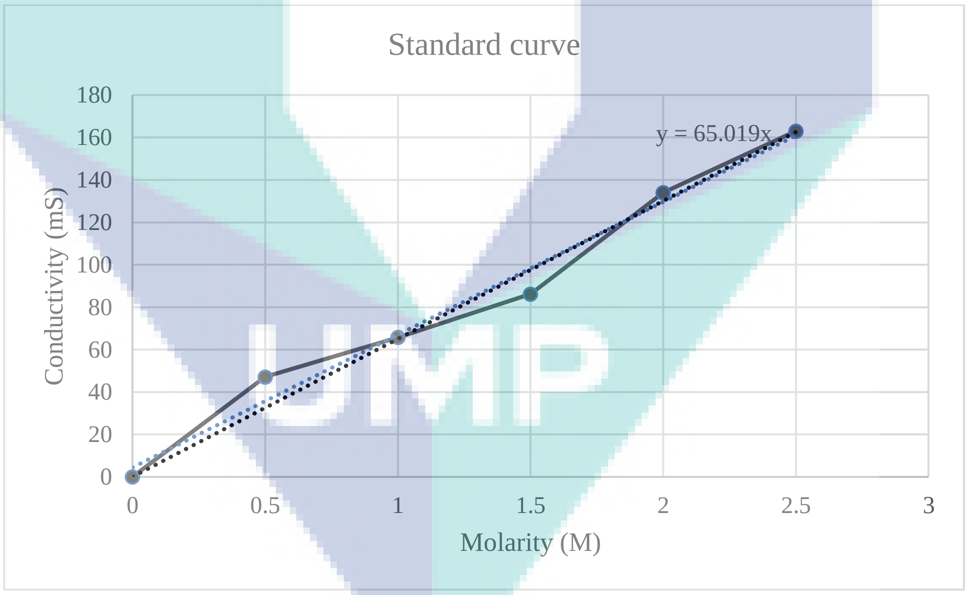

Figure A.4 Curve used to measure molarity for conductivity range between 160mS to 40 mS of NaCl solution.

APPENDIX B

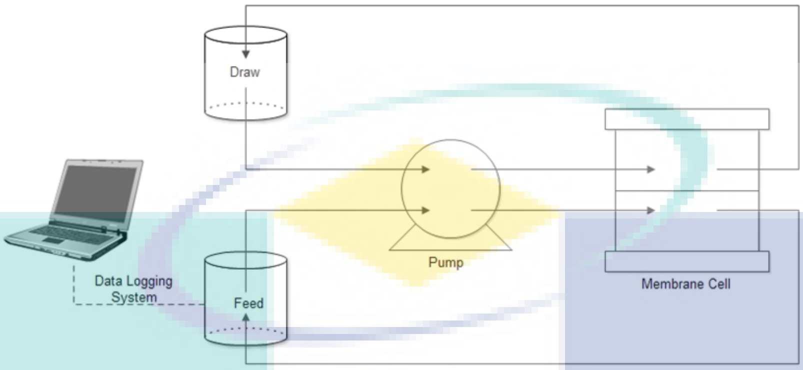

Figure 1 Schematic diagram of FO system

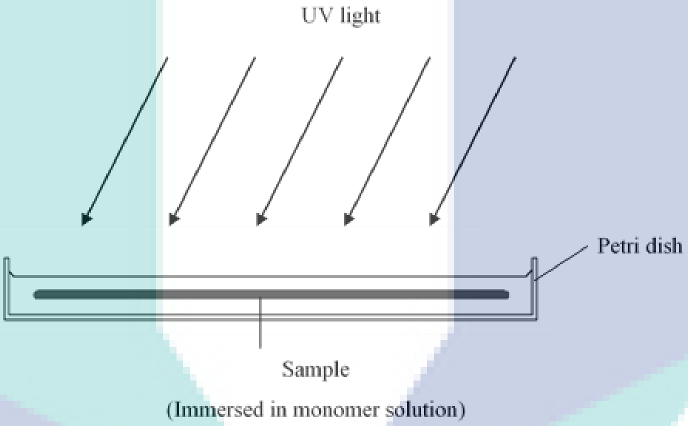

Figure 2 Schematic diagram of UV-photografting process

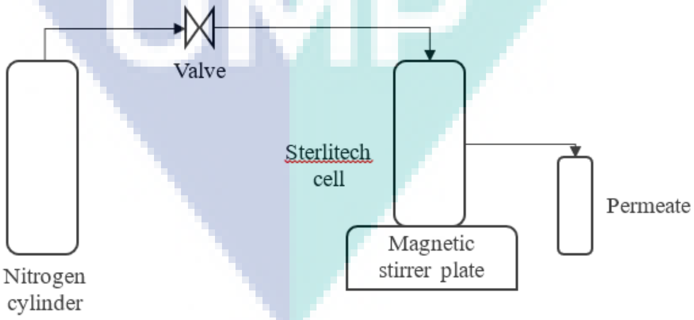

Figure 3 Schematic diagram of HP4730 Sterlitech stirred cell